Engineering

Journal of Research

of the

U.S. National Bureau of Standards

JUNE 1954

VOLUME 52 NUMBER 6

U. S. DEPARTMENT OF COMMERCE
Sinclair Weeks, Secretary
NATIONAL BUREAU OF STANDARDS
A. V. Astin, Director

JUNE • 1954
VOLUME • 52
NUMBER • 6

TA
J58

JOURNAL OF RESEARCH

of the

NATIONAL BUREAU OF STANDARDS

PERIODICALS OF THE NATIONAL BUREAU OF STANDARDS

The National Bureau of Standards is engaged in fundamental and applied research in physics, chemistry, mathematics, and engineering. Projects are conducted in thirteen fields: electricity, optics and metrology, heat and power, atomic and radiation physics, chemistry, mechanics, organic and fibrous materials, metallurgy, mineral products, building technology, applied mathematics, electronics, and radio propagation. The Bureau has custody of the national standards of measurement and conducts research leading to the improvement of scientific and engineering standards and of techniques and methods of measurement. Testing methods and instruments are developed; physical constants and properties of materials are determined; and technical processes are investigated.

JOURNAL OF RESEARCH

The Journal presents research papers by authorities in the specialized fields of physics, mathematics, chemistry, and engineering. Complete details of the work are presented, including laboratory data, experimental procedures, and theoretical and mathematical analyses. Annual subscription: domestic, $5.50; foreign, $6.75.

TECHNICAL NEWS BULLETIN

Summaries of current research at the National Bureau of Standards are published each month in the Technical News Bulletin. The articles are brief, with emphasis on the results of research, chosen on the basis of their scientific or technologic importance. Lists of all Bureau publications during the preceding month are given, including Research Papers, Handbooks, Applied Mathematics Series, Building Materials and Structures Reports, Miscellaneous Publications, and Circulars. Each issue contains 12 or more two-column pages; illustrated. Annual subscription: domestic, $1.00; foreign, $1.35.

BASIC RADIO PROPAGATION PREDICTIONS

The Predictions provide the information necessary for calculating the best frequencies for communication between any two points in the world at any time during the given month. The data are important to all users of long-range radio communications and navigation, including broadcasting, airline, steamship, and wireless services, as well as to investigators of radio propagation and ionosphere. Each issue, covering a period of one month, is released three months in advance and contains 16 large pages, including pertinent charts, drawings, and tables. Annual subscription: domestic, $1.00; foreign, $1.25.

Order all publications from the Superintendent of Documents
U. S. Government Printing Office, Washington 25, D. C.

The printing of this publication has been approved by the Director of the Bureau of the Budget, May 12, 1953.

Journal of Research of the National Bureau of Standards Vol. 52, No. 6, June 1954 Research Paper 2501

Discussion of Current-Sheet Approximations in Reference to High-Frequency Magnetic Measurements

Bohdan Kostyshyn and Peter H. Haas

The problem of violations of thin, uniform current-sheet assumptions in toroidal coils of rectangular cross section is investigated from the viewpoint of high-frequency magnetic measurements. The errors resulting by neglecting leakage flux and by assumptions as to the location of effective current sheets are investigated experimentally as a function of permeability, core dimensions, wire spacing, and wire size. Conclusions are reached as to the adequacy of at least two attempts at calculations of these errors. Finally, conclusions are drawn as to the limitations of measurements on toroidal coils by high-frequency considerations.

1. Definition of Symbols

μ = Magnetic permeability of the material (as used in this paper, the initial permeability).
L_m = Measured inductance of sample coil containing core.
L_S = Calculated value of toroidal coil inductance on basis of uniform thin current-sheet assumptions.
μ_e = Permeability of material as inferred from inductance ratio of measured to calculated inductance.
b, a, h = Outside diameter, inside diameter, and height of toroidal core, respectively.
μ_0 = Value of μ_e reached as the number of turns becomes very large.
$\Delta\mu$ = Absolute permeability error.
$\Delta\mu_1 : \Delta\mu_2$ = Components of $\Delta\mu$, see text.
x = Distance of the effective current sheet from the face of the toroid.
ΔL_m = Correction term to the measured inductance for μ_e to equal μ.
ΔL_S = Correction term to the calculated inductance for μ_e to equal μ.
D = Mean spacing between adjacent wires on toroidal coil.
ΔL_R = Correction term of the type ΔL_S as calculated from theoretical considerations by Rosa.

2. Introduction

It has commonly been the practice in the past [1] [1] to determine the initial permeability of a magnetic material at radio frequencies by winding a toroidal sample with N turns of wire, measuring its inductance, L_m, at low magnetic field strengths, calculating the geometrical inductance, L_S, of an air toroid of the same dimensions, and taking the ratio of the two, L_m/L_S, to be the permeability. Another method employed [2] has been to substitute for L_S the measured value of inductance $(L_m)_a$ of an equivalent air toroid wound on a polystyrene core of identical dimensions, with the same wire and number of turns as the magnetic core to be measured.

The assumption in applying the first method is that the given ratio does not depend on the frequency (if the permeability is truly constant), the number of turns wound on the sample, wire size, and the dimensions of the sample core. The assumption in applying the second method is that any corrections that appear for the inductances for the coils containing the magnetic core and the equivalent air core, respectively, are equal and appear in such a manner as to cancel when the ratio is taken. It is the purpose of this paper to test the validity of these assumptions.

[1] Figures in brackets indicate the literature references at the end of this paper.

3. Limitations on Test Parameters

For the test the various parameters were limited such that the following conditions were adhered to:

1. The magnetic field strength was sufficiently low that the permeability μ measured would be equal to the initial permeability; that is, that value of the permeability obtained as the magnetic induction, B, and the magnetic field intensity, H, simultaneously approach zero.
2. The frequency was low enough that capacitance effects from wire proximities could be demonstrated to be negligible, yet it was high enough that the internal inductance of the wire could be neglected.
3. The magnetic materials were chosen so that the permeability showed no change as a function of frequency until a frequency many times the test frequency was reached.
4. Realistic wire sizes allowing a tight, uniform winding were used. A toroidal winding machine was used (fig. 1) to apply single-layer windings to cores of rectangular cross section.

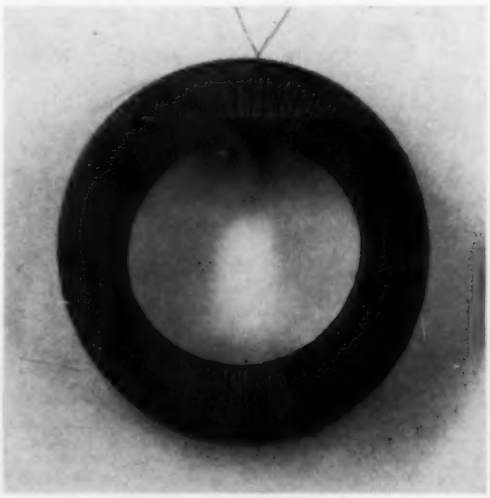

FIGURE 1. *Typical coils used.*

4. Analysis of Assumptions

We now define the effective permeability of a toroidal sample core as

$$\mu_e = \frac{L_m}{L_S}, \tag{1}$$

where μ_e is effective permeability; L_m is the measured inductance of sample coil, and L_S is the calculated inductance of an air toroid, equivalent to sample coil, assuming a thin, uniform current sheet, where L_S is equal to

$$L_S = 2N^2 h \log_e \frac{b}{a} \times 10^{-7} \text{ henry}, \tag{2}$$

where N is the number of turns of wire on sample, h is the height of sample in meters, b is the outer diameter of sample, and a is the inner diameter of sample.

If one now varies the number of turns on a given magnetic core, with given wire size and plots the effective permeability μ_e as a function of N, it is observed (see fig. 2) that the assumption that the ratio L_m/L_S is not dependent on N, as assumed earlier, does not hold, but that for small N a large value of μ_e results, and as N is increased, μ_e approaches asymptotically a value μ_a slightly higher than the true permeability μ, as determined by an NBS radio-frequency permeameter [3].

One now recognizes three values for permeability:

μ equals true initial permeability; that value of permeability obtained by using eq (1), provided a thin, uniform current sheet exists adjacent to the toroidal sample.

μ_e equals effective permeability; that value of permeability obtained from eq (1) when the sample core

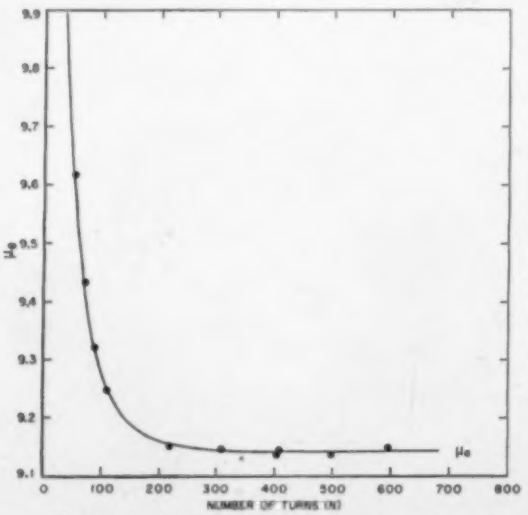

FIGURE 2. *Variation of μ_e with number of turns, N.*
Wire: Insulated No. 38. Core: Outside diameter, 1.507 in.; inside diameter, 1.004 in.; height, 0.375 in.

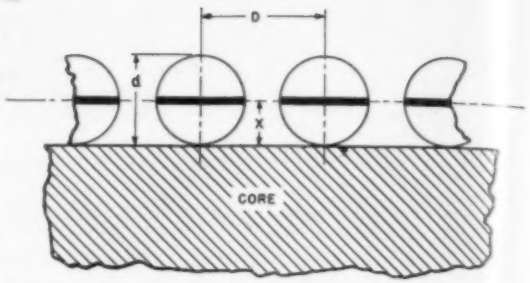

FIGURE 3. *Schematic cross section of the surface of a toroidal coil wound with round wire of diameter d.*

is wound with N turns of actual wire of finite dimensions.

μ_a equals asymptotic permeability; that value of effective permeability reached as the number of turns N becomes very large (fig. 2).

We further define

$$\Delta\mu = \Delta\mu_1 + \Delta\mu_2 = \mu_e - \mu, \tag{3}$$

$$\Delta\mu_1 = \mu_a - \mu, \tag{4}$$

$$\Delta\mu_2 = \mu_e - \mu_a. \tag{5}$$

As noted before, the assumption made in applying eq (1) and assuming it to yield the true permeability is that a constant current sheet exists about and immediately adjacent to the toroidal core. This condition requires that there be no external magnetic fields beyond the confines of the current sheet.

For an actual coil wound with wire of finite dimensions and individual turns spaced a finite distance apart (fig. 3) it is seen that a thin current sheet may not exist, but one may visualize a hypothetical current strip in each wire. If one assumes the existence of a definite current distribution, one might calculate a mean or effective current strip, located a finite distance x from the face of the core. It is further noted that as the number of turns is increased the mean wire spacing D is decreased and the current sheet is more nearly approximated. One may predict on this basis that for a few turns the predominant cause for the error $\Delta\mu_2$ is the existence of a series of current strips, rather than a current sheet. This then implies the existence of magnetic fields beyond the confines of the core. For a large number of turns one may ascribe the error $\Delta\mu_1$ to be caused by the location of an assumed current sheet at some finite distance from the faces of the core, as determined by the current distribution in the wire rather than immediately adjacent to the core.

5. Discussion of Correction Terms

It has been demonstrated in the literature [1, 4] that corrections might be made to account for these more realistic conditions.

In one case it is assumed that the magnetic flux exists only within the confines of the coil, including

that space not occupied by the core. The permeability is then calculated from

$$\mu=\frac{L_m-\Delta L_a}{L_s}, \tag{6}$$

where

$$\Delta L_a=\frac{4N^2A_a}{d_e}\times 10^{-7}\text{ henry [1]}$$

$$=4N^2x\frac{[b-a+4x+2h]}{b-a}\log_e b/a\times 10^{-7}\text{ henry}. \tag{7}$$

ΔL_a=inductance of air space between current sheet and core; A_a is the residual area of air space; d_e is effective magnetic diameter; and x is the distance of the effective current sheet from the face of the toroid. For $\mu=1$, one may alternatively apply a correction to L_s in eq (1), so that the air inductance would effectively be increased to compensate for the larger effective coil cross section. Equation (2) then becomes

$$L_{s'}=2N^2(h+2x)\log_e\frac{b+2x}{a-2x}\,10^{-7}\text{ henry}. \tag{2a}$$

It must be noted at this point that the above corrections account only for effects of finite wire dimensions. The fact that leakage fields do exist beyond the confines of the coil is not considered. A theoretical treatment from the literature of the effects of stray fields will be discussed in a later section, after a consideration of additional experimental results.

6. Experimental Results

We define the correction terms ΔL_m and ΔL_s, such that

$$\mu=\frac{L_m-\Delta L_m}{L_s} \tag{8}$$

or

$$\mu=\frac{L_m}{L_s+\Delta L_s}. \tag{9}$$

No geometrical meaning is affixed to either correction term, except that when either is applied, all necessary correction will have been taken into account.

It may be shown from eq (8) and (9) that

$$\Delta L_m=\Delta\mu L_s \tag{10}$$

$$\Delta L_s=\frac{\Delta\mu L_s^2}{L_m-\Delta\mu L_s} \tag{11}$$

$$\Delta L_s=\frac{\Delta L_m}{\mu}, \tag{12}$$

which relate the correction terms to measurable quantities.

If now the number of turns on a group of cores of the same size but different permeabilities is varied and the effective permeability, μ_e, is plotted as a function of N^2 (fig. 4), it is observed that within the limits of the test, $\Delta\mu$ is the same for all samples for any particular value of N. Thus for a given core size and wire size, $\Delta\mu$ is only a function of the number of turns on the core, i. e.,

$$\Delta\mu=f(N). \tag{13}$$

With this result in mind, a detailed study of the behavior of $\Delta\mu$ is made on a polystyrene core, and it is assumed that the conclusions that will be drawn will be applicable to all other cores of the same physical dimensions wound with the same wire. The reasons for choosing a polystyrene core for this detailed study are

1. μ is very accurately known ($\mu=1$)[5].
2. The percentage error $\Delta\mu/\mu$ is largest for the polystyrene core, and may therefore be more precisely determined.

Figure 5 shows the results of another series of measurements on a polystyrene core, similar to those for the magnetic cores, with the effective permeability, μ_e, plotted as a function of N, with a given core and wire size. It is noted that, indeed, the general shape of the curve is the same as in figures 2 and 4, and that the value of the asymptotic permeability, μ_e, is 6 percent above the true permeability.

If one now assumes a current distribution such that the current is concentrated on the periphery of the wire, and from this deduces the distance x between the current sheet and core face to be half the diameter of the wire, one may apply the correction terms in eq (7) or (2a), substituting $d/2$ for x. It is observed that both correction terms yield approximately the same result, i. e., the entire curve is shifted down and approaches the value of $\mu_e=1.03$ asymptotically. Therefore, this new assumption

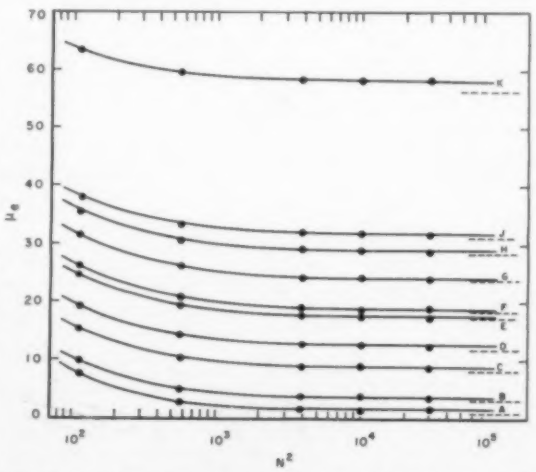

FIGURE 4. *Variation of μ_e as a function of N^2 with μ as a parameter for a group of magnetic cores of given dimensions with given wire size.*

Dotted lines indicate values of true permeability. Wire: Insulated No. 38.

decreases the error to 3 percent, but does not account entirely for the error $\Delta\mu$. This indicates that the current distribution in the wire that has now been assumed might be incorrect because of the proximity of neighboring turns of wire, which certainly will influence the distribution. Furthermore, the experimental evidence indicates that the effective current sheet is located at a still greater distance from the face of the core. It might be noted at this point that the problem of winding a wire adjacent to the core face is a difficult one, and it can be shown that even a small air space will lead to a considerable error $\Delta\mu$.

Figure 6 shows a plot of μ_e as a function of N, with wire size as a parameter. It is observed that the basic curve is shifted upward and to the left for increasing wire size. The curves indicate an increase in the value of the asymptotic permeability μ_a with increasing wire size, showing that the current distribution is altered in such a manner as to increase the distance of the effective current sheet for larger wire. At the same time, because of a greater effective "current strip width" per turn, the uniform current sheet is more closely approximated by the heavier wire for small values of N. This causes less flux to be lost from the test core by leakage, which in turn results in a smaller $\Delta\mu$. Thus it may be seen that for small N, the smaller wire yields a larger $\Delta\mu$, whereas for large N, the smaller wire yields the smaller $\Delta\mu$.

If one plots μ_e as a function of $1/N$ for a polystyrene core (as in fig. 5), it is observed that within limits a linear relationship exists. If, furthermore, the core size is varied (see table 1), and μ_e is plotted as a function of $1/N$, with a given wire size (fig. 7), it is observed that the slope is the same for all coils tested within the linear portion. Considering only the linear portion of the curve and choosing the true permeability as a base point, it is concluded that within the limits of the test, $\Delta\mu$ is a linear function of $1/N$, i. e.,

$$\Delta\mu=\frac{K_1}{N}+C_1. \tag{14}$$

Figure 8 shows a plot of μ_e as a function of $1/N$, with wire size as a parameter; it is observed that the slope K_1 is dependent on wire size.

$$K_1=f(d). \tag{15}$$

TABLE 1. *Dimensions of the cores used in figure 7*

Coil	Outside diameter	Inside diameter	Height
	in.	*in.*	*in.*
1	1.600	1.068	0.532
2	1.300	0.868	.432
3	1.000	.668	.332
4	0.700	.468	.232

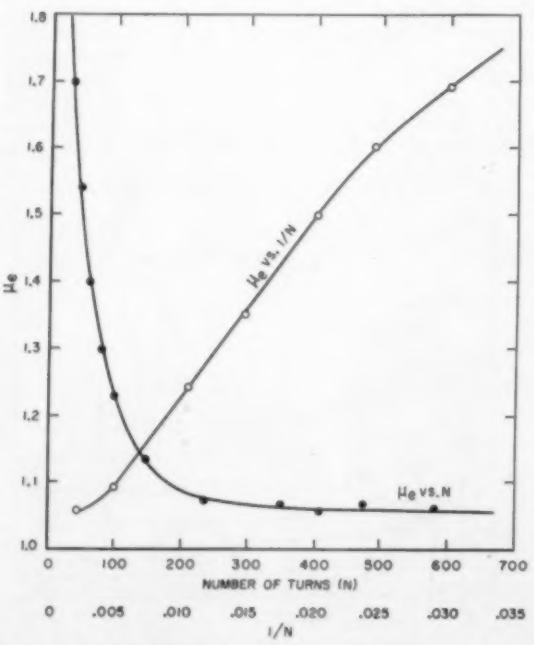

FIGURE 5. *Variation of μ_e as a function of number of turns N for a polystyrene core.*

Wire: Insulated No. 38. Core: Outside diameter, 1.504 in.; inside diameter, 1.004 in.; height, 0.373 in.

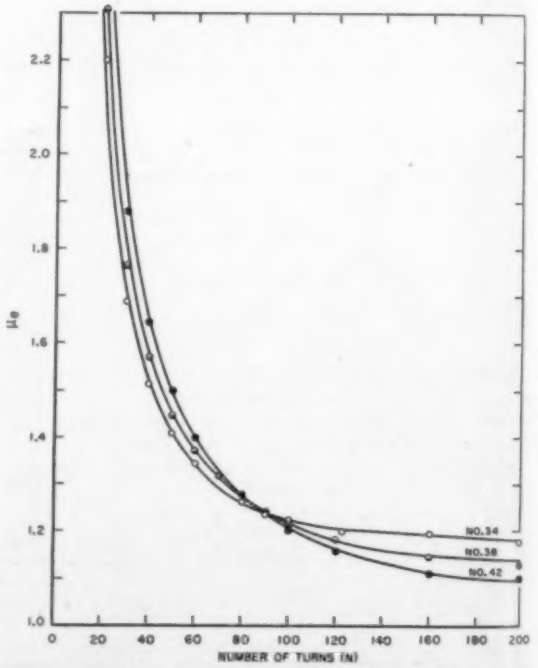

FIGURE 6. *Variation of μ_e as a function of number of turns N, with wire size as a parameter.*

Core: Outside diameter, 1.504 in.; inside diameter, 1.004 in.; height, 0.371 in.

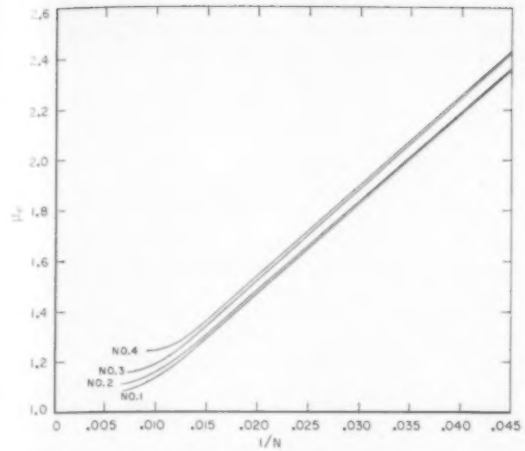

FIGURE 7. *Variation of μ_e as a function of $1/N$, with core size as a parameter.*

Wire: Insulated No. 38. See table 1 for core sizes. Experimental curves; points omitted for reasons of clarity.

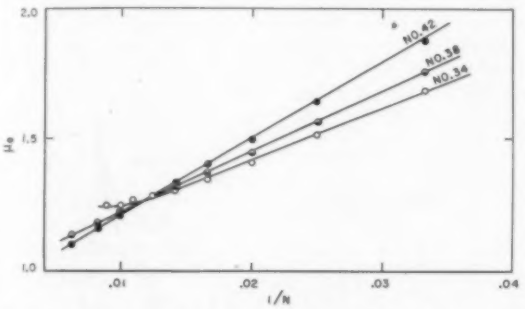

FIGURE 8. *Variation of μ_e as a function of $1/N$, with wire size as a parameter.*

Core: Outside diameter, 1.504 in.; inside diameter, 1.004 in.; height, 0.371 in.

The term C_1 is numerically small by comparison to K_1 and apparently dependent on both core and wire size.

A mean spacing between wire enters may also be defined by

$$D=\frac{\pi(b+a)}{2N}. \tag{16}$$

As D is linearly related to N, it may be concluded that within the range stated, the error is a linear function of the mean spacing between wire centers. Thus eq (14) may be written

$$\Delta\mu=K_2D+C_1, \tag{17}$$

where

$$K_2=\frac{2K_1}{\pi(b+a)}. \tag{18}$$

The data of figure 7 is replotted on figure 9, which shows a plot of μ_e as a function of D, with core size

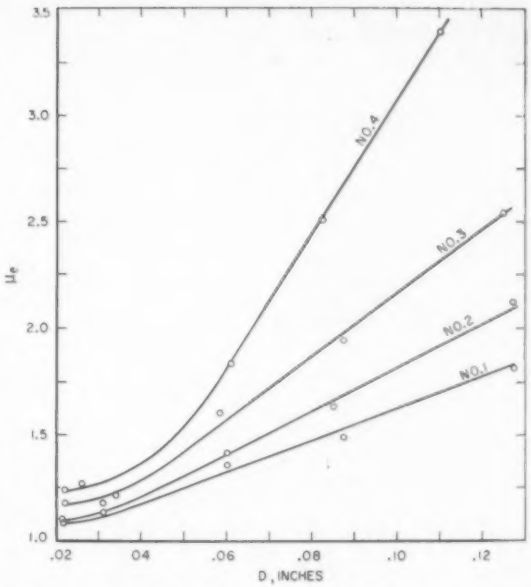

FIGURE 9. *Variation of μ_e as a function of D for various cores (see table 1).*

Wire: Insulated No. 38.

as the parameter. It is interesting to note that $\Delta\mu$ is largest for the smallest test sample, with a given wire spacing, D.

7. Effects on High-Frequency Magnetic Measurements

Sufficient experimental evidence has now been presented to allow us to draw some conclusions as to the effect of flux leakage on permeability measurements at high frequencies. The quantity of major interest in an analysis of the accuracy of a magnetic measurement is the fractional permeability error, E, given by

$$E=\frac{\Delta\mu}{\mu}. \tag{19}$$

From eq (14) we have then

$$E=\frac{K_1}{\mu N}+\frac{C_1}{\mu}. \tag{20}$$

The values of K_1 and C_1 obtained for a number of different core and wire sizes were all such that for the number of turns N usually employed at frequencies in the megacycle region, the error can be approximated by

$$\frac{\Delta\mu}{\mu}\simeq\frac{K_1}{\mu N}\simeq E. \tag{21}$$

Under these conditions, one then obtains the condition for constant error

$$\mu N = \text{constant} \tag{22}$$

(for a coil with given wire size).

Let it now be assumed that a toroidal core of permeability μ_1 has been wound with N_1 turns, yielding a measured inductance L_{m_1}. Let it furthermore be assumed that an error E_1 (this error caused by violation of current-sheet assumption only) results from a calculation of permeability by using eq (1), and that this represents a maximum error that should not be exceeded in the measurement of other cores of permeability μ_x of identical dimensions.

From eq (8) we have

$$L_{m_1} = \mu_1 L_{S_1} + \Delta L_{m_1}. \tag{23}$$

From eq (10) and (23), we have

$$\left.\begin{aligned} L_{m_1} &= (\mu_1 + \Delta\mu_1) L_S \\ &= (1 + E_1)\mu_1 N_1^2 L_a \end{aligned}\right\} \tag{24}$$

where $E_1 = \Delta\mu_1/\mu_1$ and $L_S \equiv N^2 L_a$. Now a core of permeability μ_2 is to be measured with an error, E_2, no greater than E_1. If we consider the error to be held constant, i. e., $E_1 = E_2$, then from eq (22), we have

$$N_2 = \frac{\mu_1}{\mu_2} N_1. \tag{25}$$

We now investigate the value of L_{m_2}, i. e., the measured inductance of coil 2, to satisfy the constant-error condition. As in eq (24), we have

$$\left.\begin{aligned} L_{m_2} &= (1 + E_2)\mu_2 N_2^2 L_a \\ &= (1 + E_1)\mu_1^2 N_1^2 L_a \frac{1}{\mu_2}. \end{aligned}\right\} \tag{26}$$

Dividing eq (26) by eq (24), we have, solving for L_{m_2}:

$$L_{m_2} = \frac{\mu_1}{\mu_2} L_{m_1}. \tag{27}$$

This is the value of measured inductance necessary in sample 2 for the error $\Delta\mu_2/\mu_2$ to equal the error $\Delta\mu_1/\mu_1$.

If permeability μ_2 of core 2 is assumed to be less than that of core 1, it is noted that for the errors from violation of uniform, thin current-sheet assumptions to be the same, coil 2 must possess an inductance larger than that of coil 1 by the ratio of the two permeabilities.

Up to this point only errors in the determination of high-frequency permeability caused by violating current-sheet assumptions have been considered. Errors, however, are also introduced by the presence of capacitance between the windings of the coil. In particular, if the inductance, L, of a coil, and its distributed capacitance, C, may be regarded as lumped inductance and capacitance in parallel, the effective inductance of the coil is given by

$$L_e = \frac{L}{1 - \omega^2 LC} = \frac{1}{1 - (f/f_0)^2}, \tag{28}$$

$$f_0 = \frac{1}{2\pi\sqrt{LC}}, \tag{29}$$

where L_e is effective inductance; L is actual inductance; f_0 is the self-resonant frequency of the coil. In order for the measurement to remain reasonably free from errors caused by distributed capacitance, as shown in eq (29), the measurement frequency, f, must be much lower than the natural resonant frequency, f_0.

Considering the case discussed above, wherein the error $\Delta\mu/\mu$ for cores of permeability μ_1 and μ_2 is to be constant, μ_2 being less than μ_1, it is noted that coil 2 must have a higher inductance than coil 1. However, in order to have this larger inductance, more turns had to be placed on core 2 than on core 1, resulting in an increase of capacitance for coil 2. Consequently, coil 2 will have a lower natural resonance frequency f_0 than coil 1 because of both higher inductance and capacitance. It thus appears that a smaller measurement error will result for a higher permeability at a given frequency.

It has been shown by numerous authors [2] that the effects of distributed capacitance may be corrected for by measuring the self-inductance at several frequencies. It must be pointed out, however, that this procedure assumes a constant self-inductance and thus a constant permeability with frequency. If this, however, be known a priori, a measurement at a frequency where errors from residual capacitance may be neglected would suffice.

8. Experimental Evaluation of Theoretical Corrections

As noted previously, attempts have been made to correct the approximate eq (1) for the assumptions made.

In the formulation already described, it is inferred that there are no leakage fields existing beyond the confines of the coil. If this were so, then the correction ΔL_a in eq (6) would equal the correction ΔL_m. From eq (7), we see that

$$\Delta L_a = CN^2. \tag{30}$$

It has been shown in eq (14) that

$$\Delta\mu = \frac{K_1}{N} + C_1.$$

But we also have from eq (10) and from the identity $L_S = N^2 L_a$,

$$\Delta L_m = \Delta\mu N^2 L_a. \tag{31}$$

From this equation and eq (14), we have

$$\Delta L_m = K_3 N + K_4 N^2. \tag{32}$$

For all but large values of N, ΔL_m is dominated by the term K_3N, and only for very large N is ΔL_m more nearly a function of N^2. Therefore, it may be concluded that eq (30) will apply only at large N where the assumption that a uniform current sheet exists is more nearly valid. However, for high-frequency measurements it is important, as stated, to keep the distributed capacitance down to a minumum value, which is seldom feasible if a constant, uniform current sheet is simultaneously required.

Another correction based on a theoretical approach takes into account the possibility of leakage fields existing, when the core is wound with round wire of finite dimensions. Under such conditions the self-inductance is affected by those lines of flux within the wire and by those linked with each separate turn of wire in addition to those lines of flux within the test core. The correction worked out by Rosa alters the calculated value of inductance L_s. The correction term depends on the pitch and size of wire and may be positive or negative. It is determined by considering the difference in self-inductance and mutual inductance between turns of a coil of round wire of finite dimensions from those of a coil of thin tape.

Rosa's equation for the self-inductance of an air toroid is [4]

$$L = L_S - 2Nl(A+B) \tag{33}$$

$$A = \log_e\left(1.745\,\frac{d}{D}\right), \tag{34}$$

where l is the length of one turn of wire equals $2(h+b-a)$; d is the diameter of the wire used; D is the mean wire spacing (see eq 16); B is the correction from Grover's tables [6] for mutual inductance between turns. We define Rosa's correction term

$$\Delta L_R = -2Nl(A+B). \tag{35}$$

It is noted at this point that if ΔL_R included all of the necessary corrections, it should equal the correction term ΔL_S for an air toroid, (see eq 9). We thus consider a polystyrene core and from the observed data, plot ΔL_S as given by eq (11).

$$\Delta L_S = \frac{\Delta\mu L_S^2}{L_m - \Delta\mu L_S}. \tag{11}$$

If one uses L_s as defined by eq (2) to determine ΔL_S, a plot of ΔL_S (see top curve of fig. 10) as a function of N does not compare favorably with a plot of the Rosa correction term ΔL_R. Furthermore, if we substitute a corrected value of L_S, assuming the current sheet to be a distance $d/2$ from the sample surface, it is noted that the agreement is but slightly improved. Recalling our earlier prediction as to separation of permeability errors into two parts, and

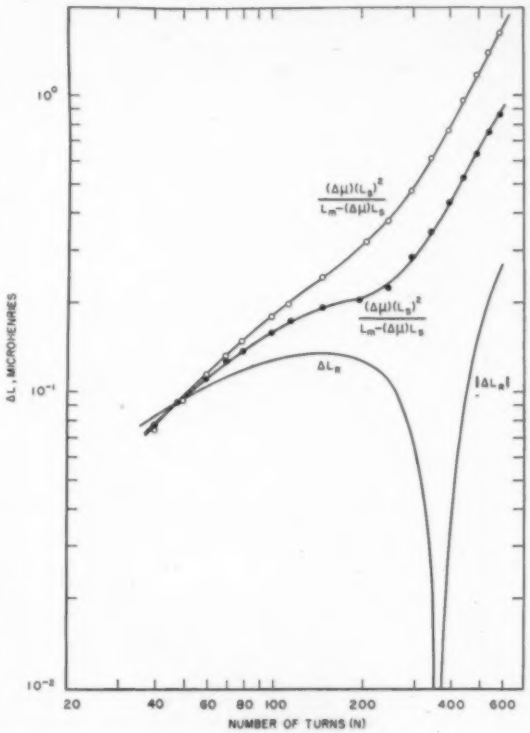

FIGURE 10. *Comparison of Rosa correction term with experimental data.*

ΔL_R is the absolute value of Rosa correction term.

on the basis that ΔL_R takes care of nonuniformity of current sheets only, we calculate ΔL_S by using $\Delta\mu_2$ as shown:

$$\Delta L_S = \frac{\Delta\mu_2 L_S^2}{L_m - \Delta\mu_2 L_S}. \tag{11a}$$

We now plot this equation as a function of N (see fig. 11) and notice that a favorable comparison with Rosa's correction term ΔL_R is obtained.

As a result of eq (10) and (12) and the experimental fact that $\Delta\mu$ is not a function of μ, we find that

$$\Delta L_S = \frac{\Delta\mu L_S}{\mu}. \tag{36}$$

Thus the values of ΔL_S for two cores of permeabilities, μ_1 and μ_2, are related by the equation

$$\Delta L_{S_2} = \frac{\mu_1}{\mu_2}\,\Delta L_{S_1}. \tag{37}$$

While Rosa's correction term is strictly valid only for an air toroid, it was pointed out earlier that in the calculation for an air toroid it takes the place of our correction term ΔL_S. In comparing its possible

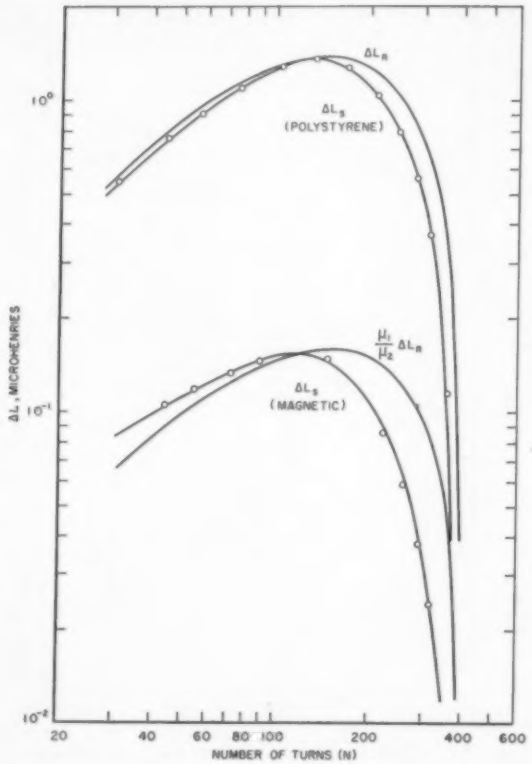

FIGURE 11. *Comparison of Rosa correction term with experimental data.*

validity for a coil with arbitrary permeability μ, we thus let it take the place of ΔL_{S_1} in eq (37), with μ_1 now equal to unity. The two curves, that is, ΔL_S for a magnetic core and ΔL_R divided by that core's permeability, are shown plotted versus N as the bottom curves on figure 11. The fairly good agreement obtained indicates a possibility of estimating a value of the permeability for a magnetic core by using Rosa's correction term in the manner indicated.

We have now shown the effects of two possible calculations of correction terms. Referring once more to eq (3),

$$\Delta\mu=\Delta\mu_1+\Delta\mu_2 \tag{3}$$

it may be stated that the error $\Delta\mu_1$ is indeed associated with violation of the assumption that the current sheet is adjacent to the toroidal sample. As shown, this may be accounted for by eq (7) or (2a), provided one knows the distance x from the face of the test sample to the location of the effective current sheet. The value of $\Delta\mu_2$ may be associated with the error caused by the presence of leakage fields beyond the confines of the coil. This error may be estimated, at least for an air coil and within limits for any coil, by applying the Rosa correction term.

9. Permeability Measurement by Air-Coil Substitution

Another method mentioned earlier for measuring high-frequency permeability utilizes the measured inductance of a coil wound on a nonmagnetic core. This coil is to have the same physical dimensions as the magnetic core whose permeability is to be determined and wound with the same number of turns and wire. For the permeability, one then takes

$$\mu_e=\frac{(L_m)_m}{(L_m)_a}. \tag{38}$$

However, by referring to eq (8) and (12), we have

$$(L_m)_m=\mu(L_S+\Delta L_{S_m}) \tag{39}$$

$$(L_m)_a=(1)(L_S+\Delta L_{S_a}), \tag{40}$$

and eq (38) becomes

$$\mu_e=\frac{\mu(L_S+\Delta L_{S_m})}{L_S+\Delta L_{S_a}}. \tag{41}$$

Only when $\Delta L_{S_a}=\Delta L_{S_m}$ will this ratio reduce to μ. On the basis of the experimental evidence and eq (10) and (12), one obtains

$$\Delta L_{S_m}=\frac{\Delta\mu}{\mu}L_S \tag{42}$$

$$\Delta L_{S_a}=\Delta\mu L_S \tag{43}$$

Equation (41) becomes, upon substituting the results of eq (42) and (43),

$$\mu_e=\frac{\mu(1+\Delta\mu/\mu)}{1+\Delta\mu} \tag{44}$$

As $\Delta\mu\neq\Delta\mu/\mu$, unless $\mu=1$, μ_{eff} will always lead to values on the low side, the absolute error becoming larger for higher permeability. A practical difficulty that may be encountered is that it is extremely difficult to wind coils exactly alike, and thus further errors might be introduced.

10. Experimental Details

The magnetic cores used for this investigation were of powdered iron. Field strengths above 1 oersted are usually required to effectively change the permeability of such cores; the field strengths employed were below 0.01 oersted in all cases. Care was taken to assure that changes in the field intensity by factors as large as 2 to 1 would not change the coil inductance by even as much as 1 part in 10,000.

The frequency used was 50 kc. The coil with the highest reactance used in this investigation was measured in the range from 1 to 50 kc. The effective inductance showed a change of less than 1 part in 10,000, which could be ascribed to capacitance effects.

The bridges used for the measurements were two high-quality Maxwell-type inductance bridges designed at Bell Telephone Laboratories. Connections between the unknown terminals of the bridges and the coils were made in such a manner that proximity effects from neighboring objects were held to a negligible minimum and that the lead inductance could be accounted for.

The true initial permeabilities of the magnetic cores were determined by a specially calibrated radio-frequency permeameter used in conjunction with calibrated capacitors.

In order to apply the windings as uniform and tight as possible without any crossovers whatever and no visible injury to the insulation, a toroidal coil winder capable of applying this type of single-layer winding was employed. Figure 1 shows an example of such windings.

WASHINGTON, January 7, 1954.

11. Summary

The errors encountered in high-frequency magnetic measurements have been discussed mostly from the viewpoint of violation of uniform, thin current-sheet assumptions. The absolute error in permeability has been shown to be independent of the permeability of the material tested, and its dependence on the spacing between turns has been formulated. The adequacy of certain correction terms suggested by other authors have been investigated. It has been shown that an approximate correction may be made utilizing a combination of several such terms, provided the extension of the leakage flux into space may be estimated.

12. References

[1] V. E. Legg, Magnetic measurements at the low flux densities using the A. C. bridge, Bell System Tech. J. **16,** 39 (1936).
[2] L. Hartshorn, Radio frequency measurements by bridge and resonance methods, p. 231 (Chapman & Hall, Ltd., London, 1941).
[3] P. H. Haas, A radio-frequency permeameter, J. Research NBS **51,** 221 (1953) RP2454.
[4] Formulas and tables for the calculation of mutual and self-inductance (Revised), NBS Sci. Paper 169, p. 125 (1912).
[5] International critical tables, vol. VI (1929).
[6] F. W. Grover, Inductance calculations, p. 148 (Van Nostrand & Co.).

294330—54——2

Journal of Research of the National Bureau of Standards Vol. 52, No. 6, June 1954 Research Paper 2502

Thermodynamic Functions for Carbon Dioxide in the Ideal Gas State

Harold W. Woolley

The thermodynamic functions C_p°/R, $(H^\circ - E_0^\circ)/RT$, $-(F^\circ - E_0^\circ)/RT$, and S°/R for carbon dioxide in the ideal gas state are given from 50° to 5,000° K, based on the latest spectroscopic data.

1. Introduction

Thermodynamic functions for carbon dioxide were computed by Kassel [1],[1] whose values were corrected to more recent values of the physical constants and extended from 3,500° to 5,000° K by Wagman, et al. [2]. Values by H. L. Johnston have been given by Ellenwood, Kulik, and Gay [3]. A subsequent calculation by Gratch [4] differed appreciably, showing a somewhat different behavior at elevated temperature. With improved spectroscopic constants, it has become possible to carry out a recalculation of greater accuracy. Values obtained for the specific heat in the main are intermediate between the previous calculations.

2. Spectroscopic Constants

The spectroscopic constants used for $C^{12}O_2^{16}$ with the vibrational energy formula are $\nu_1 = 1342.86$ cm^{-1}, $\nu_2 = 667.30$ cm^{-1}, $x_{11} = -2.20$ cm^{-1}, $x_{22} = -0.75$ cm^{-1}, $x_{12} = 3.76$ cm^{-1}, and $x_{11} = 1.03$ cm^{-1}, given by Taylor, Benedict, and Strong [5], with $\nu_3 = 2349.15$ cm^{-1}, $x_{13} = -18.54$ cm^{1}, and $x_{23} = -12.48$ cm^{-1}, as indicated in a private communication from Benedict, and $x_{33} = -12.46$ cm^{-1}, chosen to fit the observed 11496.5 cm^{-1} at $v_3 = 5$. The rotational constant B_0 was taken as 0.39038 cm^{-1}, received in a private communication from Earle K. Plyler, of the Bureau, as a preliminary value. For the stretching constant D_0, a theoretical value of 0.132×10^{-6} cm^{-1} was used on the ground that it was not ruled out by a preliminary empirical value of $(0.165 \text{ cm}^{-1} \pm 0.02 \text{ cm}^{-1}) \times 10^{-6}$ of Plyler. For rotational-vibrational interaction, the values $\alpha_1 = 0.00056$ cm^{-1} and $\alpha_2 = -0.00062$ cm^{-1} were given by Herzberg [6], and $\alpha_3 = 0.0031$ cm^{-1} was obtained from Plyler's newer data. The Fermi resonance constant W_0 was taken as 51.01 cm^{-1}, correcting for a $\sqrt{2}$ factor in the publication of Taylor, Benedict, and Strong.

3. Method of Calculation

The calculation was performed by computing the harmonic-oscillator rigid-rotator thermodynamic functions and adding corrections for deviations from this simple model. Corrections were made for anharmonicity, rotational-vibrational interaction, azimuthal quantum effects, rotational stretching, and Fermi resonance. The first three of these corrections are an extension of a method indicated by Mayer and Mayer [7] for diatomic molecules and used for polyatomic molecules by Stockmayer, Kavanagh, and Mickley [8]. The general formulas as now extended are given in another paper [9]. The constants as given in section 2 are in form for this use, with the exception of ν_2, for which the derived formulas require $\omega_2 = \nu_2 - x_{11}$. In the present application to carbon dioxide the anharmonicity formulas were carried through the second-power terms (including cross products) but not through the third-power terms. The rotational-vibrational interaction was carried through the first power, second-power terms being omitted. The azimuthal $B + g_{22}$ or $B + x_{11}$ terms were carried through the second power, third-power terms being omitted. No correction was made for the small splitting associated with azimuthal l-type doubling, on the basis that its effect is entirely negligible. Cross-product terms between azimuthal and rotational-vibrational interaction, between azimuthal and anharmonic, and between rotational-vibrational interaction and anharmonic constants were found to have small effect below 1,500° K and were omitted throughout. It may be supposed that a complete and exact representation of the energy levels would include corresponding interaction terms, so that the lack of such empirical constants may help justify the omission of related cross-product terms. In addition, the considerable uncertainty in many of the available constants provides a greater uncertainty in the resulting table than the effects of the omitted cross-product terms. The procedure used in calculating the effect of Fermi resonance and the results of that calculation are given in a separate publication [10]. No corrections were introduced for either vibrational or rotational cutoff.

The correction quantities contributing to the thermodynamic functions were calculated for $C^{12}O_2^{16}$ at 300°, 600°, 1,000°, 1,200°, 1,500°, 2,000°, 3,000°, 4,000°, and 5,000° K, and for the specific heat at several lower temperatures. The harmonic oscillator contributions were computed at closer intervals and adjusted to frequencies representing a weighted average according to the relative abundance of the isotopes. The molecular weight and rotational constant were similarly taken for the natural isotopic mixture. The values of C_p°/R interpolated to the intervals given in the final table

[1] Figures in brackets indicate literature references at the end of this paper.

allowed tabular integration to give the other functions, duplicating the directly calculated values to about one in the fourth decimal place up to 1,000° K and satisfactorily at higher temperatures. $S°/R$ is given as the sum of $(H°-E_0°)/RT$ and $-(F°-E_0°)/RT$, as tabulated. The translational contribution to the latter is (5/2) ln T+(3/2) ln M+ln $(2\pi^{3/2})\ k^{5/2}/(h^3N_0^{3/2}P_0)$, evaluated as (5/2) ln T+2.0121, based on M=44.01 for molecular weight and values for the physical constants. The value used for hc/k is 1.43847 cm deg.

4. Thermodynamic Functions

The thermodynamic functions calculated for carbon dioxide include heat capacity, enthalpy, free energy, and entropy for the standard ideal gas state. The properties are listed in the dimensionless forms $C_p°/R$, $(H°-E_0°)/RT$, $-(F°-E_0°)/RT$, and $S°/R$ in table 1. The corrections added to the harmonic-oscillator rigid-rotator functions based on ν_1, ν_2, and ν_3, to obtain $C_p°/R$, $(H°-E_0°)/RT$, and $-(F°-E_0°)/RT$ for $C^{12}O_2^{16}$, are given in table 2.

The amounts by which the functions for the natural mixture (omitting entropy of isotope mixing and of nuclear spin) exceed those for $C^{12}O_2^{16}$ are given in table 3.

Although it was desired to produce an accurate table of thermodynamic functions, the new values have considerable uncertainty. Using some arbitrarily assigned uncertainties for some of the constants, rough estimates of the magnitude of the uncertainties for the functions $C_p°/R$, $(H°-E_0°)/RT$, and $-(F°-E_0°)/RT$ are listed in table 4 for 300°, 1,000°, 3,000°, and 5,000° K. Uncertainties of 0.1 cm^{-1} for ν_2 and x_{22} have been taken arbitrarily and may be too small. A 2-percent uncertainty in the Fermi effect as computed is consistent with the order of magnitude of the 1.3−cm^{-1} difference in different values of W_0. For α_1 and α_2 Herzberg

TABLE 1. *"Ideal gas" thermodynamic properties of* CO_2 *(natural isotopic mixture)*

T	$C_p°/R$	$(H°-E_0°)/RT$	$-(F°-E_0°)/RT$	$S°/R$	T	$C_p°/R$	$(H°-E_0°)/RT$	$-(F°-E_0°)/RT$	$S°/R$	T	$C_p°/R$	$(H°-E_0°)/RT$	$-(F°-E_0°)/RT$	$S°/R$
°K					°K					°K				
50	3.5001	3.4963	15.5922	19.0885	550	5.5371	4.3602	24.3981	28.7583	1,250	6.826	5.453	28.415	33.868
60	3.5002	3.4969	16.2297	19.7266	560	5.5691	4.3815	24.4769	28.8584	1,300	6.872	5.506	28.630	34.136
70	3.5006	3.4974	16.7688	20.2662	570	5.6006	4.4026	24.5546	28.9572	1,350	6.913	5.558	28.839	34.397
80	3.5020	3.4979	17.2358	20.7337	580	5.6315	4.4235	24.6314	29.0549	1,400	6.952	5.607	29.042	34.649
90	3.5055	3.4985	17.6479	21.1464	590	5.6618	4.4443	24.7072	29.1515	1,450	6.988	5.654	29.239	34.893
100	3.5128	3.4995	18.0165	21.5160	600	5.6915	4.4648	24.7820	29.2468	1,500	7.021	5.699	29.432	35.131
110	3.5249	3.5013	18.3501	21.8514	610	5.7207	4.4852	24.8560	29.3412	1,600	7.082	5.783	29.802	35.585
120	3.5432	3.5039	18.6549	22.1588	620	5.7494	4.5053	24.9291	29.4344	1,700	7.134	5.861	30.155	36.016
130	3.5680	3.5079	18.9355	22.4434	630	5.7775	4.5253	25.0013	29.5266	1,800	7.180	5.933	30.492	36.425
140	3.5995	3.5133	19.1957	22.7090	640	5.8052	4.5451	25.0728	29.6179	1,900	7.222	6.000	30.815	36.815
150	3.6372	3.5202	19.4383	22.9585	650	5.8324	4.5647	25.1434	29.7081	2,000	7.258	6.062	31.124	37.186
160	3.6804	3.5289	19.6657	23.1946	660	5.8591	4.5841	25.2132	29.7973	2,100	7.291	6.120	31.421	37.541
170	3.7282	3.5392	19.8800	23.4192	670	5.8853	4.6033	25.2823	29.8856	2,200	7.320	6.174	31.707	37.881
180	3.7800	3.5511	20.0826	23.6337	680	5.9110	4.6223	25.3506	29.9729	2,300	7.347	6.224	31.983	38.207
190	3.8347	3.5646	20.2750	23.8396	690	5.9363	4.6412	25.4183	30.0595	2,400	7.371	6.271	32.249	38.520
200	3.8916	3.5795	20.4582	24.0377	700	5.9611	4.6599	25.4852	30.1451	2,500	7.393	6.316	32.506	38.822
210	3.9502	3.5957	20.6332	24.2289	710	5.9855	4.6784	25.5514	30.2298	2,600	7.414	6.358	32.754	39.112
220	4.0097	3.6132	20.8009	24.4141	720	6.0094	4.6967	25.6170	30.3137	2,700	7.433	6.397	32.995	39.392
230	4.0695	3.6317	20.9619	24.5936	730	6.0329	4.7149	25.6819	30.3968	2,800	7.451	6.435	33.228	39.663
240	4.1296	3.6512	21.1169	24.7681	740	6.0559	4.7328	25.7461	30.4789	2,900	7.468	6.470	33.455	39.925
250	4.1892	3.6716	21.2663	24.9379	750	6.0786	4.7506	25.8098	30.5604	3,000	7.484	6.503	33.675	40.178
260	4.2484	3.6926	21.4107	25.1033	760	6.1009	4.7682	25.8728	30.6410	3,100	7.499	6.535	33.888	40.423
270	4.3068	3.7143	21.5505	25.2648	770	6.1228	4.7857	25.9353	30.7210	3,200	7.513	6.566	34.096	40.662
280	4.3643	3.7365	21.6860	25.4225	780	6.1442	4.8030	25.9971	30.8001	3,300	7.526	6.595	34.299	40.894
290	4.4208	3.7591	21.8175	25.5766	790	6.1653	4.8201	26.0584	30.8785	3,400	7.539	6.622	34.496	41.118
300	4.4763	3.7821	21.9453	25.7274	800	6.1860	4.8370	26.1192	30.9562	3,500	7.551	6.649	34.688	41.337
310	4.5307	3.8054	22.0697	25.8751	810	6.2064	4.8538	26.1794	31.0332	3,600	7.563	6.674	34.876	41.550
320	4.5840	3.8289	22.1909	26.0198	820	6.2264	4.8704	26.2390	31.1094	3,700	7.575	6.698	35.059	41.757
330	4.6361	3.8525	22.3091	26.1616	830	6.2460	4.8869	26.2982	31.1851	3,800	7.586	6.721	35.238	41.959
340	4.6871	3.8763	22.4244	26.3007	840	6.2653	4.9032	26.3568	31.2600	3,900	7.597	6.743	35.413	42.156
350	4.7371	3.9002	22.5371	26.4373	850	6.2843	4.9193	26.4149	31.3342	4,000	7.608	6.765	35.584	42.349
360	4.7859	3.9241	22.6473	26.5714	860	6.3029	4.9353	26.4725	31.4078	4,100	7.618	6.786	35.751	42.537
370	4.8335	3.9481	22.7552	26.7033	870	6.3212	4.9511	26.5297	31.4808	4,200	7.628	6.806	35.915	42.721
380	4.8801	3.9720	22.8608	26.8328	880	6.3392	4.9668	26.5863	31.5531	4,300	7.638	6.825	36.075	42.900
390	4.9257	3.9959	22.9643	26.9602	890	6.3569	4.9823	26.6426	31.6249	4,400	7.647	6.843	36.233	43.076
400	4.9704	4.0197	23.0657	27.0854	900	6.3742	4.9977	26.6983	31.6960	4,500	7.657	6.861	36.387	43.248
410	5.0140	4.0434	23.1653	27.2087	910	6.3913	5.0129	26.7536	31.7665	4,600	7.666	6.879	36.538	43.417
420	5.0566	4.0670	23.2630	27.3300	920	6.4080	5.0280	26.8085	31.8365	4,700	7.676	6.896	36.686	43.582
430	5.0983	4.0905	23.3590	27.4495	930	6.4244	5.0429	26.8629	31.9058	4,800	7.685	6.912	36.831	43.743
440	5.1392	4.1139	23.4533	27.5672	940	6.4406	5.0577	26.9169	31.9746	4,900	7.694	6.928	36.974	43.902
450	5.1792	4.1371	23.5460	27.6831	950	6.4565	5.0723	26.9705	32.0428	5,000	7.702	6.943	37.114	44.057
460	5.2183	4.1602	23.6372	27.7974	960	6.4721	5.0868	27.0237	32.1105					
470	5.2566	4.1831	23.7269	27.9100	970	6.4874	5.1012	27.0765	32.1777					
480	5.2942	4.2059	23.8152	28.0211	980	6.5025	5.1154	27.1289	32.2443					
490	5.3310	4.2285	23.9022	28.1307	990	6.5173	5.1295	27.1809	32.3104					
500	5.3671	4.2509	23.9878	28.2387	1,000	6.5318	5.1434	27.2325	32.3759					
510	5.4024	4.2731	24.0722	28.3453	1,050	6.601	5.211	27.485	32.696					
520	5.4371	4.2952	24.1553	28.4506	1,100	6.664	5.276	27.729	33.005					
530	5.4711	4.3170	24.2374	28.5544	1,150	6.723	5.337	27.965	33.302					
540	5.5044	4.3387	24.3183	28.6570	1,200	6.776	5.396	28.193	33.589					

TABLE 2. *Corrections added in obtaining table 1, due to* x_{ii}, x_{ij}, α_i, x_{ll}, W_0, *and* $\Delta\nu_2=\nu_2-\omega_2$

T	C_p°/R	H°/RT	$(-F^\circ/RT)$
°K			
50	0.00012	−0.0037	0.0039
100	.00016	−.0018	.0021
150	−.00026	−.0012	.0014
200	−.00072	−.0010	.0011
250	−.0004	−.0009	.0009
300	−.0001	−.0008	.0007
400	+.0006	−.0006	.0006
500	.0018	−.0002	.0005
600	.0038	+.0003	.0005
700	.0071	.0010	.0006
800	.0112	.0020	.0008
900	.0161	.0033	.0011
1,000	.0213	.0048	.0015
1,200	.0325	.0085	.0027
1,500	.0495	.0150	.0053
2,000	.0775	.0271	.0112
2,500	.1055	.0400	.0187
3,000	.1338	.0533	.0272
3,500	.1631	.0669	.0364
4,000	.1935	.0808	.0462
4,000	.2252	.0951	.0565
5,000	.2584	.1097	.0673

TABLE 3. *Amounts by which the thermodynamic functions for* CO_2 *for the natural isotopic mixture exceed those for* $C^{12}O^{16}_2$

[The entropy of mixing of the different isotopic molecules and nuclear-spin entropies have been omitted.]

T	C_p°/R	$(H^\circ-E_0^\circ)/RT$	$-(F^\circ-E_0^\circ)/RT$	S°/R
°K				
100	0.00006	0.00001	0.00092	0.00093
200	.0007	.0002	.0010	.0012
300	.0009	.0004	.0011	.0015
400	.0009	.0005	.0013	.0018
500	.0008	.0006	.0014	.0020
600	.0008	.0006	.0015	.0021
700	.0008	.0007	.0016	.0023
800	.0008	.0007	.0017	.0024
900	.0007	.0007	.0018	.0025
1,000	.0007	.0007	.0018	.0025
1,200	.0006	.0007	.0019	.0026
1,500	.0005	.0007	.0021	.0028
2,000	.0003	.0006	.0023	.0029
2,500	.0002	.0005	.0024	.0029
3,000	.0002	.0005	.0025	.0030
3,500	.0001	.0004	.0026	.0030
4,000	.0001	.0004	.0026	.0030
4,500	.0001	.0003	.0027	.0030
5,000	.0001	.0003	.0027	.0030

indicates an uncertainty of ± 0.00010 cm^{-1}, or about one-sixth of their values. For each temperature the sum of the separate uncertainties has been obtained. It is to be recognized that the actual uncertainty is probably considerably greater in view of the arbitrary values assigned and the neglect of part of the constants in making these estimates.

A comparison of table values with the experimental values reported by Masi and Petkof follows:

Temperature	C_p°/R (calculated)	C_p°/R (experimental)
°K		
243.16	4.1483	4.148
273.16	4.3250	4.324
323.16	4.6005	4.604
363.16	4.8009	4.804

TABLE 4. *Partial list of uncertainties*

Constants	C_p/R	H/RT	$(-F/RT)$
Temperature 300° K			
ν_2	0.0002	0.0001	0.00004
x_{22}	.0002	.00006	.00002
W_0	.00002	.000005	.000001
α	.0003	.00007	.00002
Sum	0.0007	0.0002	0.00008
Temperature 1,000° K			
ν_2	0.00004	0.0001	0.0002
x_{22}	.002	.0007	.0004
W_0	.00007	.00004	.00002
α	.001	.0006	.0003
Sum	0.003	0.0015	0.001
Temperature 3,000° K			
ν_2	0.000006	0.00004	0.0003
Linear x_{22}	.006	.003	.002
Quadratic x_{22}	.001	.0003	.0001
Cubic x	.001	.0002	.0001
W_0	.0002	.0001	.0001
α	.004	.002	.002
Sum	0.012	0.006	0.005
Temperature 5,000° K			
ν_2	0.000002	0.00003	0.0003
Linear x_{22}	.01	.005	.004
Quadratic x_{22}	.003	.0009	.0004
Cubic x	.0047	.0012	.0004
W_0	.0004	.0002	.0002
α	.007	.003	.003
Sum	0.025	0.01	0.008

Values of coefficients of change of thermodynamic properties with respect to small changes of spectroscopic constants are given in tables 5, 6, and 7, for the anharmonicity, rotation-vibration interaction, and the azimuthal $B+x_{ll}$ constants. If ensuing revisions of these constants involve only small changes, the corresponding revised thermodynamic functions can be adequately approximated with small proportionate changes.

TABLE 5. *Coefficients for change of* C_p°/R *with change of spectroscopic constants*

Values given are $10^2 c_i d(C_p^\circ/R)/dc_i$.

T	$c_i=x_{11}$	x_{22}	x_{33}	x_{12}	x_{13}	x_{23}	α_1	α_2	α_3	$B+x_{ll}$
°K										
300	0.008	1.26	0	−0.19	0	0.012	0.10	−1.57	0.013	−3.6
600	.59	6.9	.09	−3.6	.45	2.6	.70	−3.9	.92	−5.4
1,000	2.3	13.8	1.78	−9.8	3.9	14.3	1.42	−6.6	3.54	−8.4
1,200	3.2	17.2	3.4	−12.6	6.2	21	1.74	−7.9	4.8	−9.9
1,500	4.5	22	6.3	−16.8	9.9	31	2.2	−9.9	6.5	−12.0
2,000	6.5	31	11.6	−23	15.9	48	3.0	−13.3	9.1	−15.4
3,000	10.3	49	23	−36	28	83	4.5	−20	14.0	−21
4,000	14.0	69	35	−50	41	122	5.9	−27	18.8	−26
5,000	17.9	92	49	−64	55	165	7.4	−33	23	−30

TABLE 6. *Coefficients for change of* $(H^\circ - E_0^\circ)/RT$ *with change of spectroscopic constants*

Values are $10^2\, c_i d[(H^\circ - E_0^\circ)/RT]/dc_i$.

T	$c_i = x_{11}$	x_{22}	x_{33}	x_{12}	x_{13}	x_{23}	α_1	α_2	α_3	$B+x_{11}$
°K										
300	0.001	0.22	0	−0.022	0	0.001	0.015	−0.45	0.001	−1.48
600	.105	2.1	.009	−.82	.056	.38	.20	−1.61	.161	−3.0
1,000	.64	5.4	.30	−3.2	.80	3.4	.55	−3.1	.98	−4.5
1,200	1.00	7.1	.67	−4.5	1.51	5.8	.72	−3.8	1.51	−5.3
1,500	1.57	9.6	1.51	−6.6	2.8	9.9	.97	−4.8	2.3	−6.4
2,000	2.5	13.8	3.4	−9.9	5.4	17.4	1.37	−6.5	3.7	−8.3
3,000	4.5	23	8.0	−16.6	10.9	33	2.2	−9.9	6.3	−11.7
4,000	6.4	32	13.2	−23	16.8	51	2.9	−13.2	8.9	−14.7
5,000	8.3	41	18.9	−30	23	69	3.6	−16.6	11.3	−17.4

TABLE 7. *Coefficients for change of* $-(F^\circ - E_0^\circ)/RT$ *with change of spectroscopic constants.*

Values given are $10^2\, c_i d[-(F^\circ - E_0^\circ)/RT]/dc_i$.

T	$c_i = x_{11}$	x_{22}	x_{33}	x_{12}	x_{13}	x_{23}	α_1	α_2	α_3	$B+x_{11}$
°K										
300	0	0.039	0	−0.002	0	0	0.002	−0.136	0	−0.60
600	.018	.70	.001	−.188	.007	.058	.060	−.81	.029	−2.1
1,000	.182	2.5	.049	−1.13	.169	.84	.24	−1.98	.280	−4.0
1,200	.33	3.7	.134	−1.83	.38	1.67	.36	−2.6	.51	−4.9
1,500	.61	5.5	.37	−3.1	.85	3.40	.55	−3.6	.93	−6.2
2,000	1.20	8.9	1.05	−5.4	2.0	7.3	.88	−5.2	1.80	−8.3
3,000	2.6	16.1	3.3	−10.7	5.2	17.3	1.59	−8.4	3.8	−12.3
4,000	4.2	24	6.2	−16.4	9.2	29	2.3	−11.7	6.0	−16.1
5,000	5.8	32	9.8	−22	13.5	43	3.0	−15.1	8.2	−19.7

5. References

[1] L. S. Kassel, J. Am. Chem. Soc. **56,** 1838 (1934).
[2] Selected values of chemical thermodynamic properties, series III, National Bureau of Standards (June 30, 1948).
[3] F. O. Ellenwood, N. Kulik, and N. R. Gay, Engineering Experiment Station Bulletin No. 30 (Cornell University, October 1942).
[4] S. Gratch, Trans. ASME **71,** 897 (1949).
[5] J. H. Taylor, W. S. Benedict, and J. Strong, J. Chem. Phys. **20,** 1884 (1952).
[6] G. Herzberg, Molecular spectra and molecular structure, II infrared and Raman spectra of polyatomic molecules, p. 395 (Van Nostrand Co., Inc., New York, N. Y., 1945).
[7] J. E. Mayer and M. G. Mayer, Statistical mechanics, p. 162 (John Wiley & Sons, Inc., New York, N. Y., 1940).
[8] W. H. Stockmayer, G. M. Kavanagh, and H. S. Mickley, J. Chem. Phys. **12,** 408 (1944).
[9] H. W. Woolley, J. Research NBS **53,** (1954).
[10] H. W. Woolley, J. Research NBS **53,** (1954).
[11] J. F. Masi and B. Petkof, J. Research NBS **48,** 179 (1952) RP2303.

WASHINGTON, October 16, 1953.

Journal of Research of the National Bureau of Standards Vol. 52, No. 6, June 1954 Research Paper 2503

Optical Spectroscopic Determination of Hydrogen Isotopes in Aqueous Mixtures

Herbert P. Broida, Harold J. Morowitz,[1] and Margaret Selgin

Extension of the optical spectroscopic method of isotope analysis of gaseous mixtures of hydrogen and deuterium to mixtures of water and heavy water provides a direct method for determining the total water content of materials. A determination can be made on a sample of less than 0.1 milliliter in less than 10 minutes to an accuracy of a few percent. Using a sample of at least 1 milliliter, an accuracy of the order of 0.1 percent is obtained in an hour or less. This paper describes the system and the investigation of optimum operating conditions and effect of variations in operating conditions on precision and accuracy of measurement, as well as limitations of the technique. A sample of blood or serum can be measured directly almost as easily as one of distilled water. The optical spectroscopic method can be used to determine the water content of most materials, whether in the solid, liquid, or gas phase.

1. Introduction

Following initial work on an optical spectroscopic analysis of gaseous mixtures of hydrogen and deuterium [1, 2],[2] a similar technique was tried with mixtures of water and heavy water. A preliminary study [3] indicated that it was possible to carry out such analyses to an accuracy of better than 3 percent. The work discussed in the present paper represents an extension of the preliminary study in an effort to improve both the precision and the range and to determine present limitations of the analysis. A detailed study was made to determine the influence of operating variables on precision and accuracy of measurement in order to find the optimum operating conditions. In these studies the following accuracy was obtained: (a) 0.1 percent of the intensity ratio, in the isotope ratio range 0.01 to 1.0; (b) 1 percent, in the range 0.00015 to 0.01 (see table 5).

In addition to the above the rather practical problems of developing the method into a routine analytical technique were taken into consideration. For this reason efforts were made to achieve a rapid analysis, and operating conditions were viewed with the possibility of constructing a simple flow system and optical system for routine use. Several types of routine measurements were made concurrently with the study of the technique.

The technique used is as follows: The vapor from an aqueous sample containing a mixture of H_2O and D_2O is pumped through a tube where a high-frequency electrodeless discharge is maintained. The light emitted from the discharge tube contains lines of the Balmer series of hydrogen and deuterium with a very small amount of background radiation. The emitted light is dispersed by a monochromator, and the relative intensities of the β lines of the Balmer series of hydrogen and deuterium are recorded and measured. The ratio of the intensities of the two lines is a monotonic function of the relative concentration of the isotopes, and to a high degree of accuracy is equal to the ratio of the isotope concentrations. For precise work the measurement is a relative, rather than an absolute one, in that the relationship between intensity ratio and concentration ratio is obtained from calibration curves taken on standard samples whose compositions are determined by independent measurements.

The statistical terms [4, 5] used in this report are defined as follows: "Precision" refers to the variation encountered during readings taken in close succession under identical conditions. "Reproducibility" refers to the variation among readings when they are spread over a considerable time period. It is not a fixed quantity but depends somewhat on the time interval and the history of the apparatus in that interval. "Accuracy" refers to the variation of the measured concentration from the true value and is determined from the precision and reproducibility of the measurements and from the accuracy of the calibrated samples. The relationship between reproducibility and time determines how frequently it is necessary to take calibration points. These factors are all dependent on the stability of operating conditions.

The above variations are expressed either as standard deviation or as the coefficient of variation. These terms apply either for single measurements or for averages. As the standard deviation of the average is dependent on the number of readings taken, this value is most useful when compared to other sets of the same number of readings. For the purposes of this study, all standard deviations of the average refer to sets of 10 readings.

Stability of this system may be viewed in the following manner. Consider the measured ratio of intensities of the DβBalmer line to the HβBalmer line at 4860.0 A and 4861.3 A, respectively, and represent this ratio by D_l/H_l. This ratio is a function of a large number of variables such as the actual concentration ratio in the sample D/H, the tempera-

[1] Present address, National Heart Institute, National Institutes of Health, Bethesda, Md.

[2] Figures in brackets indicate the literature references at the end of this paper.

ture, the pressure, the flow rate, etc., and may be represented in the following fashion:

$$D_1/H_1 = D/H\ f(D/H, X_1, X_2 \ldots X_n),$$

where $X_1 \ldots$ are independent variables. In practice, operating conditions are found such that f is very nearly unity.

A completely stable set of operating conditions is one in which D_1/H_1 is a function of D/H only, and is unaffected by small changes of $X_1, X_2 \ldots X_n$. From a practical point of view, the conditions of stability are that changes of D_1/H_1 due to variations of the X's are small compared with changes due to variations of D/H. Many of the experimental curves shown in the following sections are graphs of the ratio D_1/H_1 as a function of one of the independent variables, with all other variables kept as constant as possible.

The samples employed in these experiments are in all cases aqueous solutions or suspensions in which the solvent is a mixture of hydrogen oxide, H_2O, and deuterium oxide, D_2O. The number used to describe concentrations is, unless otherwise specified, the atom ratio of deuterium to hydrogen, D/H. This figure depends only upon the number of atoms of hydrogen and deuterium in the sample and is independent of the equilibrium between H_2O, HDO, and D_2O.

In taking measurements of isotope ratios the vapor is pumped from the liquid through the discharge tube. This procedure raises two questions; what is the relationship between D/H in the liquid and the vapor and what fractionation (isotope separation) occurs in the flow process? The first question is purely academic with respect to the analysis of water. A given ratio of D to H in the liquid will always give rise to a reproducible ratio in the vapor, and as all measurements are taken relative to calibration samples, the measurement taken is, in all cases, referred back to the liquid.

Because of the difference in vapor pressure between H_2O, HDO, and D_2O, the process of evaporating liquid from samples involves some degree of fractional distillation. This has been investigated experimentally to study the over-all effect and will be discussed in a later section.

The processes occurring in the breakdown of water vapor in the radio-frequency field are imperfectly understood and will be discussed only briefly. The discharge through the water vapor in the tube causes excitation, ionization, and dissociation, giving rise to the following atoms and molecules from a mixture of normal and heavy water:

H, D, HD, H_2, D_2, OH, OD, H_2O_2, D_2O_2, H_2O, HDO, D_2O, HDO_2,

as well as other groupings, most of which may exist as normal, excited, or ionized molecules. The emission spectrum from the discharge contains lines and bands from many of these components. The Balmer lines of hydrogen and deuterium are prominent in this spectrum.

The β line of the Balmer series was chosen because the largest output signal was obtained for this line. This is a result of the product of the actual intensity and the phototube sensitivity being a maximum in the region of the β Balmer line of the hydrogen spectrum. The α lines at 6561.0 A and 6562.8 A for D and H, respectively, also can be used; this pair has the advantage of a somewhat larger separation than the β pair. (1.8 A compared to 1.3 A).

2. Equipment

2.1. Glass Flow System

A glass flow system was employed to provide a steady flow of sample vapor through the discharge tube. A flow system decreases problems of contamination by previous samples and simplifies the preparation of the sample for analysis. The system, shown photographically in figure 1 and schematically in figure 2, consists of the following components:

1. *Sample bottles.* The sample bottles are equipped with an inverted standard taper ground-glass joint so that rapid change of samples can be made.

2. *Sample connectors.* The connectors are standard taper ground-glass joints corresponding to those on the bottles. A special vacuum line (fig. 2) provides a means of evacuating the air from the sample chamber before admitting sample into the main flow system.

3. *Pressure regulator.* In order to vary and control pressure in the discharge tube a parallel network is provided, consisting of a capillary and a continuously variable metal leak valve. In most of the studies described in this paper, the variable metal leak valve was used because fine pressure control and frequent adjustments were necessary. However, for routine measurements a fixed nonmetallic orifice is preferable.

4. *Pressure gage.* To measure pressure in the system, a pressure line connects through stopcocks to various critical locations. Pressure measurement is made by means of a commercial ionization gage, which utilizes alpha particles from a radium source to provide ionization. The gage can be used from pressures of 1μ to 1 cm. Pressures used in this report are gage readings. Absolute pressure of water vapor is found by multiplying by 1.163, the factor supplied by the gage manufacturer.

5. *Discharge tube.* The discharge tube consists of a glass inner cylinder surrounded by a glass water jacket. Water flows through the jacket at a constant rate controlled by a regulator at the tap. Air bubbles in the water, which might affect intensity measurements, are eliminated by an extractor shown at point G in figure 1.

6. *Pumps.* The two main vacuum lines shown in figure 2 connect with independent pumping systems. The left-hand line goes to a trap, single stage oil diffusion pump and forepump while the right-hand line goes only to a trap and mechanical pump. The diffusion pump was used in these investigations because a wide variation in conditions was to be studied.

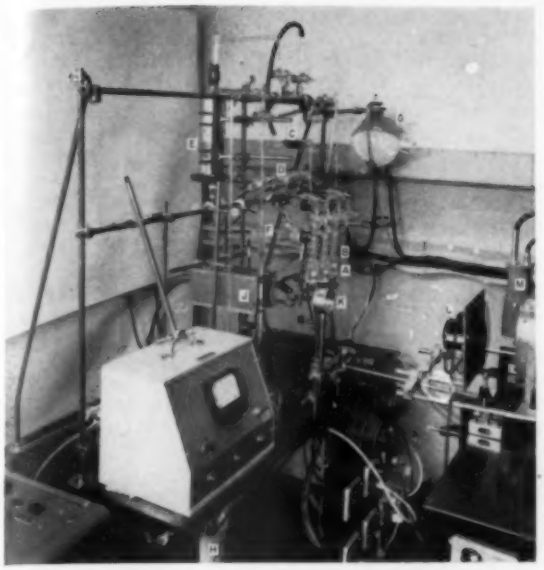

FIGURE 1. *Flow system for* H–D *analysis.*

A, Sample bottles; B, sample connectors; C, metal leak valve; D, glass capillary; E, pressure gage; F, discharge tube; G, bubble extractor; H, trap; J, shield for high-frequency source; K, lens; L, chopper; M, photomultiplier tube.

2.2. High-Frequency Source

The energy necessary to excite the spectrum of the sample was provided by a commercial 150-Mc 150-w oscillator. The energy is carried through a radio-frequency cable, which terminates in a tunable quarter-wavelength tank circuit with antennas held near the discharge tube. This terminal circuit is shown diagramatically in figure 2. A radio-frequency shield (point J in fig. 1) cuts down stray radiation, which might affect other electronic equipment.

2.3. Monochromator

The apparatus used to analyze the spectrum consists of a high-resolution grating monochromator with a photomultiplier detector and associated amplifier and recorder.[3] A detailed discussion of the original monochromator is given by Fastie [6].

The plane diffraction grating used in the monochromator is 3 by 3 inches and is ruled with 30,000 lines per inch; the instrument has a practical resolving power ($\lambda/\Delta\lambda$) of 55,000. This resolution is sufficient to observe some of the fine structure splitting of H_α and D_α lines. The choice of optimum resolving power is governed by two considerations: it must be sufficient to resolve the lines to be analyzed

[3] This equipment was on field trial loan to the National Bureau of Standards from the Research Division of the Leeds & Northrup Co.

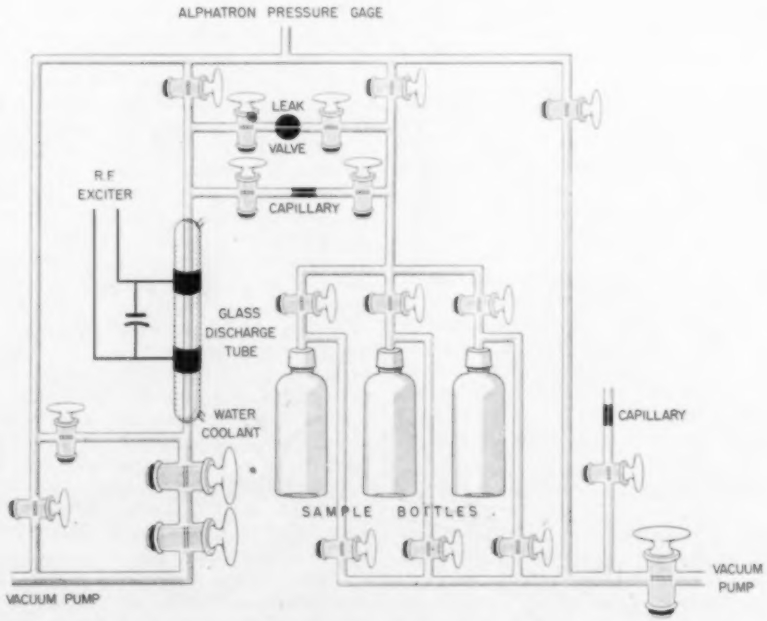

FIGURE 2. *Schematic diagram of flow system.*

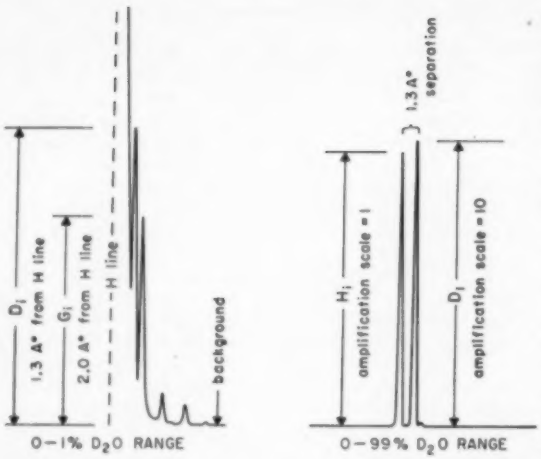

FIGURE 3. *Method of measuring intensities* (H_1, D_1, G_1).

Height of H line (H_1) is approximately 500 times that of H ghost line (G_1). The zero line is arbitrarily taken 6.6 A from the H line, and intensities are measured as distances above the zero line. From left to right, traces are of 0.4-percent and 10-percent D_2O samples, respectively.

and at the same time be low enough to allow for the integrated intensity of a line to be approximated by the peak height of that line. The resolving power was varied by varying the width of the entrance and exit slits until the β line of deuterium could be resolved in a normal water discharge (D/H=0.00015) [7]. Figure 3 shows the H, D, and H ghost lines resolved, and indicates, on the basis of the half width of the line, a resolving power of 20,000. This resolving power proved suitable for subsequent studies.

The first Rowland ghost of the β line of hydrogen was spaced about 2.0 A from the line and was approximately one five-hundredths as intense. The β line of deuterium appears between the H line and its first ghost. The ratio of ghost intensity to line intensity is a function of the optics of the system only, and under conditions of fixed optics may be taken as a constant. For low deuterium concentrations the ratio between the deuterium line and the H ghost is a fixed multiple of the ratio between the D and H lines. This fact proves useful in allowing comparison to be made between signals taken at the same scale of amplification, the calibration in this range being independent of the ratio of amplification for different scales.

2.4. Power Supply, Amplifier, and Recorder

A chopper before the entrance slit of the monochromator converts the input signal to 60 cps. This signal is fed into a narrow band-pass synchronous amplifier, the output of which is recorded by a pen on 10-inch chart paper. The recorder has a response time of 1 second. The power supply for the photomultiplier is continuously variable from 500 to 1,300 v. By using the photomultiplier with a sensitive linear a-c amplifier, which has an accurate amplification factor ranging from 2 to 800, very small signals can be observed.

3. Experimental Results

The primary purpose of this study was to determine the effects of numerous interrelated variables on the speed, accuracy, and sensitivity of the method. The variables include pressure in the flow system, flow rate, sample size, solute composition of the sample, temperature, and oscillator characteristics. These variables will be considered in detail. The percentage change in ratio per unit change in variable was computed for each operating curve and can be used to determine how closely each variable must be controlled to achieve a desired precision (see table 7).

The methods of measuring intensity ratios for the 0- to 1-percent D_2O range and the 1- to 99-percent D_2O range are shown in figure 3. As previously discussed, the deuterium to ghost ratio is used instead of the deuterium to hydrogen ratio in the 0- to 1-percent range. In the 1- to 99-percent range the D and H lines were measured directly at a lower amplification. In both concentration ranges the baseline, or background, is somewhat arbitrary and is taken at a fixed distance from the deuterium peak. This causes no error in the final measurement because the calibration is made in the same manner as the measurement.

3.1. Contamination by a Previous Sample

The speed with which a measurement can be taken is largely dependent on the time required to clean the system of one sample and saturate it with another so that a constant ratio is obtained. Metal parts are troublesome, but the metal leak valve usually was employed to gain fine pressure control in spite of its tendency to retain water with which it has previously been in contact.

Figure 4 shows a series of experiments under extreme conditions in which a pure water sample was run and then switched to commercial heavy water. Curve *a* shows the effect, under the slowest conditions, of using the metal leak valve with no intermediate pumping or flushing. Curve *b* shows the effect of using a glass capillary tube and a glass stopcock for pressure control with no intermediate pumping or flushing. For routine measurement the capillary tube and stopcock were used under the following conditions. The system was pumped with and without sample between extreme pressures in the ratio of at least 15 to 1. These changes were made rapidly for approximately 2 min, and then the pressure was stabilized to 400μ. The effect of contamination by the previous sample was thereby reduced to that shown in curve *c*.

These curves show that an all-glass system, with intermediate flushing, most quickly reduces contamination. Even with an extreme change in concentration, equilibrium is reached to within 1 percent in

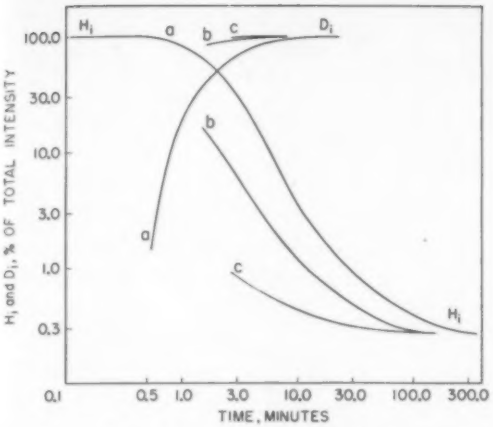

FIGURE 4. *Residual contamination.*

Pressure equals 400 μ. *a*, Metal leak valve, with no intermediate pumping or flushing between samples; *b*, glass stopcock, with no intermediate pumping or flushing; *c*, glass stopcock, with intermediate pumping and flushing.

less than 3 min and complete equilibrium in approximately 1 hr. The flow system shown in figure 2 was designed for maximum variability, but for routine use, a much simpler system is advantageous. Also the elimination of side projections should reduce the time to remove the previous sample.

3.2. Pressure

The operating pressure in the discharge tube has an effect on the intensity ratio, especially in the 0- to 1-percent D_2O range (see fig. 5). Flow rate was not held constant, so actually the traces show ratio versus a combination of pressure and flow rate at constant pumping speed as determined by settings of the metal leak valve and the speed of the pump. The flow rate in milligrams per minute decreased from 0.011 at a pressure of 900μ to 0.0023 at 400μ and 0.001 at 200μ. The pressure gage used had the disadvantage of large metal surfaces, resulting in appreciable delay in removing traces of previous samples, an effect that is particularly undesirable when the concentration is being changed frequently. Therefore, the gage was isolated from the system after initial pressure setting and during the course of most intensity-ratio measurements. The disadvantage of not taking continuous pressure readings was overcome by using the discharge length as a pressure indicator because it is a sensitive function thereof. Although this variation could not be used for absolute measurement of pressure, it provided a good check on the constancy and reproducibility of pressure and flow conditions.

Intensity as a function of pressure was investigated at various concentrations, and the results are shown in figure 6. The curves are quite similar at all concentrations. An operating pressure of approximately 400μ was chosen for routine use because it makes use of maximum intensity and the flattest portion of the

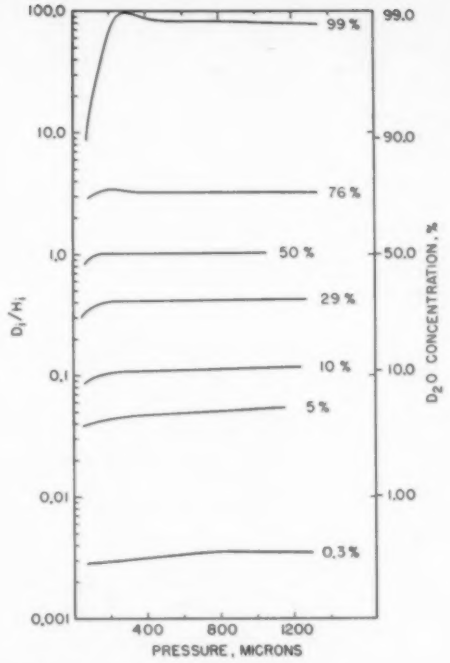

FIGURE 5. *Intensity ratio versus pressure—seven samples at various concentrations.*

The calibrated concentration of each sample by weighing is given at end of each trace.

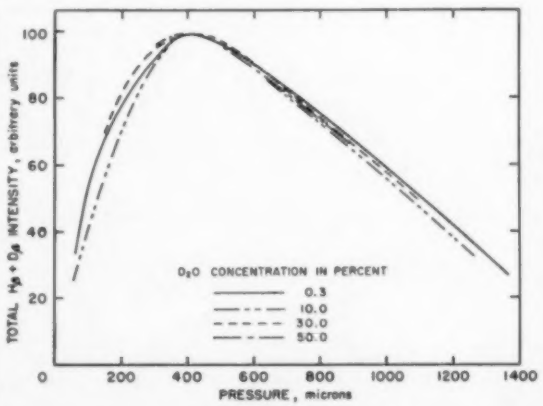

FIGURE 6. *Total* H_2+D_2 *intensity versus pressure at various concentrations.*

intensity versus pressure curve. It also occurs at regions of the ratio versus pressure curves that are reasonably flat. The percentage change of ratio per unit change in pressure at 400μ as computed from figure 5 is 0.020 percent per micron. This means that the pressure must be held to $\pm 5\mu$ to achieve a precision of ± 0.1 percent.

3.3. Fractionation

At 20° C there is a difference of 2.3 mm of mercury between the vapor pressure of H_2O and D_2O, with HDO having an intermediate pressure [7]. Thus a sample that is being evaporated will begin to concentrate deuterium. To check on the error to be expected from this effect, a 0.5-ml sample was run continuously to dryness, with frequent checks made on the D/H ratio. The results at an operating pressure of 200 μ are shown in figure 7. From this curve the minimum sample size can be computed for a given flow rate and allowable error. This is shown in detail in section 5.

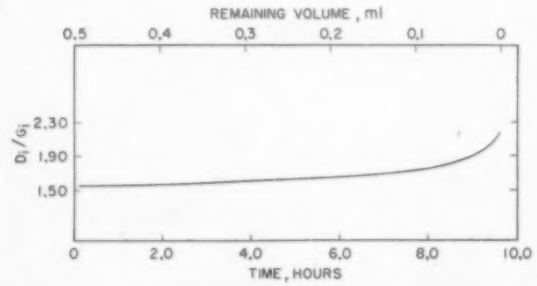

FIGURE 7. *Fractionation effect.*

Flow was continuous at 0.063 ml/hr. D_1/G_1 scale is greatly expanded.

3.4. Temperature

The ratio of the vapor pressure of H_2O, D_2O, and HDO changes with temperature, so that some error might be expected from variation of sample temperature. To study this effect, sample bottles were immersed in a constant-temperature bath during these determinations. Table 1 shows the results obtained at temperatures ranging from 0.4° to 25.8° C. From this table the percentage change in ratio per unit change in sample temperature was computed to be 0.15 percent per deg C.

TABLE 1. *Intensity ratio versus sample temperature*

Pressure equals 500 μ.

Sample	Temperature	Ratio D_1/H_1
	°C	
S-4	4.0	0.3895
	25.8	.3965
S-9	0.4	.0454
	3.0	.0452
	17.0	.0466
	22.0	.0470

3.5. Flow-Rate

Flow rate affects the D/H ratio, the rate of fractionation, and the size of the smallest sample measurable. It is a function of pressure, the geometry of the flow system, and the speed of the pump. Table 2 gives data obtained for D_1/H_1 ratio as a function of the flow rate at constant pressure. This table shows that D_1/H_1 decreases with decreased flow rate and indicates that at least part of the effect of change of pressure (fig. 5) is caused by the reduced flow rate at lower pressures. The percentage change of ratio per unit change of flow rate computed from table 2 is 0.5 percent per gram a minute.

TABLE 2. *Intensity ratio versus flow rate*

Pressure equals 400 μ. Flow rate obtained by weighing sample before and after flow.

Flow	Ratio D_1/H_1
g/min	
0.01125	0.899
.00983	.894
.00331	.857

3.6. Oscillator and Discharge Characteristics

The discharge characteristics can be varied by changes in oscillator plate current, antenna tuning, position of electrodes with respect to the tube, and the temperature of the cooling stream in the jacket of the discharge tube. Plate current is variable between 100 and 200 ma, and the tuning is adjusted by the tuning capacitor in figure 2 as well as by the position of the radio-frequency shield and electrodes. The radio-frequency shield and electrodes were placed to obtain maximum intensity, and the tuning capacitor was varied to give a range of discharge lengths. Ratio of D_1/H_1 as a function of discharge length is shown in table 3. The effect on D_1/H_1 of changing the oscillator plate current is shown in table 4. It is seen that there is no appreciable effect of the discharge length or plate current on the measured ratio. The temperature of the cooling stream was varied by changing the water flow rate through the discharge-tube jacket. D_1/H_1 varied less than 1 percent over the extreme range of temperature from a stream of the coldest water available from the tap (approximately 18° C) to no cooling (greater than 200° C).

TABLE 3. *Intensity ratio versus percentage maximum discharge length*

Pressure equals 500 μ

Sample	Percentage of maximum discharge length	Ratio D_1/H_1
S-9	100	4.71
	88.6	4.78
	73.8	4.85
	49.4	4.48
S-12	100	49.74
	98	49.5
	91.8	49.71
	82.7	49.79
	75.1	49.97
	64.7	50.17
	52.0	50.04
	49.0	49.79

TABLE 4. *Intensity ratio versus oscillator plate current*

Pressure equals 500 μ

Sample	Plate current	Ratio D_1/H_1
	ma	
S-9	100	0.0503
	122	.0499
	140	.0491
	175	.0491
	190	.0490
S-12	100	1.015
	125	1.016
	130	1.013
	150	1.015
	185	1.012
	200	1.012
	210	1.012

3.7. Solute Composition

As the optical spectroscopic method of analysis may be extended for use with many aqueous solutions, preliminary investigation was made of the variation of D_1/H_1 ratio with the amount of solids dissolved in the sample. This test was made with NaCl. With concentrations of 0 percent, 1 percent, 10 percent, and a saturated solution, no variation of D_1/H_1 was found within the experimental error.

4. Calibration Curves, Precision, and Reproducibility

Calibration curves were necessary to achieve the highest accuracy. Figure 8 shows the 0- to 1-percent D_2O range and figure 9 the 1- to 80-percent D_2O range.[4] Samples were made by mixing portions of distilled water and commercial D_2O (99.8%) that had been weighed to an accuracy of 0.1 mg.

Table 5 gives examples of the isotope content expressed, for comparison, in ratio and in percent, and shows the precision obtained under optimum conditions.

TABLE 5. *Comparison of ratio method and percentage concentration method of expressing isotope content*

Ratio D/H	Standard deviation of average of ratio [a]	Coefficient of variation of average [b]	Deuterium concentration 100D/D+H	Standard deviation of average of concentration [a]	Coefficient of variation of average [b]
			%		
500	5.0	1.0	99.8	0.002	0.002
100	0.1	0.1	99.0	.001	.001
10	.01	.1	90.9	.01	.01
1	.001	.1	50.0	.25	.05
.1	.0001	.1	9.09	.01	.01
.01	.00001	.1	0.99	.001	.1
.001	.000007	.7	.100	.0007	.7
.0001	.000002	2.0	.01	.0002	2.0

[a] Based on a set of 10 readings.
[b] Standard deviation of average, expressed in percent.

[4] Calibration curves were taken on samples up to 99.8 percent of D_2O (commercially available), but no extensive measurements were made in the high-concentration range. The analysis in this range differs from that in the low ranges only in the method of preparing standard samples.

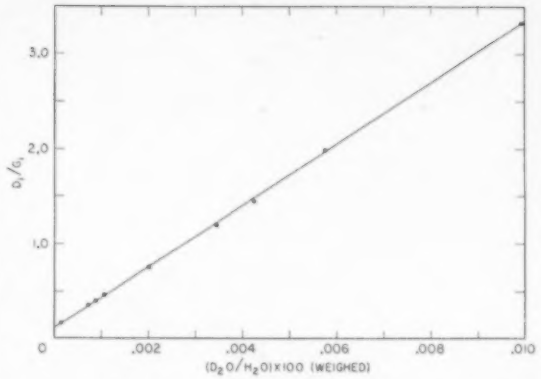

FIGURE 8. *Calibration curve for 0- to 1-percent D_2O concentration range.*

Samples were made up by weighing.

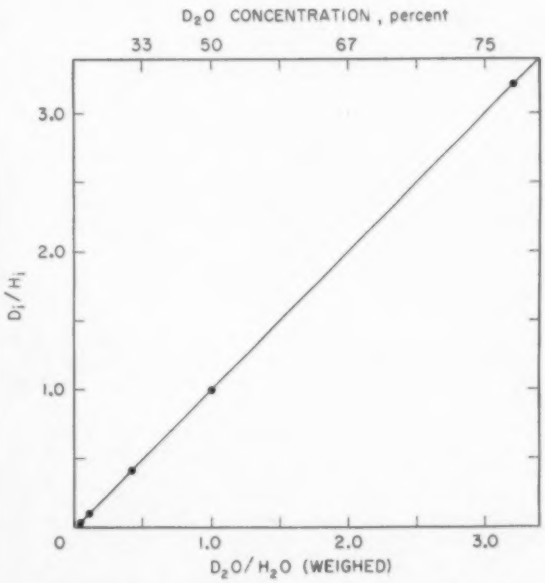

FIGURE 9. *Calibration curve for 1- to 80-percent D_2O concentration range.*

80- to 99-percent portion of the curve is omitted because of the extended scale. Samples were made up by weighing.

Reproducibility was measured on a 21-percent D_2O sample and a 0.2-percent D_2O sample. Measurements were taken at varying time intervals, and in some cases with major changes taking place during the interval, both in the apparatus and in the concentration ratios. Results are shown in figure 10 for 4 portions of the 21-percent sample.

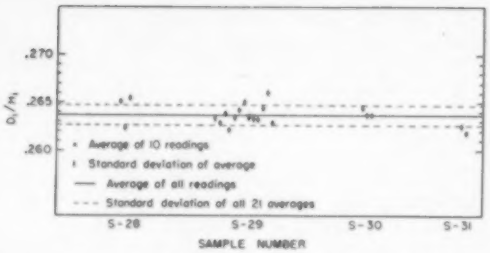

FIGURE 10. *Precision and reproducibility for 21-percent D_2O samples.*

The data were taken over a period of 3 months, and dates are given below, reading from left to right on figure 10.

Sample	Date	Sample	Date
S–28	Dec. 9, 1952 Dec. 9, 1952 Dec. 23, 1952	S–30	Dec. 4, 1952 Dec. 4, 1952 Dec. 23, 1952
S–29	Dec. 1, 1952 Dec. 1, 1952 Dec. 2, 1952 Dec. 2, 1952 Dec. 3, 1952 Dec. 3, 1952 Dec. 4, 1952 Dec. 5, 1952 Dec. 5, 1952 Dec. 5, 1952 Dec. 5, 1952 Dec. 22, 1952 Feb. 25, 1953	S–31	Dec. 19, 1952 Dec. 19, 1952

Each point shows the average of 10 readings, with the precision depicted as vertical spread. The grand average is a solid horizontal line, and the standard deviation computed directly from all 21 averages is shown by dotted lines on either side of the grand average. Thus the relation between precision and reproducibility at this stage of development can be seen at a glance. The results obtained for the 0.2-percent sample were similar. Data for it are listed in table 6.

TABLE 6. *Reproducibility of intensity ratio for a 0.2-percent D_2O sample over a 1-month period.*

Each ratio is the average of 10 readings. Pressure equals 200μ.

Date, 1953	D_1/G_1 *	Date, 1953	D_1/G_1 *
April 28	0.760	May 11	.753
May 1	.737	May 15	.740
May 2	.736	May 18	.769
May 4	.733	Do	.754
May 7	.729	May 19	.765
Do	.724	May 20	.753
Do	.744		
May 8	.751	Average	0.746
Do	.743		

* G_1 is the measured intensity of the ghost of the H line.

5. Discussion

The great number of variables that influence the measurement of D/H ratios makes it impossible to be certain that the final operating conditions are in fact the optimum ones. Indeed, it is not necessary to assume that there is a unique set of optimum conditions for this analysis. The operating conditions chosen therefore are the "best set", based upon data available and the nature of the measurements to be performed. Some of the final data used to evaluate operating conditions are shown in table 7. This table illustrates that there is no extreme problem in keeping the operating conditions constant enough so that the measurement can be made within the desired accuracy.

TABLE 7. *Operating variables*

Operating condition varied	Percentage change of ratio per unit change of variable	Routine operating conditions
Sample temperature	0.15 percent per deg C	Room temperature.
Pressure	0.020 percent per micron	400 microns.
Salt concentration	0 percent per mole/liter	Any.
Flow rate	0.5 percent per g/min	Depending on sample size and desired speed of measurement.
Tuning	0 percent per percentage change in discharge length.	Maximum discharge length.
Oscillator plate current.	0 percent per ma	175 ma.
Discharge tube temperature.	0.005 percent per deg C	Room temperature.

Accessory factors enter into the choice of best conditions. The fractionation curve (fig. 7) can be represented as $RS^k=K$, where R is the isotope ratio, S is the sample size, and k and K are experimental constants. In differential form the fractionation curve can be represented as $dR/R=-(k/S)dS$, where the left-hand term represents the percentage change of ratio due to fractionation. Setting dR/R equal to ϵ, the maximum tolerable fractionation error, and realizing that $dS=-f\Delta t$, the flow-rate times the time increment, we arrive at the following expression for minimum sample size:

$$S=\frac{0.068 f\Delta t}{\epsilon}.$$

The value of k, 0.068, was obtained from the data shown in figure 7. As has been mentioned previously, flow-rate depends on operating pressure, flow-geometry, and pumping speed, and the time of measurement depends on the time required to clean the system of the previous sample and to equalize the pressure. Hence, sample size is some complex function of the major operating variables. Under normal conditions at a 400-μ operating pressure the flow rate was 0.0023 ml/min, and the time per determination was 20 min. The minimum sample size is therefore $0.00313/\epsilon$, or 0.3 ml, for a 1-percent error. The absolute minimum sample size under present conditions involves an operating pressure of 200 μ and a maximum error of 3 percent. Under

these conditions, a 7-min measurement is possible, and the minimum sample size is 0.02 ml.

The operating conditions that were found to be most suitable with the equipment described are shown in table 7.

This study is not exhaustive, inasmuch as there are many combinations of variables that were not tried. In addition, no attempt was made to vary systematically such things as the oscillator frequency or discharge-tube geometry. A few preliminary experiments with a 2,240-Mc oscillator indicate that a stable set of operating conditions can be set up at that frequency.

As pointed out in the beginning of this paper, the chief object of these studies was to determine how to minimize error, sample size, and time of determination. Of course, it is impossible to minimize all three factors at once. Highest precision requires many determinations per sample, hence a long time and large sample size. The minimum values attainable at the present stage of development and the maximum values obtained while minimizing the others are given as follows:

Factor	Minimum	Maximum
Precision (coefficient of variation of the average)	0.1 to 2 percent.	3 percent
Sample size	0.02 ml	1 ml
Time per sample	7 min	60 min

With respect to precision and time per determination, the optical spectroscopic case compares favorably with other methods. It finds particular application where the water samples contain impurities. Whereas other methods require one or two stages of purification, the sample vapor can be analyzed directly by this method. This method appears to be considerably more rapid and, for similar accuracy, less expensive than other methods.

While it is not the function of this paper to discuss, in detail, applications of hydrogen-deuterium analysis, we shall review briefly in the following paragraphs some of the most important uses to which the optical spectroscopic method has been placed. The dilution technique for determining the total water content of materials involved in these uses is described in reference [3]. Essentially, it consists in dissolving or suspending a known amount of the material to be analyzed in a mixture of D_2O and H_2O and then determining spectroscopically the resulting change in the ratio of D_2O to H_2O.

1. *Determination of* D_2O *content of blood.* In this application the blood, serum, or plasma is placed in the sample bottle and the vapor analyzed in the usual manner. No prior preparation of the blood is necessary and high precision is obtainable. This technique finds application in the determination of total body water by D_2O dilution and in the study of water exchange in capillary beds. Over 150 blood samples have been run, and no difficulty has been encountered in adapting the techniques to routine analysis.

2. *Determination of water of hydration or water of crystallization.* The crystal to be analyzed is dissolved in D_2O, and the final intensity ratio gives a measure of the H_2O originally in the crystal. Several hydrates have been tried, and the results agree with other methods.

3. *Determination of labile hydrogen.* A weighed quantity of dry material containing labile hydrogen is dissolved in D_2O and the resultant ratio measured. From the number of exchangeable hydrogen atoms per molecule, information about structure of the molecule is obtained.

The most extensive work has been done with blood, for which a brief description of the routine application follows.

Army Medical Service gave injections of 100 g of commercially pure D_2O to several hemorrhagic fever patients and sampled blood at various time intervals. The serum samples were analyzed at the National Bureau of Standards to determine the total body water content of the patients. Seventy-three samples in the concentration range 0.029 to 0.425 percent gave precisions of the order of 0.7-percent coefficient of variation of the average. Ten readings were taken per sample, using the metal leak valve for pressure control. The time per sample ranged between 25 and 55 min, depending on stability of operating conditions.

Reference [8] gives details of a study of transcapillary exchange rates of D_2O and thiocyanate in the forearm of man. A study has since been made of the exchange rates from the artery of one arm to the vein of the other. In this case only five readings were taken per sample and metal parts were eliminated, thus cutting the total time per sample down to 15 min, plus data calculation time. The precision of measurement was of the order of 1.5-percent coefficient of variation of the average for 17 samples in the concentration range 0.015 to 2.00 percent of D_2O.

6. References

[1] H. P. Broida and J. W. Moyer, Spectroscopic analysis of deuterium in hydrogen-deuterium mixtures, J. Opt. Soc. Am. **42,** 37 (1952).

[2] H. P. Broida and G. H. Morgan, Optical spectrophotometric analysis of hydrogen-deuterium mixtures in presence of air, Anal. Chem. **24,** 799 (1952).

[3] H. J. Morowitz and H. P. Broida, Rapid spectroscopic determination of total water content, Anal. Chem. **24,** 1657 (1952).

[4] W. J. Youden, Statistical methods for chemists (John Wiley & Sons, Inc., New York, N. Y., 1951).

[5] ASTM Manual on quality control of materials, Am. Soc. Testing Materials (Philadelphia, Pa., January 1951).

[6] William G. Fastie, A small plane grating monochromator, J. Opt. Soc. Am. **42,** 641 (1952).

[7] I. Kirshenbaum, Physical properties and analysis of heavy water, p. 396 (McGraw-Hill Book Co., New York, N. Y., 1951).

[8] Edward D. Freis, Thomas F. Higgins, and Harold J. Morowitz, Transcapillary exchange rates of deuterium oxide and thiocyanate in the forearm of man, J. Appl. Physiol. **5,** 526 (1953).

WASHINGTON, November 25, 1953.

Journal of Research of the National Bureau of Standards Vol. 52, No. 6, June 1954 Research Paper 2504

Refractive Indices of Five Selected Optical Glasses*

Robert E. Stephens and William S. Rodney

The refractive indices of typical samples of five optical glasses made at the National Bureau of Standards were measured over a range of wavelengths from 0.35 to 2.32 microns. This was done in such a way that the values obtained in the visible and invisible portions of the spectrum are consistent with one another. The results are expressed for each glass by a six-constant dispersion formula.

Precise data on optical glasses should be readily available in considerable detail in order to satisfy the complex requirements of optical engineers and designers. Only for the visual range of wavelengths are refractive indices satisfactorily available for either domestic or imported glasses, and almost no data are available on spectral transmittances.

The five glasses considered here were made and annealed in the Glass Section at the National Bureau of Standards under the direction of Clarence H. Hahner, who has furnished the weight percentages shown in table 1, descriptive of their chemical composition as computed from the batch composition. With the exception of the rare-earth glass, these are typical optical glasses and are probably very similar to the corresponding Bausch and Lomb glasses $n=1.517$, $\nu=64.5$; $n=1.573$, $\nu=57.4$; $n=1.621$, $\nu=36.2$; and $n=1.649$, $\nu=33.8$, as listed in their catalogs under these D-line indices and ν values.

The refractive indices of these glasses were accurately determined in the visible region by means of the high-precision spectrometer made by E. R. Watts & Son, Ltd., London.[1] Measurements in the infrared and in the near ultraviolet regions were made on each of two spectrometers. The first was of the Wadsworth mirror type, improvised from a Zeiss monochromator, the same instrument that was used for index determinations on magnesium oxide.[2] The second was the Gaertner spectrometer equipped with mirrors and a lead sulphide detector, the same apparatus that was used for index determinations on potassium bromide.[3]

The independently observed indices in the infrared and also in the near ultraviolet regions were in fair agreement, and no systematic differences were detected. The values resulting from the second set (Gaertner spectrometer) should be somewhat more accurate because of a potentially higher accuracy in angle measurement, and accordingly much more weight is given to the Gaertner data in computing averages.

The indices of refraction of these glasses were represented by dispersion equations of the form

$$n^2=a^2-k\lambda^2-p\lambda^4+\frac{v}{\lambda^2}+\frac{m}{\lambda^2-l^2}$$

where λ is in microns, and the parameters have appropriate values for the various glasses as given in table 2. The parameters were adjusted by the NBS Com-

TABLE 1. *Chemical compositions of glasses* [a]

Oxide	Borosilicate crown (BSC) $n=1.517$ $\nu=64.5$	Light barium crown (LBC) $n=1.574$ $\nu=57.7$	Flint (F) $n=1.620$ $\nu=36.2$	Dense flint (DF) $n=1.6^{\circ}9$ $\nu=33.8$	Rare earth $n=1.673$ $\nu=56.2$
SiO_2	65.6	47.4	45.6	41.2	18.5
B_2O_3	13.0	4.9	.....	.....	20.8
Na_2O	7.6	0.9	2.7	0.7	.....
K_2O	12.1	7.0	5.7	6.5	.....
ZnO	1.2	7.5	.....	.....	.....
PbO	.....	.....	45.5	51.1	.....
BaO	.....	30.0	.....	.....	30.6
BeO	.....	.....	.....	.....	2.0
La_2O_3	.....	.....	.....	.....	19.6
CaO	.....	.....	.....	.....	8.5
As_2O_3	0.5	0.3	0.5	0.5	.....
Sb_2O_3	.....	.5	.....	.....	.....
Al_2O_3	.....	1.5	.....	.....	.....

[a] n=index of refraction for the sodium-D line, and ν, the Abbe value $=(n-1)/(n_F-n_C)$, where n_F and n_C are refractive indices for the hydrogen F and C lines, respectively.

TABLE 2. *Parameters of dispersion equations*

Parameter	BSC $n=1.517$ $\nu=64.5$	LBC $n=1.574$ $\nu=57.7$	F $n=1.620$ $\nu=36.2$	DF $n=1.649$ $\nu=33.8$	Rare earth $n=1.673$ $\nu=56.2$
a^2	2.2723379	2.4372255	2.5551726	2.6383102	2.749265
k	.00961954	.00840627	.00825919	.00832968	.0109904
p	.0000982107	.0000834459	.0000894995	.0000939503	.0013455
v	.006027086	.005289321	.0100231789	.010094553	.0034447
m	.004855199	.008838177	.01340333	.01568233	.0146030
l^2	.0237050	.0217633	.0432000	.0451527	.017689
Average residual ultraviolet	1.9×10^{-3}	0.9×10^{-3}	2.6×10^{-4}	2.2×10^{-4}	1.3×10^{-4}
Visible	0.3	.2	.3	.8	.3
Infrared	1.4	1.0	.7	1.7	1.1

*The companion papers in this issue present values of the spectral transmissive properties, densities, and coefficients of linear thermal expansion for five different types of optical glasses produced by the Optical Glass Section of the National Bureau of Standards. These measurements have been made in the different organizational parts of the Bureau appropriate to each type of measurement, and are, therefore, presented separately. For each type of glass the samples have been taken from the same melt, and, therefore, these papers present, collectively, a consistent set of data for the five glasses studied.

[1] Robert J. Spindler and William S. Rodney, Refractivity of potassium bromide for visible wavelengths, J. Research NBS **49,** 253 (1952) RP2361.

[2] Robert E. Stephens and Irving H. Malitson, Index of refraction of magnesium oxide, J. Research NBS **49,** 249 (1952) RP2360.

[3] Robert E. Stephens, Earle K. Plyler, William S. Rodney, and Robert J. Spindler, Refractive index of potassium bromide for infrared radiant energy, J. Opt. Soc. Am. **43,** 110 (1953).

TABLE 3. *Computed values of refractive indices of glasses*

Wavelength	BSC $n=1.517$ $\nu=64.5$	LBC $n=1.574$ $\nu=57.7$	F $n=1.620$ $\nu=36.2$	DF $n=1.649$ $\nu=33.8$	Rare earth $n=1.673$ $\nu=56.2$
Microns					
0.3341	1.54287				
.3404	1.54141				
.3467	1.54001	1.60313	1.67080		
.3612	1.53713	1.59937	1.66870	1.70384	1.70407
.3650	1.53643	1.59846	1.66678	1.70162	1.70295
.3655	1.53635	1.59836	1.66656	1.70136	1.70282
.3663	1.53620	1.59816	1.66615	1.70088	1.70259
.4047	1.53044	1.59072	1.65113	1.68360	1.69366
.4078	1.53004	1.59022	1.65014	1.68247	1.69305
.4340	1.52709	1.58643	1.64290	1.67421	1.68850
.4358	1.52691	1.58620	1.64247	1.67372	1.68822
.4678	1.52402	1.58253	1.63569	1.66602	1.68380
.4800	1.52308	1.58133	1.63352	1.66357	1.68236
.4861	1.52263	1.58076	1.63249	1.66241	1.68167
.5086	1.52112	1.57886	1.62911	1.65860	1.67938
.5461	1.51900	1.57620	1.62446	1.65338	1.67618
.5770	1.51754	1.57439	1.62136	1.64990	1.67400
.5791	1.51745	1.57428	1.62116	1.64968	1.67386
.5893	1.51702	1.57375	1.62026	1.64867	1.67322
.6438	1.51502	1.57130	1.61617	1.64411	1.67027
.6563	1.51463	1.57082	1.61538	1.64323	1.66969
.6907	1.51363	1.56992	1.61342	1.64105	1.66823
.7065	1.51321	1.56911	1.61261	1.64015	1.66762
.7081	1.51317	1.56906	1.61252	1.64006	1.66756
.7729	1.51166	1.56729	1.60971	1.63695	1.66542
1.0140	1.50766	1.56282	1.60310	1.62972	1.66001
1.1287	1.50617	1.56128	1.60102	1.62748	1.65812
1.3570	1.50341	1.55859	1.59767	1.62394	1.65483
1.3673	1.50328	1.55847	1.59754	1.62380	1.65468
1.3951	1.50295	1.55816	1.59717	1.62342	1.65430
1.5295	1.50132	1.55666	1.59546	1.62164	1.65245
1.6932	1.49925	1.55480	1.59343	1.61955	1.65009
1.7092	1.49905	1.55461	1.59323	1.61935	1.64992
1.8131	1.49766	1.55338	1.59193	1.61802	1.64839
1.9701	1.49544	1.55145	1.58992	1.61599	1.64598
2.2493	1.49108	1.54770	1.58611	1.61214	1.64128
2.3254	1.48979	1.54659	1.58501	1.61103	1.63989

putation Laboratory, using the method of least squares. The magnitude and distribution of the plus and minus residuals are such that the formulas are unquestionably adequate for representing the data. The computed values, which are adjudged to be better than the observed, values are presented in table 3.

The necessity of using a dispersion equation with six constants was not anticipated. Trials with four carefully adjusted constants, however, proved inadequate in that for the first four glasses there were evident systematic differences between the observed and the computed indices. Such systematic failures for four-constant formulas were as large as 5 or 10×10^{-5} outside the visible region, and the deviations were more convincing in the infrared because of more observed points there than in the violet. Moreover, the character of the systematic failures was similar for the different glasses, and thus the equation was considered inadequate in form.

The addition of a term in λ^4 was obviously a suitable expedient for the infrared and one in $1/\lambda^2$ improved the ultraviolet end, and both seemed necessary. The resulting residuals are all less than $\pm5\times10^{-5}$, with the exception of 2 (of opposite sign) in the ultraviolet and, similarly, 2 in the infrared. One-half of all residuals are smaller than $\pm0.7\times10^{-5}$. The remaining systematic trends between observed and computed values are not over ±1 or 2×10^{-5}.

WASHINGTON, November 19, 1953.

Journal of Research of the National Bureau of Standards Vol. 52, No. 6, June 1954 Research Paper 2505

Spectral Transmissive Properties of Five Selected Optical Glasses*

Harry J. Keegan, Marion A. Belknap, and Dorothy J. Cordrey [1]

Measurements of the spectral transmittance and internal transmittance of five optical glasses for the wavelength region 200 to 1,000 millimicrons are reported.

1. Introduction

The transmittance, T, of a plate is defined as the ratio of radiant flux (P_2) transmitted by the plate to the flux (P_1) incident upon it. Internal transmittance (T_i) is defined as the ratio of the flux (P) arriving at the second surface of the plate to that flux (P_0) penetrating the first surface. All values of T and T_i are functions of wavelength.

The transmittances and internal transmittances reported were determined for glasses of the NBS melts for which the chemical compositions are given in Research Paper 2504.

The samples were prepared in the NBS Optical Shop in the form of cylinders or plates, 30 mm in diameter, with surfaces plane, parallel, and polished. The rare earth glass, $n=1.673$,[2] $\nu=56.2$, was prepared in thicknesses of 5 and 105 mm. The other four glasses were prepared in a thickness of 1 mm in addition to greater thicknesses. The thin samples were compared against a blank beam, and spectral transmittance was so obtained. The thick samples were compared to the thin sample of the same kind of glass, the resulting ratios being taken as internal transmittance for a sample of thickness equal to the difference between thick and thin specimens.[3]

2. Spectrophotometric Measurements

Most spectrophotometers are designed primarily for samples between 0- and 10- to 50-mm thickness, but can be used with samples of somewhat greater thickness. The greater the thickness, however, the more the instrument is subject to errors resulting from refraction of the various rays in the beam, for although these rays are approximately parallel and at right angles to the surfaces, they are in general not strictly so. The result is, in effect, a change in P_1 to P_0 of the above defining relations for transmittance, P_2/P_1, or for internal transmittance, P/P_0. This is particularly true when, as in the present measurements with the thick samples, the compensation beam of the spectrophotometer does not contain a sample of the same length (as it usually does, for example, in measuring the transmittance of a solution relative to its solvent).

Four types of spectrophotometers were available for this work. The designs of two of these instruments (the General Electric recording spectrophotometer and the König-Martens visual spectrophotometer) are such as to give confidence in the results for thick samples. The other two instruments (the Beckman quartz photoelectric spectrophotometer and the Gibson photoelectric spectrophotometer [9])[4] were sensitive to beam disturbance with thick samples. In the work on the rare-earth glass 1.673, it was found that the latter instrument was too sensitive to beam disturbance on insertion of the thick sample to give valid results, and it therefore was not used in the later measurements on the other glasses.

In the General Electric spectrophotometer (GE) [1, 2, 3] the beam of radiant energy, after transmission through the sample, is incident upon a diffusing white surface of uniform reflectance forming part of the interior wall of a white-lined integrating sphere. Any deviation or dispersion of the beam should not, therefore, cause appreciable error, if not so great that part of the beam impinges on the entrance aperture of the sphere.

On the König-Martens spectrophotometer (K-M) [4] the reverse but equivalent condition exists. The radiant energy is reflected from a diffusing surface of MgO, which is part of an enclosure completely covered with MgO, except for the part containing the bases of the lamps from which the radiant energy originates. Multiple reflections should give a wall surface of essentially uniform radiance, and any displacement of this source in the photometric field by the thick sample should not introduce important error in the results.

The principal value of the K-M measurements was to confirm the reliability of the GE data even for the thickest samples. However, the precision of the visual measurements is less than the photoelectric, and except with the rare-earth glass 1.673, only a few check measurements were made on the K-M spectrophotometer.

The Beckman quartz photoelectric spectrophotometer (model DU) (BQ) [5, 6] is somewhat susceptible to errors resulting from beam disturbance on insertion of the sample, and the thicker the sample the greater may be the error. On this instrument, the

*The companion papers in this issue present values of the index of refraction, densities, and coefficients of linear thermal expansion for five different types of optical glasses produced by the Optical Glass Section of the National Bureau of Standards. These measurements have been made in the different organizational parts of the Bureau appropriate to each type of measurement, and are, therefore, presented separately. For each type of glass the samples have been taken from the same melt, and, therefore, these papers present, collectively, a consistent set of data for the five glasses studied.

[1] Now Mrs. Frederick J. Doss, E. I. duPont de Nemours & Co., Inc., Parlin, N. J.

[2] n=index of refraction for the sodium D lines, and ν, the Abbe value=$(n-1)/(n_F-n_C)$, where n_F and n_C are refractive indices for the hydrogen F and C lines, respectively.

[3] Glass DF, $n=1.649$, $\nu=33.5$ was prepared in greater thickness of 97 mm and compared to the 5-mm sample. Values of T_i for 100 mm for this glass are computed from the values of T_i for 92 mm so determined.

[4] Figures in brackets indicate the index references at the end of this paper.

beam of radiant energy, after passage through the sample, is incident directly on the photocell. Although the window of the photocell is made diffusing, this is undoubtedly far from completely so, and any deviation or dispersion of the beam may well affect the response because of varying sensitivity of the photosensitive surface. The principal value of the Beckman spectrophotometer in the present work was to obtain the values of transmittance or internal transmittance in the ultraviolet, and it was not used at wavelengths longer than 460 millimicrons (mμ).

Consistent with the above, the GE recording spectrophotometer was used over the range 400 to 1,000 mμ, and the Beckman spectrophotometer over the range from 460 mμ toward shorter wavelengths into the ultraviolet as far as there was measurable transmission. The transmittance values obtained on the GE spectrophotometer were taken as a reference and the Beckman values adjusted to them when necessary in accordance with the following procedure: [5] (1) The GE transmittance values were used from 460 to 1,000 mμ, subject to an occasional smoothing not exceeding 0.001; (2) from 410 to 460 mμ the GE data were used to compute an adjustment factor to apply to all of the Beckman data. This adjustment factor was the average of the ratios (T_{GE}/T_{BQ}) at each of the six wavelengths from 410 to 460 mμ. In this range the adopted values were then based on both the GE data and the adjusted Beckman data; (3) from 400 mμ toward shorter wavelengths the adopted values were based on these adjusted Beckman data.

All the values by the Beckman spectrophotometer were obtained with the samples at 25° C.[6] Values by the GE spectrophotometer (visible and infrared) were obtained at a room temperature close to 25° C, and should be valid also at 25° C.

3. Spectrophotometric Results

Curves of the transmittances for 1-mm thickness for four glasses are shown in figure 1 (numbered 1 to 4), together with the transmittance curve for the 5-mm thickness of the rare-earth glass 1.673, numbered 5 in the figure.

Curves for the internal transmittances for 4- and 100-mm thicknesses of the same four glasses are shown in figure 2, together with the internal transmittance curve for the 100-mm thickness of the rare-earth glass 1.673.

The values of transmittance and internal transmittance are given in table 1. All are subject to slight uncertainty in the last figure. Examination of the values of T_i for 100 mm for the rare-earth glass 1.673 shows traces of the absorption bands near 580 and 740 mμ commonly found in didymium glasses.

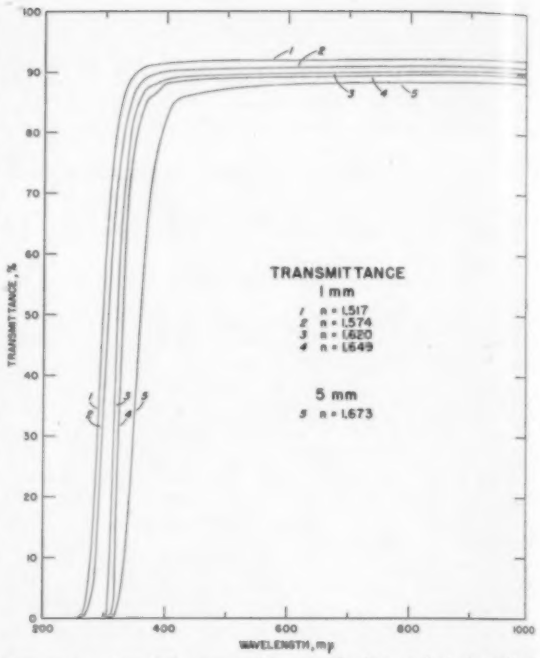

FIGURE 1. *Spectral transmittance of five selected optical glasses made at NBS for the ultraviolet, visible, and near-infrared spectrum.*

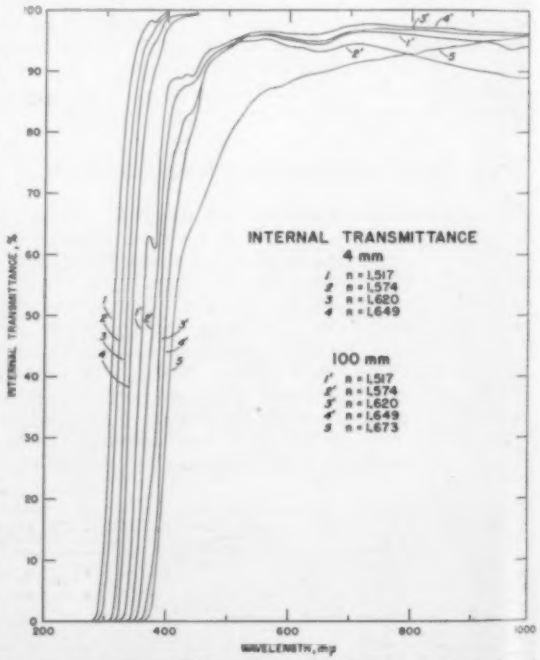

FIGURE 2. *Spectral internal transmittance of five selected optical glasses made at NBS for the ultraviolet, visible, and near-infrared spectrum.*

[5] This indicated procedure was followed for 4 of the 5 glasses. For rare-earth glass 1.673, a slightly different procedure was used.

[6] At the steep portions of the curves (figs. 1 and 2), the transmittance and internal transmittance vary importantly with temperature, in these cases in the ultraviolet region of the spectrum [7].

TABLE 1. *Spectral transmittance and internal transmittance data of five selected optical glasses made at NBS for the indicated thicknesses and for the wavelength range 200 to 1,000 millimicrons*

Wavelength	Glass BSC $n=1.517$ $\nu=64.5$			Glass LBC $n=1.574$ $\nu=57.7$			Glass F $n=1.620$ $\nu=36.2$			Glass DF $n=1.649$ $\nu=33.8$			Rare-earth glass $n=1.673$ $\nu=56.2$	
	1 mm	4 mm	100 mm	1 mm	4 mm	100 mm	1 mm	4 mm	100 mm	1 mm	4 mm	100 mm	5 mm	100 mm
	T	T_i	T_i	T	T_i	T_i	T	T_i	T_i	T	T_i	T_i	T	T_i
mμ														
250	0.000													
260	.002	------	------	0.000										
270	.026	0.000	------	.008										
280	.12	.001	------	.054	0.000	------	------	------	------	------	------	------	0.000	
290	.33	.019	------	.17	.003	------	------	------	------	------	------	------	.001	
300	.56	.14	------	.37	.039	------	0.000	0.000	------	0.000	------	------	.002	
310	.72	.39	------	.56	.16	------	.10	.002	------	.003	0.000	------	.004	
320	.813	.64	0.000	.71	.39	------	.46	.072	------	.17	.003	------	.014	
330	.862	.802	.004	.80	.62	0.000	.69	.36	------	.51	.11	------	.063	
340	.887	.896	.065	.847	.79	.002	.79	.63	0.000	.70	.39	------	.18	
350	.900	.945	.24	.873	.884	.046	.840	.79	.003	.79	.63	0.000	.36	
360	.907	.972	.48	.886	.939	.21	.864	.885	.047	.832	.78	.002	.53	0.000
370	.910	.982	.63	.893	.966	.42	.876	.934	.18	.857	.867	.030	.66	.004
380	.911	.981	.61	.896	.975	.53	.879	.949	.26	.864	.905	.09	.74	.042
390	.913	.992	.79	.899	.985	.66	.885	.974	.49	.874	.946	.26	.795	.15
400	.915	.996	.875	.901	.992	.80	.888	.987	.694	.881	.971	.50	.825	.32
410	.915	------	.889	.902	------	.856	.890	.990	.765	.882	.981	.633	.847	.47
420	.916	------	.889	.902	------	.869	.891	.991	.794	.883	.986	.705	.856	.575
430	.916	------	.895	.903	------	.878	.892	.993	.827	.884	.990	.775	.860	.625
440	.916	------	.892	.903	------	.880	.892	.993	.835	.885	.992	.804	.862	.645
450	.917	------	.910	.904	------	.892	.893	.995	.864	.887	.993	.842	.864	.667
460	------	------	.929	------	------	.912	------	------	.899	------	------	.900	------	.696
470	------	------	.936	------	------	.925	------	------	.916	------	------	.913	------	.723
480	------	------	.940	------	------	.932	------	------	.923	------	------	.923	------	.748
490	------	------	.944	------	------	.938	------	------	.931	------	------	.932	------	.773
500	.918	------	.949	.905	------	.942	.895	------	.938	.889	------	.940	.873	.794
510	------	------	.953	------	------	.946	------	------	.947	------	------	.948	------	.811
520	------	------	.956	------	------	.948	------	------	.952	------	------	.955	------	.826
530	------	------	.957	------	------	.949	------	------	.956	------	------	.959	------	.840
540	------	------	.958	------	------	.950	------	------	.958	------	------	.962	------	.852
550	.919	------	.959	.906	------	.952	.896	------	.959	.890	------	.964	.877	.862
560	------	------	.960	------	------	.953	------	------	.961	------	------	.965	------	.869
570	------	------	.958	------	------	.951	------	------	.960	------	------	.965	------	.873
580	------	------	.955	------	------	.947	------	------	.958	------	------	.964	------	.874
590	------	------	.952	------	------	.943	------	------	.956	------	------	.962	------	.878
600	.919	------	.951	.907	------	.941	.897	------	.955	.891	------	.961	.879	.883
610	------	------	.950	------	------	.939	------	------	.953	------	------	.961	------	.887
620	------	------	.947	------	------	.938	------	------	.951	------	------	.961	------	.890
630	------	------	.945	------	------	.935	------	------	.949	------	------	.960	------	.893
640	------	------	.944	------	------	.933	------	------	.949	------	------	.960	------	.895
650	.920	------	.944	.908	------	.932	.898	------	.949	.892	------	.961	.881	.898
660	------	------	.946	------	------	.933	------	------	.950	------	------	.962	------	.901
670	------	------	.951	------	------	.935	------	------	.954	------	------	.966	------	.903
680	------	------	.956	------	------	.940	------	------	.959	------	------	.969	------	.906
690	------	------	.960	------	------	.943	------	------	.962	------	------	.973	------	.909
700	.920	------	.962	.908	------	.945	.899	------	.965	.893	------	.974	.882	.911
710	------	------	.963	------	------	.945	------	------	.966	------	------	.976	------	.913
720	------	------	.963	------	------	.944	------	------	.967	------	------	.977	------	.916
730	------	------	.964	------	------	.942	------	------	.969	------	------	.977	------	.917
740	------	------	.964	------	------	.940	------	------	.969	------	------	.976	------	.918
750	.921	------	.963	.909	------	.938	.900	------	.969	.894	------	.976	.882	.919
760	------	------	.963	------	------	.936	------	------	.969	------	------	.975	------	.923
770	------	------	.963	------	------	.934	------	------	.969	------	------	.975	------	.924
780	------	------	.962	------	------	.931	------	------	.968	------	------	.974	------	.926
790	------	------	.961	------	------	.929	------	------	.968	------	------	.974	------	.927
800	.921	------	.960	.909	------	.926	.900	------	.968	.895	------	.973	.882	.927
810	------	------	.959	------	------	.923	------	------	.967	------	------	.972	------	.928
820	------	------	.958	------	------	.920	------	------	.966	------	------	.972	------	.932
830	------	------	.957	------	------	.918	------	------	.966	------	------	.972	------	.934
840	------	------	.956	------	------	.916	------	------	.965	------	------	.971	------	.936
850	.922	------	.955	.909	------	.913	.901	------	.965	.896	------	.971	.883	.937
860	------	------	.954	------	------	.911	------	------	.964	------	------	.970	------	.939
870	------	------	.953	------	------	.909	------	------	.963	------	------	.969	------	.940
880	------	------	.952	------	------	.907	------	------	.963	------	------	.968	------	.941
890	------	------	.951	------	------	.905	------	------	.962	------	------	.967	------	.943
900	.922	------	.950	.909	------	.903	.901	------	.962	.896	------	.966	.884	.945
910	------	------	.949	------	------	.901	------	------	.961	------	------	.966	------	.947
920	------	------	.948	------	------	.900	------	------	.961	------	------	.965	------	.948
930	------	------	.947	------	------	.898	------	------	.961	------	------	.965	------	.950
940	------	------	.946	------	------	.897	------	------	.960	------	------	.964	------	.952
950	.922	------	.942	.909	------	.895	.901	------	.960	.896	------	.964	.884	.953
960	------	------	.937	------	------	.891	------	------	.959	------	------	.963	------	.954
970	------	------	.936	------	------	.890	------	------	.959	------	------	.962	------	.956
980	------	------	.938	------	------	.890	------	------	.959	------	------	.962	------	.957
990	------	------	.940	------	------	.890	------	------	.959	------	------	.962	------	.958
1000	.922	------	.941	.909	------	.890	.902	------	.959	.896	------	.962	.885	.960

Values of T_i for 4 mm are not tabulated above 400 or 450 mμ where the values exceed 0.995. As there is uncertainty of 0.001 or 0.002 in such values, it would be preferable, where the absorption is so slight, to compute the values of T_i for 4 mm (or for any other small thickness) from the values of T_i for 100 mm than to measure them directly.

The slight error in T_i resulting from the multiple reflections through different thicknesses of glass [8] is ignored in these results. For either high or low transmittance the error is of the order of 0.001. In view of the equal or greater uncertainties indicated above, computation of such corrections was considered unwarranted.

The authors express their appreciation to K. S. Gibson, Chief, NBS Photometry and Colorimetry Section, who coordinated the work of these spectrophotometric measurements and results; to Kenneth L. Kelly for his assistance in the computations; and to John C. Schleter for the preparation of the graphs.

4. References

[1] A. C. Hardy, History of the design of the recording spectrophotometer, J. Opt. Soc. Am. **28,** 360 (1938).
[2] J. L. Michaelson, Construction of the General Electric recording spectrophotometer, J. Opt. Soc. Am. **28,** 365 (1938).
[3] K. S. Gibson and H. J. Keegan, Calibration and operation of the General Electric recording spectrophotometer of the National Bureau of Standards, J. Opt. Soc. Am. **28,** 372 (1938).
[4] H. J. McNicholas, Equipment for routine spectral transmission and reflection measurements, BS J. Research **1,** 793 (1928) RP30.
[5] H. H. Cary and A. O. Beckman, A quartz photoelectric spectrophotometer, J. Opt. Soc. Am. **31,** 682 (1941).
[6] K. S. Gibson and M. M. Balcom, Transmission measurements on the Beckman quarts spectrophotometer, J. Research NBS **38,** 601 (1947) RP1798; also J. Opt. Soc. Am. **37,** 593 (1947).
[7] K. S. Gibson, Spectrophotometry, NBS Circular 484 (1949). See figures 29 and 30.
[8] T. Smith, Note on measurements of glass absorption, Proc. Phys. Soc. **58,** 473 (1946).
[9] K. S. Gibson, Direct-reading photoelectric measurement of spectral transmission, J. Opt. Soc. Am. and Rev. Sci. Instr. **7,** 693 (1923).

Washington, November 19, 1953.

Journal of Research of the National Bureau of Standards Vol. 52, No. 6, June 1954 Research Paper 2506

Densities of Five Selected Optical Glasses*

Charles T. Collett

Densities of five optical glasses were determined by the hydrostatic weighing method. Values are presented by type of glass, index of refraction, and Abbe value.

Each sample of glass used in these measurements was in the form of a cylindrical disk 30 mm in diameter and 5 mm thick. The observed densities of the samples were derived from their masses, determined by weighing in air, and their volumes, determined by hydrostatic weighing, with corrections for buoyancy.

For the hydrostatic weighing, a basket was suspended from the left pan of the balance by a wire that passed down through a hole in the case into a cabinet insulated against changes in temperature and air currents. The immersing liquid was distilled water in a Dewar flask closed by a stopper, through which holes of small diameter admitted the suspension wire, a glass stirring rod, and a platinum resistance thermometer. A galvanometer and Mueller-type resistance bridge continuously indicated the resistance of the thermometer, from which the water temperature was calculated.

The effect of surface tension was reduced as much as possible by the use of gold-plated platinum wire of small diameter (0.20 mm) at the region of intersection with the water surface. The errors caused by surface tension were further reduced by cancellation between the two steps of the weighing process next described.

A constant load remained on the right pan of the balance, and the immersed basket was at all times suspended from the left pan. The first step was to place each glass on the left pan with weights, W_1, sufficient to produce equilibrium. For the second step, the sample was transferred to the basket, and equilibrium was restored by increasing the weights on the pan to the value W_2.

Provided that W_1 and W_2 were determined while no change of density occurred in the water or air, the volume of the glass sample, V_s, was given by the equation

$$V_s = \frac{(W_2 - W_1)\left(1 - \frac{\rho_a}{8.4}\right)}{\rho_w - \rho_a},$$

where ρ_a and ρ_w represents the densities in grams per milliliter of air and water and 8.4 the density of the brass weights. The air density was determined by means of a special buoyancy balance.[1]

Weights were observed to 0.1 mg, and temperatures to 0.001 deg C. The observed values of density are shown in table 1.

TABLE 1. *Densities of some optical glasses, at 23° C*

Glass [a]	Observed densities	Densities computed from factors after—	
		Winkelmann and Schott [b]	Russ [c]
	g/cm³	g/cm³	g/cm³
BSC, n=1.517, ν=64.5	2.510₅	2.33	2.44
LBC, n=1.574, ν=57.7	3.191₃	3.11	3.18
F, n=1.620, ν=36.2	3.609₈	3.59	3.66
DF, n=1.649, ν=33.8	3.865₄	3.85	3.90
Rare earth, n=1.673, ν=56.2	3.786₇	[d]	[d]

[a] n is the index of refraction for the sodium D line, and ν, the Abbe value, equals $(n-1)/(n_F - n_C)$, where n_F and n_C are refractive indices for the hydrogen F and C lines, respectively.
[b] From Winkelmann and Schott's factors for oxides in glass (see footnote 2).
[c] From Russ' factors for oxides in glass (see footnote 2).
[d] No factors were given for rare-earth oxides.

Winkelmann and Schott, and Russ,[2] among others, made density determinations on selected glasses and derived factors for various component oxides. By use of these factors, the density of the glass could be roughly computed.

The last two columns in table 1 give density values thus computed. The differences between these and the observed values vary from less than 0.5 percent to more than 7 percent. This is not surprising, in view of Hovestadt's [3] comparisons of 29 glasses, where trial density computations based on these factors revealed differences as large as 10 percent.

*The companion papers in this issue present values of the index of refraction, spectral transmissive properties, and coefficients of linear thermal expansion for five different types of optical glasses produced by the Optical Glass Section of the National Bureau of Standards. These measurements have been made in the different organizational parts of the Bureau appropriate to each type of measurement, and are, therefore, presented separately. For each type of glass the samples have been taken from the same melt, and, therefore, these papers present, collectively, a consistent set of data for the five glasses studied.

[1] N. S. Osborne, E. C. McKelvy, and H. W. Bearce, Bul. BS **9**,327 (1913) S197 (see p. 378).
[2] Geo. W. Morey, The properties of glass, p. 223 (Rheinhold Publishing Corp., New York, N. Y., 1938).
[3] H. Hovestadt, Jena glass and its scientific and industrial applications, p. 148 (Macmillan & Co., Ltd., London, 1902).

WASHINGTON, August 14, 1953.

Journal of Research of the National Bureau of Standards Vol. 52, No. 6, June 1954 Research Paper 2507

Thermal Expansion of Five Selected Optical Glasses [1]

Peter Hidnert

Coefficients of linear thermal expansion of five optical glasses were determined by a strain gage method for the range between room temperature and 60° C. The coefficients of expansion of two crown glasses are 7.6×10^{-6} per deg C. A rare-earth glass was found to have a slightly lower coefficient of expansion, but the coefficients of expansion of two flint glasses are 10 percent larger than the other glasses.

This paper gives coefficients of linear thermal expansion of five samples of optical glasses. The chemical composition of these glasses are given in Research Paper 2504.

The diameter of each sample of glass was 30 mm. The length of each sample was 105 mm, except sample DF (table 1), which was 97 mm long. Determinations were made on the linear thermal expansion of these glasses on heating and cooling between 23° and 60° C. An electric-resistance strain-gage method was used. When a strain gage, consisting of a fine wire, is attached to a sample of solid material, changes in length of the wire accompanying thermal expansion of the sample are proportional to the changes in electrical resistance of the wire. Information about commercially available types of wire strain gages has been given by Ramberg.[2]

Two SR4 (type A 11) strain gages connected in series, were attached with a cellulose nitrate cement on opposite sides of each sample of glass and of each of three reference samples. These reference samples were duplicates of samples of invar, glass, and steel on which coefficients of linear thermal expansion had previously been determined by the precision micrometric method [3] of the Bureau. After the cement was sufficiently dried, the cemented gages were coated with wax. The glass and reference samples with their attached gages were then subjected to two cycles of heating and cooling between room temperature and 60° C, in order to allow the gages to adjust themselves to the samples before observations were made. During these cycles of heating and cooling, all samples were held at the maximum temperature for 2 hours.

The samples of glass and the reference samples with attached strain gages were supported vertically in an electrically controlled temperature cabinet. Two copper leads extended from each sample and from each reference sample to an SR4 strain indicator (type K). Four copper-constantan thermocouples placed symmetrically in the region of the glass samples and the reference samples were connected to a precision potentiometer.

Observations were made at room temperature and at 60° C, during three cycles of heating and cooling, on each sample of glass in conjunction with each reference sample of known expansion. These observations at constant temperatures, consisted of strain-indicator readings recorded to the nearest microinch per inch and of potentiometer readings recorded to the nearest microvolt. The latter readings were converted to temperatures to the nearest 0.1 deg C. The coefficients of linear thermal expansion of the five samples of glass given in table 1, were derived from the data. These coefficients of expansion are believed to be accurate to $\pm0.1\times10^{-6}$.

TABLE 1. *Coefficients of linear thermal expansion of some optical glasses*

Glass [a]	Observed average coefficient of expansion per deg C between 23° and 60° C	Computed [b] coefficient of expansion per deg C
BSC, $n=1.517$, $\nu=64.5$	7.6×10^{-6}	7.6×10^{-6}
LBC, $n=1.574$, $\nu=57.7$	7.6	7.8
F , $n=1.620$, $\nu=36.2$	8.4	8.5
DF , $n=1.649$, $\nu=33.8$	8.3	8.5
Rare earth, $n=1.673$, $\nu=56.2$	7.5	(c)

[a] n=index of refraction for the sodium D line, and ν, the Abbe value$=(n-1)/(n_F-n_C)$, where n_F and n_C are refractive indices for the hydrogen F and C lines, respectively.

[b] From English and Turner's factors for oxides in glass for the range from 25° to 90° C (see footnote 4).

[c] No factor was given by English and Turner for La_2O_3 in this glass.

The last column in table 1 gives coefficients of expansion computed from English and Turner's [4] factors.[5] One-third of the sum of the products of the factors and the precentages of the corresponding constituent oxides of a glass gives a computed coefficient of linear thermal expansion. The agreement between the observed and computed coefficients of linear expansion of the glasses is good.

[1] The companion papers in this issue present values of the index of refraction, spectral transmissive properties, and densities for five different types of optical glasses produced by the Optical Glass Section of the National Bureau of Standards. These measurements have been made in the different organizational parts of the Bureau appropriate to each type of measurement, and are, therefore, presented separately. For each type of glass the samples have been taken from the same melt, and, therefore, these papers present, collectively, a consistent set of data for the five glasses studied.

[2] W. Ramberg, Contributions of electricity to mechanics, J. Wash. Acad. Sci. **39**, 281 (Sept. 1949).

[3] P. Hidnert and W. Souder, Thermal expansion of solids, NBS Circular 486 (1950).

[4] S. English and W. E. S. Turner, Relationship between chemical composition and the thermal expansion of glasses, J. Am. Ceram. Soc. **10**, 551 (1927); Corrections on "Relationship between chemical composition and the thermal expansion of glasses," J. Am. Ceram. Soc. **12**, 760 (1929).

[5] For computing coefficients of cubical expansion.

The coefficients of expansion of the two crown glasses (BSC 1.517 and LBC 1.574) and the rare earth glass 1.673 are practically the same and about 10 percent smaller than the coefficients of expansion of the two flint glasses (F 1.620 and DF 1.649).

The author acknowledges his indebtedness to R. C. Valore, Jr. of the NBS Structural Engineering Section for helpful suggestions in the application of the strain-gage method and to H. S. Krider of the Length Section for assistance in the experimental work.

WASHINGTON, July 14, 1953.

Journal of Research of the National Bureau of Standards Vol. 52, No. 6, June 1954 Research Paper 2508

Evaluation of the Exponential Integral for Large Complex Arguments

John Todd

Two methods of evaluating the exponential integral for (large) complex arguments are discussed. It is shown that the Laguerre quadrature method is more efficient than the asymptotic expansion. Examples are given to show the practicability of the Laguerre method.

1. Introduction

An extensive table of the exponential integral

$$E_1(z)=\int_z^\infty (e^{-u}/u)du \qquad z=x+iy$$

has been prepared by the National Bureau of Standards [1];[1] the introduction to the table gives a precise definition of this function. This table covers the range $|x|\leq 20$, $|y|\leq 20$, with arguments variously spaced. In order to compute $E_1(z)$ outside this range, (or within this range, at points where interpolation is awkward, which are those with comparatively large argument), several methods can be considered. We examine two in detail and recommend the Laguerre quadrature, which is certainly practicable in the case of isolated arguments.

2. Asymptotic Series

The first of these is the use of the asymptotic series (see e. g., [1]),

$$E_1(z)\sim e^{-z}\left(\frac{1}{z}-\frac{1!}{z^2}+\frac{2!}{z^3}-\frac{3!}{z^4}+\cdots\right).$$

The remainder after n terms in the expansion for $e^zE_1(z)$ can be obtained by integration by parts and is

$$R_n=(-)^n n!e^z\int_z^\infty \frac{e^{-u}}{u^{n+1}}\,du.$$

If we put $u=z+\rho$, where ρ is real, then

$$R_n=(-)^n n!\int_0^\infty \frac{e^{-\rho}d\rho}{[(x+\rho)+iy]^{n+1}},$$

which can be estimated as

$$|R_n|\leq S_n=n![x^2+y^2]^{-\frac{1}{2}(n+1)} \qquad \text{if } x\geq 0$$

$$|R_n|\leq T_n=n!|y|^{-n-1} \qquad \text{if } x\leq 0,$$

from which the asymptotic character of the series is evident. In fact,

$$\frac{S_{n+1}}{S_n}=\frac{n+1}{(x^2+y^2)^{\frac{1}{2}}},$$

and so S_n decreases as n increases until n exceeds $(x^2+y^2)^{\frac{1}{2}}$. To obtain the least the least value of S_n we have to take $n\doteq(x^2+y^2)^{\frac{1}{2}}=|z|$. For this value of n, we find, using Stirling's formula, that S_n is about $(2\pi/n)^{\frac{1}{2}}e^{-n}$. In the second case, the least value of T_n is formally the same, but

[1] Figures in brackets indicate the literature references at the end of this paper.

now $n \doteq |y|$. The decrease in the effectiveness of this representation as z approaches the negative real axis is apparent from the estimates.

We note that the evaluation of the sums of the first n terms of the series for $e^z E_1(z)$, as a polynomial in z^{-1}, by successive multiplication by z^{-1} for instance, involves about $4n$ real multiplications, z being complex.

3. Laguerre Quadrature

The second method is the use of a Laguerre quadrature. We shall show that this is more efficient than the asymptotic series method just described.

We have

$$e^z E_1(z) = I_1 - iI_2,$$

where

$$I_1 = \int_0^\infty e^{-\rho} \cdot \frac{x+\rho}{(x+\rho)^2+y^2} \cdot d\rho, \quad I_2 = \int_0^\infty e^{-\rho} \cdot \frac{y}{(x+\rho)^2+y^2} \cdot d\rho.$$

It is well known [3] that, for any n,

$$I = \int_0^\infty e^{-t} \cdot f(t) \cdot dt \doteq \Sigma \lambda_i^{(n)} f(x_i^{(n)}) = Q,$$

where the $x_i^{(n)}$ are the zeros of the Laguerre polynomial $L_n(t)$, and the $\lambda_i^{(n)}$ are the corresponding Christoffel numbers. The $x_i^{(n)}$, $\lambda_i^{(n)}$ have been tabulated for $n=1(1)15$, $i=1(1)n$ by Salzer and Zucker [2].

Moreover, it is known [3] that for some ξ, $0 \leq \xi \leq \infty$,

$$R = [I-Q] = (n!)^2 \frac{f^{(2n)}(\xi)}{(2n)!}.$$

We shall now estimate this error. It is convenient to handle the two integrals separately. We calculate the $2n$th derivatives of

$$f_1(t) = \frac{x+t}{(x+t)^2+y^2}, \quad f_2(t) = \frac{y}{(x+t)^2+y^2}$$

and find

$$R_1 = (n!)^2 r_1^{-2n-1} \cos(2n+1)\theta_1,$$

$$R_2 = (n!)^2 r_2^{-2n-1} \sin(2n+1)\theta_2,$$

where the $\xi_i = \xi_i(x, y)$ satisfy $0 \leq \xi_i \leq \infty$, $r_i = [(x+\xi_i)^2+y^2]^{\frac{1}{2}}$, and θ_i is defined by $\cos\theta_i = (x+\xi_i)/r_i$, $\sin\theta_i = y/r_i$.

Hence

$$|R_i| \leq \frac{(n!)^2}{[x^2+y^2]^{n+\frac{1}{2}}} \qquad x \geq 0,$$

$$|R_i| \leq \frac{(n!)^2}{|y|^{2n+1}} \qquad x \leq 0.$$

The difficulties that were noticed in section 2, as z approaches the negative real axis, are still present. As before, there is an optimum value of n, which is about $|z|$ in the first case, $|y|$ in the second. With this choice of n, the value of our bounds for the R_i are about $2\pi e^{-2n}$ in each case.

The important fact to notice is that our estimate for the error committed by using an n-point Laguerre quadrature is approximately the square of that for the estimate of the error committed by neglecting all terms in the asymptotic series after the nth. This, together with the fact that about the same number ($4n$) of real multiplications are required in both methods, indicates that the Laguerre method is more efficient.

4. Examples

In order to demonstrate the practicability of the Laguerre method, and to show that our conclusions are not dependent on the crudity of our appraisals of the remainders, we give three examples in detail. We choose $n=5$, which is optimum in one but not in the others. For completeness, we repeat (from [2]) the values of $x_i^{(5)}$, $\lambda_i^{(5)}$.

$x_i^{(5)}$	$\lambda_i^{(5)}$
0. 26356 03197 18	0. 52175 56105 83
1. 41340 30591 07	. 39866 68110 83
3. 59642 57710 41	. 07594 24496 817
7. 08581 00058 59	. 00361 17586 7992
12. 64080 08442 76	. 00002 33699 723858

The superscripts (5) will be dropped from now on.

We shall work to about 10 decimals throughout our examples. We begin with a case of z real: $z=10$ and follow with $z=1+10i$, and then $z=-10+5i$; it is only in the last case that we are, with $n=5$, near the optimum number of terms.

(a) $z=10$.

In this case $f_2=0$, and we have only to deal with

$$I_1=\int_0^\infty e^{-t}\cdot\frac{1}{(10+t)}\cdot dt\doteq\sum\lambda_i\cdot\frac{1}{10+x_i}=Q_1.$$

A complete worksheet for this calculation follows. The sum Q_1 is cumulated on the machine, there being no reason to record individual products.

$\alpha_i=10+x_i$	α_i^{-1}
10. 26356 03197	0. 09743 20771
11. 41340 30591	. 08761 62872
13. 59642 57710	. 07354 87412
17. 08581 00059	. 05852 81002
22. 64080 08443	. 04416 80490

$$Q_1=\sum\lambda_i\alpha_i^{-1}=0.\ 09156\ 33319$$

The correct value of $e^{10}E_1(10)$ is 0. 09156 3334. The actual error is about 2×10^{-9}, whereas our estimate is 144×10^{-9}. Using five terms of the asymptotic series, we obtain the value 0.09164. There is thus an actual error of about 8×10^{-5}, compared with an estimated error of 12×10^{-5}.

(b) $z=1+10i$.

In this case we have

$$e^{1+10i}E_1(1+10i)=I_1-iI_2,$$

where

$$I_1=\int_0^\infty e^{-t}\cdot\frac{1+t}{(1+t)^2+100}\cdot dt\doteq\sum\lambda_i\cdot\frac{1+x_i}{(1+x_i)^2+100}=\sum(1+x_i)\left\{\frac{\lambda_i}{(1+x_i)^2+100}\right\}$$

and

$$I_2=\int_0^\infty e^{-t}\cdot\frac{10}{(1+t)^2+100}\cdot dt\doteq\sum\lambda_i\cdot\frac{10}{(1+x_i)^2+100}=\sum10\left\{\frac{\lambda_i}{(1+x_i)^2+100}\right\}.$$

A complete work sheet for this calculation follows. It is convenient to compute the common factors γ_i, in braces { } above, and then obtain the sums $\sum\alpha_i\gamma_i$ and $\sum 10\gamma_i$ by accumulation on the machine.

$\alpha_i=1+x_i$	$\beta_i=100+\alpha_i^2$	$\gamma_i=\lambda_i/\beta_i$
1. 26356 0320	101. 59658 47	0. 00513 55625
2. 41340 3059	105. 82451 43	. 00376 72444
4. 59642 5771	121. 12712 99	. 00062 69648
8. 08581 0006	165. 38032 35	. 00002 18391
13. 64080 0844	286. 07144 76	. 00000 00817

$$\mathscr{R}e^{1+10i}E_1(1+10i)\doteq\sum\alpha_i\gamma_i=0.01864\ 0471$$

$$\mathscr{I}e^{1+10i}E_1(1+10i)\doteq-\sum 10\gamma_i=-0.09551\ 6925$$

The correct value of $e^{1+10i}E_1(1+10i)$ is $0.01864\ 049-0.09551\ 688i$.
The actual error is of the order of 5×10^{-8}, whereas our estimate is about 144×10^{-8}. Using five terms of the asymptotic series gives

$$0.018595-0.095600i.$$

There is thus an actual error of about 1×10^{-4}, compared with an estimated error of about 1.2×10^{-4}.

(c) $z=-10+5i$

$\alpha_i=-10+x_i$	$\beta_i=25+\alpha_i^2$	$\gamma_i=\lambda_i/\beta_i$
−9. 73643 9680	119. 79825 76	0. 00435 52855
−8. 58659 6941	98. 72964 70	. 00403 79645
−6. 40357 4229	66. 00576 29	. 00115 05428
−2. 91418 9994	33. 49250 33	. 00010 78378
2. 64080 0844	31. 97382 91	. 00000 07309

$$\mathscr{R}e^{-10+5i}E_1(-10+5i)\doteq\sum\alpha_i\gamma_i=-0.08475\ 7264$$

$$\mathscr{I}e^{-10+5i}E_1(-10+5i)\doteq-\sum 5\gamma_i=-0.04826\ 1807$$

The correct value of $e^{-10+5i}E_1(-10+5i)$ is

$$-.08475\ 749-0.04826\ 039i.$$

The actual error is of the order of 2×10^{-8}, whereas our estimate is about 3×10^{-4}. Using five terms of the asymptotic series, we obtain the value

$$-0.084855-0.048277i.$$

There is thus an actual error of about 1×10^{-4}, compared with an estimated error of about 8×10^{-3}.

5. Remarks

1. A third method of attack is conceivable: The integration in the complex plane of the differential equation for $E_1(z)$, taking z^{-1} as the independent variable, extending the ideas of Fox and Miller [4].

2. It is conceivable that the Laguerre method would be effective in cases when the integrand is not precisely of the form $e^{-t}f(t)$. A case of importance might be that of the generalized exponential integral $\int^\infty(e^{-w}/w)du$, where $w=(a^2+u^2)^{\frac{1}{2}}$. In such a case it would be convenient to follow the device of A. Reiz [5] and use the quadrature in the form

$$\int_0^\infty F(t)dt\doteq\sum\mu_i^{(n)}F(x_i^{(n)}),$$

where $\mu_i^{(n)}=\lambda_i^{(n)} \exp x_i^{(n)}$; the $\mu_i^{(n)}$ have been tabulated by Salzer and Zucker [2].

3. The table of Mashiko [6] gives $E_1(z)$, or rather auxiliary functions from which this can be obtained, for $z=re^{i\theta}$ when $r^{-1}=0.01(0.01)0.2$ and $\theta=0(2°)60°(1°)90°$.

6. References

[1] National Bureau of Standards, Tables of $E_1(z)$, (publication pending).

[2] H. E. Salzer and Ruth Zucker, Table of the zeros and weight factors of the first fifteen Laguerre polynomials, Am. Math. Soc. Bul. **55,** 1004–1012 (1949).

[3] G. Szegö, Orthogonal polynomials, Amer. Math. Soc. Coll. Publications **23,** 369 (1939).

[4] L. Fox and J. C. P. Miller, Table-making for large arguments. The exponential integral, MTAC **5,** 163–167 (1951).

[5] A. Reiz, On the numerical solution of certain types of integral equations, Arkiv for Mat., Astron. Fysik, **29** (A); No. 29 (1943).

[6] M. Mashiko, Tables of generalized exponential-, sine-, and cosine-integrals, Numerical Computation Bureau, Report No. 7 (Tokyo,1953).

WASHINGTON, February 2, 1954.

Journal of Research of the National Bureau of Standards Vol. 52, No. 6, June 1954 Research Paper 2509

On Nearly Triangular Matrices [1]

A. M. Ostrowski [2]

A discussion is presented of the change in the inverse of a triangular matrix if on one side the zeros are replaced by sufficiently small numbers and on the other side the non-vanishing elements are varied by sufficiently small amounts.

1. Introduction

Consider a system of linear equations

$$\sum_{\nu=1}^{n} a_{\mu\nu}x_\nu = y_\mu \qquad (\mu=1, \ldots, n), \tag{1}$$

with the matrix A, in which all diagonal elements $a_{\mu\mu}$ $(\mu=1, \ldots, n)$ are not equal to 0 and the elements off the diagonal satisfy for two positive numbers m, M the inequalities

$$\left.\begin{aligned} |a_{\mu\nu}| &\leqq m|a_{\mu\mu}| \quad (\nu<\mu;\ \mu=1, \ldots, n), \\ |a_{\mu\nu}| &\leqq M|a_{\mu\mu}| \quad (\nu>\mu;\ \mu=1, \ldots, n-1). \end{aligned}\right\} \tag{2}$$

If m is very small, the system does not essentially differ from the corresponding "triangular" system in which all $a_{\mu\nu}$ with $\nu<\mu$ are replaced by zeros and the matrix of which will be denoted by $A^{(0)}$. It then appears plausible that the solution of this triangular system does not differ very much from that of the system (1).

However, the value of the determinant of the order n

$$\begin{vmatrix} 1 & -M & 0 & & & 0 & 0 \\ 0 & 1 & -M & & & & 0 \\ & & \cdot & \cdot & & & \\ & & & \cdot & \cdot & & \\ & & & & \cdot & \cdot & \\ & & & & & \cdot & \cdot \\ 0 & & & & & 1 & -M \\ -m & 0 & & & & 0 & 1 \end{vmatrix} = 1-mM^{n-1},$$

shows that if M is, for instance, greater than or equal to 10, the determinant of our system will not be necessarily different from zero unless $m<10^{-(n-1)}$. A detailed study of the problems connected with the matrices characterized by (2) appears, therefore, to be of importance and interest.

As the first problem in this connection, we give a necessary and sufficient condition that any matrix A satisfying conditions (2) be nonsingular. If $m<M$, this condition is given by

$$\frac{m}{(1+m)^n}<\frac{M}{(1+M)^n}, \tag{3}$$

[1] This paper was prepared under a National Bureau of Standards contract with American University.

[2] American University and University of Basle, Switzerland.

and, if $m=M$, by [3]

$$m<\frac{1}{n-1}. \tag{3^o}$$

In order to obtain a precise measure of the influence of the change from A to $A^{(0)}$, we have to discuss the estimates (for convenient norms) of the norm of the matrix $A^{-1}-A^{(0)-1}$.

We consider, in particular, two such norms defined in section 5 and denoted by $|A^{-1}-A^{(0)-1}|_p$, $(p=1,\infty)$, which are particularly suitable for the problems of numerical analysis. Assuming, without loss of generality, that $a_{\mu\mu}=1$ $(\mu=1, \ldots, n)$, we show that for given values of m, M such that $M\leqq 1.5/n$, $n\geqq 4$, we have

$$|A^{-1}-A^{(0)-1}|_p\leqq(1+M)^{n-1}\frac{\delta}{1-\delta}\quad\left(M\leqq\frac{1.5}{n},\ n\geqq 4\right), \tag{4}$$

where $1-\delta$ is the smallest modulus of the determinant attainable for the matrices A and is connected with m by the relation

$$\delta=\frac{M_n m}{1-\theta\dfrac{m}{M}},\qquad 0<\theta<1, \tag{5}$$

with

$$M_n=\frac{(1+M)^n-nM-1}{M}. \tag{6}$$

If $M<1.5/n$, the formula (4) need not be valid any longer, but we can prove in this case the relation

$$|A^{-1}-A^{(0)-1}|_p\leqq\frac{6nm}{1-2nm}\qquad(M\leqq 1.5/n) \tag{7}$$

is valid as long as m remains less than $1/2n$.

The estimate (7) is not a "best" estimate for all values of $M\leqq 1.5/n$, but still it is not far from the best, since for $m=M\leqq 1/(n-1)$ we have

$$|A^{-1}-A^{(0)-1}|_p\leqq\frac{(n-1)m}{1-(n-1)m}\qquad\left(m=M<\frac{1}{n-1}\right), \tag{8}$$

which cannot be improved for any value of $m<1/(n-1)$.

The condition (3) is derived in section 4, theorem B. However, we derive it as a special case of a more general theorem, where in the inequalities (2) the expressions m, M *depend on* μ, that is to say, change from one row to another. The necessary and sufficient condition for all matrices A to be regular (theorem A, section 4) is in this case rather unwieldy, but still may be very useful in some cases because it contains $2n-2$ instead of two essential parameters. The direct derivation of theorem B is, of course, much simpler, since, as the reader will immediately see, the computations of the determinant Ω_n in section 2 can be considerably shortened in this case. The connection between the formal algebra of sections 2 and 3 and theorems A and B is provided by a result concerning the so-called H-determinants and M-determinants published 16 years ago [1]. The results about the norms $|A^{-1}-A^{(0)-1}|_p$ are obtained by using the explicit representation of the inverse matrix of a certain matrix Δ_n, which provides a majorant for all matrices A^{-1}. The formulas giving Δ_n^{-1} are derived in the second part of section 3, and in section 6 the norms $|\Delta_n^{-1}-\Delta_n^{(0)-1}|_p$ are derived and discussed. The corresponding inequalities for $|A^{-1}-A^{(0)-1}|_p$ are then obtained in section 8, by using a new theorem (lemma III) concerning the connection between the H-determinants and the M-determinants.

---

[3] This condition (3°) is already contained in some results in a paper [2][4], and also can be deduced from a well-known theorem of the theory of determinants discussed in [6].

[4] Figures in brackets indicate the literature references at the end of this paper.

In this section is given another application of this theorem in estimating the variation in the inverse matrix of a triangular matrix satisfying the conditions (2) with $m=0$. We obtain an unexpectedly simple and elegant formula (120).

In section 8, the results are applied explicitly to the problems concerning the linear system (1). It may be finally remarked that these results, with obvious changes, remain valid if in the matrix of (1) the rows and the columns are interchanged, although no mention is made of it explicitly at every step.[5]

2. Value of the Determinant Ω_n

Let K_n be defined by

$$K_n=\begin{vmatrix} \kappa_n & \delta_n & 0 & 0 & \cdots & 0 & 0 \\ \kappa_{n-1} & \kappa_{n-1} & \delta_{n-1} & 0 & \cdots & 0 & 0 \\ \kappa_{n-2} & \kappa_{n-2} & \kappa_{n-2} & \delta_{n-2} & \cdots & 0 & 0 \\ \cdot & \cdot & \cdot & \cdot & \cdots & \cdot & \cdot \\ \cdot & \cdot & \cdot & \cdot & \cdots & \cdot & \cdot \\ \cdot & \cdot & \cdot & \cdot & \cdots & \cdot & \cdot \\ \kappa_2 & \kappa_2 & \kappa_2 & \kappa_2 & \cdots & \kappa_2 & \delta_2 \\ \kappa_1 & \kappa_1 & \kappa_1 & \kappa_1 & \cdots & \kappa_1 & \kappa_1 \end{vmatrix} \qquad (n\geqq 3), \tag{9}$$

$$K_1=\kappa_1, \qquad K_2=\begin{vmatrix} \kappa_2 & \delta_2 \\ \kappa_1 & \kappa_1 \end{vmatrix}=\kappa_1(\kappa_2-\delta_2),$$

where in the μ-th row all elements to the left of the main diagonal and on this diagonal are equal to $\kappa_{n-\mu+1}$, the next element to the right is $\delta_{n-\mu+1}$, and all other elements are 0. κ_μ, δ_μ are here independent variables. In subtracting the second column from the first, we obtain $K_n=(\kappa_n-\delta_n)K_{n-1}$, and therefore the following formula, valid also for $n=1, 2$:

$$K_n=\kappa_1 \prod_{\nu=2}^{n}(\kappa_\nu-\delta_\nu). \tag{10}$$

Consider now for $n\geqq 3$ the determinant

$$T_n=\begin{vmatrix} \delta_n & 0 & 0 & 0 & \cdots & 0 & \beta_n \\ \gamma_{n-1} & \delta_{n-1} & 0 & 0 & \cdots & 0 & \beta_{n-1} \\ \gamma_{n-2} & \gamma_{n-2} & \delta_{n-2} & 0 & \cdots & 0 & \beta_{n-2} \\ \cdot & \cdot & \cdot & \cdot & \cdots & \cdot & \cdot \\ \cdot & \cdot & \cdot & \cdot & \cdots & \cdot & \cdot \\ \cdot & \cdot & \cdot & \cdot & \cdots & \cdot & \cdot \\ \gamma_2 & \gamma_2 & \gamma_2 & \gamma_2 & \cdots & \delta_2 & \beta_2 \\ 1 & 1 & 1 & 1 & \cdots & 1 & 0 \end{vmatrix} \qquad (n\geqq 3). \tag{11}$$

[5] Some of the results contained in the sections 2 to 5 have been published without proof in [3].

We have in particular

$$T_3=\begin{vmatrix}\delta_3 & 0 & \beta_3\\ \gamma_2 & \delta_2 & \beta_2\\ 1 & 1 & 0\end{vmatrix}=-(\delta_3\beta_2+\beta_3(\delta_2-\gamma_2)). \tag{12}$$

Developing T_n in the elements of the first line and using the value (10) of K_n, we obtain for $n\geqq 4$

$$T_n=\delta_n T_{n-1}-\beta_n\prod_{\nu=2}^{n-1}(\delta_\nu-\gamma_\nu),$$

$$\frac{T_n}{\delta_2\dots\delta_n}=\frac{T_{n-1}}{\delta_2\dots\delta_{n-1}}-\frac{\beta_n}{\delta_n}\prod_{\nu=2}^{n-1}\left(1-\frac{\gamma_\nu}{\delta_\nu}\right),$$

and therefore generally for $n\geqq 4$

$$\frac{T_n}{\delta_2\dots\delta_n}=-\left[\frac{\beta_n}{\delta_n}\prod_{\nu=2}^{n-1}\left(1-\frac{\gamma_\nu}{\delta_\nu}\right)+\frac{\beta_{n-1}}{\delta_{n-1}}\prod_{\nu=2}^{n-2}\left(1-\frac{\gamma_\nu}{\delta_\nu}\right)+\dots+\frac{\beta_4}{\delta_4}\prod_{\nu=2}^{3}\left(1-\frac{\gamma_\nu}{\delta_\nu}\right)\right]+\frac{T_3}{\delta_2\delta_3}. \tag{13}$$

Since by (12)

$$\frac{T_3}{\delta_2\delta_3}=-\frac{\beta_2}{\delta_3}\left(1-\frac{\gamma_2}{\delta_2}\right)-\frac{\beta_2}{\delta_2}$$

we obtain

$$\frac{-T_n}{\delta_2\dots\delta_n}=\sum_{\mu=2}^{n}\frac{\beta_\mu}{\delta_\mu}\prod_{\nu=2}^{\mu-1}\left(1-\frac{\gamma_\nu}{\delta_\nu}\right),$$

where $\prod_{\nu=2}^{1}$ is identically 1, and therefore finally

$$T_n=-\sum_{\mu=2}^{n}\beta_\mu\prod_{\nu=\mu+1}^{n}\delta_\nu\prod_{\nu=2}^{\mu-1}(\delta_\nu-\gamma_\nu). \tag{14}$$

If we now put

$$T_n^*=\begin{vmatrix}\delta_1 & 0 & 0 & \dots & 0 & \beta_1\\ \gamma_2 & \delta_2 & 0 & \dots & 0 & \beta_2\\ \cdot & \cdot & \cdot & \dots & \cdot & \cdot\\ \cdot & \cdot & \cdot & \dots & \cdot & \cdot\\ \cdot & \cdot & \cdot & \dots & \cdot & \cdot\\ \gamma_{n-1} & \gamma_{n-1} & \gamma_{n-1} & \dots & \gamma_{n-1} & \beta_{n-1}\\ 1 & 1 & 1 & \dots & 1 & 0\end{vmatrix}\quad(n\geqq 3), \tag{15}$$

$$T_3^*=\begin{vmatrix}\delta_1 & 0 & \beta_1\\ \gamma_2 & \delta_2 & \beta_2\\ 1 & 1 & 0\end{vmatrix},$$

this becomes T_n if the indices of β_ν, γ_ν, δ_ν are replaced by their complements with respect to $n+1$. We obtain then from (14)

$$T_n^*=-\sum_{\mu=2}^{n}\beta_{n+1-\mu}\prod_{\nu=\mu+1}^{n}\delta_{n+1-\nu}\prod_{\nu=2}^{\mu-1}(\delta_{n+1-\nu}-\gamma_{n+1-\nu}),$$

or in replacing the summation index μ by $n+1-\kappa$

$$T_n^* = -\sum_{\kappa=1}^{n-1} \beta_\kappa \prod_{\nu=n+2-\kappa}^{n} \delta_{n+1-\nu} \prod_{\nu=2}^{n-\kappa} (\delta_{n+1-\nu} - \gamma_{n+1-\nu})$$

and finally, if in both products ν is replaced by $n+1-\lambda$,

$$T_n^* = -\sum_{\kappa=1}^{n-1} \beta_\kappa \prod_{\lambda=1}^{\kappa-1} \delta_\lambda \prod_{\lambda=\kappa+1}^{n-1} (\delta_\lambda - \gamma_\lambda). \tag{16}$$

Consider now for $n \geqq 3$ the determinant

$$\Omega_n = \begin{vmatrix} \alpha_1 & -M_1 & -M_1 & \cdot & \cdot & \cdot & -M_1 \\ -m_2 & \alpha_2 & -M_2 & \cdot & \cdot & \cdot & -M_2 \\ -m_3 & -m_3 & \alpha_3 & \cdot & \cdot & \cdot & -M_3 \\ \cdot & \cdot & \cdot & \cdot & \cdot & \cdot & \cdot \\ \cdot & \cdot & \cdot & \cdot & \cdot & \cdot & \cdot \\ \cdot & \cdot & \cdot & \cdot & \cdot & \cdot & \cdot \\ -m_n & -m_n & -m_n & \cdot & \cdot & \cdot & \alpha_n \end{vmatrix}. \tag{17}$$

If we subtract here the last column from each of the preceding ones, we obtain

$$\begin{vmatrix} M_1+\alpha_1 & 0 & 0 & \cdot & \cdot & \cdot & 0 & -M_1 \\ M_2-m_2 & M_2+\alpha_2 & 0 & \cdot & \cdot & \cdot & 0 & -M_2 \\ M_3-m_3 & M_3-m_3 & M_3+\alpha_3 & \cdot & \cdot & \cdot & 0 & -M_3 \\ \cdot & \cdot & \cdot & \cdot & \cdot & \cdot & \cdot & \cdot \\ \cdot & \cdot & \cdot & \cdot & \cdot & \cdot & \cdot & \cdot \\ \cdot & \cdot & \cdot & \cdot & \cdot & \cdot & \cdot & \cdot \\ M_{n-1}-m_{n-1} & M_{n-1}-m_{n-1} & M_{n-1}-m_{n-1} & \cdot & \cdot & \cdot & M_{n-1}-m_{n-1} & -M_{n-1} \\ -(\alpha_n+m_n) & -(\alpha_n+m_n) & -(\alpha_n+m_n) & \cdot & \cdot & \cdot & -(\alpha_n+m_n) & \alpha_n \end{vmatrix}.$$

Here the subdeterminant corresponding to the last element of the last row is obviously $\prod_{\nu=1}^{n-1} (M_\nu+\alpha_\nu)$, so that Ω_n is the sum of $\alpha_n \prod_{\nu=1}^{n-1} (M_\nu+\alpha_\nu)$, and

$$-(\alpha_n+m_n) \begin{vmatrix} M_1+\alpha_1 & 0 & 0 & \cdot & \cdot & \cdot & 0 & -M_1 \\ M_2-m_2 & M_2+\alpha_2 & 0 & \cdot & \cdot & \cdot & 0 & -M_2 \\ M_3-m_3 & M_3-m_3 & M_3+\alpha_3 & \cdot & \cdot & \cdot & 0 & -M_3 \\ \cdot & \cdot & \cdot & \cdot & \cdot & \cdot & \cdot & \cdot \\ \cdot & \cdot & \cdot & \cdot & \cdot & \cdot & \cdot & \cdot \\ \cdot & \cdot & \cdot & \cdot & \cdot & \cdot & \cdot & \cdot \\ M_{n-1}-m_{n-1} & M_{n-1}-m_{n-1} & M_{n-1}-m_{n-1} & \cdot & \cdot & \cdot & M_{n-1}+\alpha_{n-1} & -M_{n-1} \\ 1 & 1 & 1 & \cdot & \cdot & \cdot & 1 & 0 \end{vmatrix}.$$

This last determinant becomes T_n^* if we put

$$\delta_\nu = M_\nu + \alpha_\nu, \quad \gamma_\nu = M_\nu - m_\nu, \quad \beta_\nu = -M_\nu \qquad (\nu = 1, \ldots, n-1),$$

and has therefore by (16) the value

$$-\sum_{\varkappa=1}^{n-1}(-M_\varkappa)\prod_{\lambda=1}^{\varkappa-1}(M_\lambda+\alpha_\lambda)\prod_{\lambda=\varkappa+1}^{n-1}(m_\lambda+\alpha_\lambda).$$

We obtain therefore for Ω_n the expression

$$\Omega_n = \alpha_n \prod_{\nu=1}^{n-1}(M_\nu+\alpha_\nu) - \sum_{\varkappa=1}^{n-1} M_\varkappa \prod_{\lambda=1}^{\varkappa-1}(M_\lambda+\alpha_\lambda)\prod_{\lambda=\varkappa+1}^{n}(m_\lambda+\alpha_\lambda). \tag{18}$$

The determinant Ω_n can be also written in the form

$$\Omega_n = \begin{vmatrix} \alpha_n & -m_n & -m_n & \ldots & -m_n & -m_n \\ -M_{n-1} & \alpha_{n-1} & -m_{n-1} & \ldots & -m_{n-1} & -m_{n-1} \\ -M_{n-2} & -M_{n-2} & \alpha_{n-2} & \ldots & -m_{n-2} & -m_{n-2} \\ \cdot & \cdot & \cdot & \ldots & \cdot & \cdot \\ \cdot & \cdot & \cdot & \ldots & \cdot & \cdot \\ \cdot & \cdot & \cdot & \ldots & \cdot & \cdot \\ -M_2 & -M_2 & -M_2 & \ldots & \alpha_2 & -m_2 \\ -M_1 & -M_1 & -M_1 & \ldots & -M_1 & \alpha_1 \end{vmatrix}, \tag{19}$$

and we obtain therefore from (18)

$$\Omega_n = \alpha_1 \prod_{\nu=2}^{n}(m_\nu+\alpha_\nu) - \sum_{\varkappa=2}^{n} m_\varkappa \prod_{\mu=\varkappa+1}^{n}(m_\mu+\alpha_\mu)\prod_{\mu=1}^{\varkappa-1}(M_\mu+\alpha_\mu). \tag{20}$$

3. The Matrix Δ_n and Its Inverse

We consider now the matrix

$$\Delta_n = \begin{pmatrix} 1 & -M & -M & \ldots & -M \\ -m & 1 & -M & \ldots & -M \\ \cdot & \cdot & \cdot & \ldots & \cdot \\ \cdot & \cdot & \cdot & \ldots & \cdot \\ \cdot & \cdot & \cdot & \ldots & \cdot \\ -m & -m & -m & \ldots & 1 \end{pmatrix} \tag{21}$$

Its determinant is obtained from Ω_n in putting in (20)

$$\alpha_1 = \alpha_2 = \ldots \alpha_n = 1; \quad m_2 = m_3 = \ldots = m_n = m; \quad M_1 = M_2 = \ldots = M_{n-1} = M.$$

We obtain

$$|\Delta_n| = (m+1)^{n-1} - m\sum_{\varkappa=2}^{n}(m+1)^{n-\varkappa}(M+1)^{\varkappa-1},$$

and this becomes, if $M \neq m$,

$$|\Delta_n| = (m+1)^{n-1} - m(M+1)\frac{(M+1)^{n-1}-(m+1)^{n-1}}{M-m}$$

$$= \frac{1}{M-m}[(m+1)^{n-1}(M-m+m(M+1)) - m(M+1)^n],$$

$$|\Delta_n| = \frac{1}{M-m}[M(m+1)^n - m(M+1)^n] \qquad (m \neq M),^6 \tag{22}$$

while for $m=M$ we obtain from (22) in letting $M \to m$:

$$|\Delta_n| = [1-(n-1)m](1+m)^{n-1} \qquad (m=M). \tag{23}$$

In particular, if $0<m<M$, a necessary and sufficient condition for $|\Delta_n|>0$ is

$$\frac{m}{(m+1)^n} < \frac{M}{(M+1)^n}. \tag{24}$$

We assume now in particular

$$0<m<M. \tag{25}$$

If we introduce the abbreviations

$$M_n = \frac{(1+M)^n - nM - 1}{M}, \quad m_n = \frac{(1+m)^n - nm - 1}{m}, \tag{26}$$

we can write (22) in the form

$$(M-m)|\Delta_n| = M(1+nm+mm_n) - m(1+nM+MM_n) = M-m-mM(M_n-m_n),$$

and therefore, if we put

$$\delta = 1-|\Delta_n|, \tag{27}$$

$$\frac{\delta}{mM} = \frac{M_n - m_n}{M-m}. \tag{28}$$

It follows from (25) for $n>2$

$$\frac{M_n-m_n}{M-m} = \sum_{\nu=2}^{n}\binom{n}{\nu}\frac{M^{\nu-1}-m^{\nu-1}}{M-m} > \sum_{\nu=2}^{n}\binom{n}{\nu}M^{\nu-2} = \frac{(1+M)^n-1-nM}{M^2} = \frac{M_n}{M},$$

so that from (28) we have

$$\frac{M_n}{1-\frac{m}{M}} > \frac{\delta}{m} > M_n. \tag{29}$$

It follows in particular that if (24) holds, then $\delta>0$, $0<|\Delta_n|<1$.

In solving (29) with respect to m and δ, we obtain

$$\frac{\delta}{M_n+\frac{\delta}{M}} < m < \frac{\delta}{M_n}, \quad m = \frac{\delta}{M_n+\theta\frac{\delta}{M}}, \quad 0<\theta<1, \tag{30}$$

$$M_n m < \delta < \frac{M_n m}{1-\frac{m}{M}}, \quad \delta = \frac{M_n m}{1-\theta\frac{m}{M}}, \quad 0<\theta_1<1. \tag{30'}$$

[6] This formula can be also obtained from the formulas given in the proof of theorem III in [3a, p. 113].

In order to discuss the meaning of the condition (24), consider the curve

$$y=f(x)=\frac{x}{(1+x)^n}; \tag{31}$$

we have

$$f'(x)=\frac{1-(n-1)x}{(1+x)^{n+1}}, \quad f''(x)=n\,\frac{(n-1)x-2}{(1+x)^{n+2}}.$$

For $x>0$ the curve (31) has one maximum at $x=1/(n-1)$ and an inflection point at $x=2/(n-1)$.

In figure 1 the curve (31) is drawn (computed for $n=5$). The portion of this curve from the point 0 to the highest point T will be denoted as the *ascending branch* and the portion between T and $x=\infty$ as the *descending branch*.

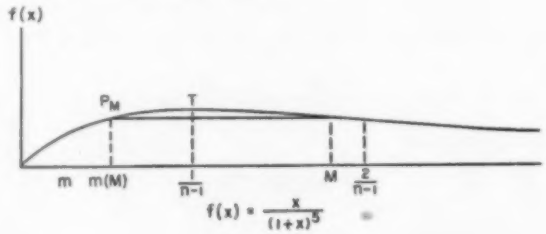

FIGURE 1.

If we assume that in (24) m is less than M, we see that either

$$0<m<\frac{1}{n-1}, \quad M>\frac{1}{n-1} \tag{32}$$

or

$$m<M\leqq\frac{1}{n-1}. \tag{32°}$$

In order to find for a given $M>1/(n-1)$ the range of values of m satisfying (24) we find on the curve the second point P_M with the same ordinate as the point $x=M$; then if the abcissa $m(M)$ corresponds to P_M, we have $0<m<m(M)$.

Finally we prove from (24) and $m<M$ that it always follows that

$$mM^{n-1}<1. \tag{33}$$

Indeed, in proving (33) we can obviously assume that M is greater than 1 and therefore on the descending branch in the diagram. But then we have

$$\frac{1}{1+\dfrac{1}{M^{n-1}}}=\frac{M^{n-1}}{1+M^{n-1}}>\frac{M}{1+M},$$

and therefore in raising it to the nth power

$$\frac{\dfrac{1}{M^{n-1}}}{\left(1+\dfrac{1}{M^{n-1}}\right)^n}>\frac{M}{(1+M)^n}.$$

We see that $1/M^{n-1}$ must lie, in figure 1, between M and $m(M)$, and it follows that $1/M^{n-1}>m$, that is (33).

We are now going to determine the inverse matrix

$$\Delta_n^{-1}=(\alpha_{\mu\nu}) \qquad (\mu,\nu=1,\ \ldots,n) \tag{34}$$

of Δ_n, if its determinant (22) resp. (23) is not equal to 0. It is sufficient for this purpose to solve the corresponding linear system

$$x_\mu - m\sum_{\nu=1}^{\mu-1} x_\nu - M\sum_{\nu=\mu+1}^{n} x_\nu = z_\mu \qquad (\mu=1,\ \ldots,n) \tag{35}$$

for indeterminate z_μ. Put

$$\left.\begin{aligned} &x_1+\ \ldots\ +x_n=s, \qquad \frac{m-M}{M+1}=\sigma,\\ &\frac{M}{1+M}=\lambda, \qquad 1+\sigma=\frac{1+m}{1+M}=q,\\ &\frac{z_\nu}{1+M}=\alpha_\nu, \qquad \alpha_\nu+\lambda s=y_\nu \end{aligned}\right\}. \tag{36}$$

Then the system (35) is equivalent with

$$(1+M)x_\mu=(m-M)(x_1+\ \ldots\ +x_{\mu-1})+Ms+z_\mu \quad (\mu=1,\ \ldots,n),$$

$$x_\mu=\sigma(x_1+\ \ldots\ +x_{\mu-1})+y_\mu \qquad (\mu=1,\ \ldots,n),$$

or in putting

$$S_\nu=x_1+\ \ldots\ +x_\nu \quad (\nu=1,\ \ldots,n), \qquad S_0=0:$$

$$S_\mu-S_{\mu-1}=\sigma S_{\mu-1}+y_\mu, \qquad S_\mu=(1+\sigma)S_{\mu-1}+y_\mu=qS_{\mu-1}+y_\mu,$$

$$S_\mu q^{-\mu}=S_{\mu-1}q^{-\mu+1}+y_\mu q^{-\mu} \quad (\mu=1,\ \ldots,n),$$

$$S_\mu q^{-\mu}=\sum_{\nu=1}^{\mu} y_\nu q^{-\nu},$$

$$S_\mu=\sum_{\nu=1}^{\mu} y_\nu q^{\mu-\nu} \qquad (\mu=1,\ \ldots,n), \tag{37}$$

$$x_\mu=\sum_{\nu=1}^{\mu-1} y_\nu (q-1)\,q^{\mu-\nu-1}+y_\mu \qquad (\mu=1,\ \ldots,n). \tag{38}$$

From (37) for $\mu=n$ we have by (36)

$$S_n=s=\sum_{\nu=1}^{n} y_\nu q^{n-\nu}=\lambda s\sum_{\nu=1}^{n} q^{n-\nu}+\sum_{\nu=1}^{n}\alpha_\nu q^{n-\nu},$$

$$s=\lambda s\,\frac{q^n-1}{q-1}+\sum_{\nu=1}^{n}\alpha_\nu q^{n-\nu}, \tag{39}$$

where for $m=M$, $q=1$ the coefficient of λs is to be replaced by n. Since for $m\neq M$

$$1-\lambda\,\frac{q^n-1}{q-1}=\frac{m-Mq^n}{m-M}=\frac{Mq^n-m}{M-m},$$

we have from (39) and (22)

$$s=Q\sum_{\nu=1}^{n}\alpha_\nu q^{n-\nu} \qquad (m\neq M), \tag{40}$$

$$Q=\frac{M-m}{Mq^n-m}=\frac{(M+1)^n}{|\Delta_n|} \qquad (m\neq M), \tag{41}$$

while for $m=M$ we obtain again (40) in defining Q by

$$Q=\frac{m+1}{1-(n-1)m}=\frac{(m+1)^n}{|\Delta_n|} \qquad (m=M). \tag{41°}$$

If we now replace in (38) y_ν by $\lambda s+\alpha_\nu$ and use for s the expression from (40),

$$x_\mu=(q-1)\sum_{\nu=1}^{n-1}\alpha_\nu q^{n-\nu-1}+\alpha_\mu+\lambda s\left[(q-1)\sum_{\nu=1}^{n-1}q^{n-\nu-1}+1\right].$$

But here the expression within the brackets is q^{n-1}, and we obtain therefore

$$x_\mu=\sum_{\nu=1}^{n-1}\alpha_\nu q^{n-\nu-1}(q-1)+\alpha_\mu+\lambda Q q^{n-1}\sum_{\nu=1}^{n}\alpha_\nu q^{n-\nu} \qquad (\mu=1,\ldots,n)$$

and finally in introducing α_μ from (36)

$$x_\mu=\sum_{\nu=1}^{n-1}z_\nu q^{n-\nu-1}\frac{q-1}{M+1}+\frac{z_\mu}{M+1}+\frac{\lambda Q q^{n-1}}{M+1}\sum_{\nu=1}^{n}z_\nu q^{n-\nu} \qquad (\mu=1,\ldots,n). \tag{42}$$

Introduce the two following triangular matrices:

$$U_n(q)=(u_{\mu\nu})=\begin{pmatrix}0&0&.&.&.&.&.&0\\1&0&.&.&.&.&.&.\\q&1&0&&&&&.\\q^2&q&.&.&&&&.\\.&.&.&.&.&&&.\\.&.&.&.&.&.&&.\\.&.&.&.&.&.&.&.\\.&.&.&.&q^2&q&1&0\end{pmatrix}, \tag{43}$$

$$u_{\mu\nu}=\begin{cases}q^{n-\nu-1} & (\mu>\nu)\\ 0 & (\mu\leqq\nu),\end{cases} \tag{44}$$

$$V_n(q)=(v_{\mu\nu})=\begin{pmatrix}0&q^{-1}&q^{-2}&q^{-3}&\ldots&q^{-n+1}\\0&0&q^{-1}&q^{-2}&\ldots&q^{-n+2}\\.&.&.&.&\ldots&.\\.&.&.&.&\ldots&.\\.&.&.&.&\ldots&.\\0&0&0&0&\ldots&0\end{pmatrix}, \tag{45}$$

$$v_{\mu\nu}=\begin{cases}0 & (\mu\geqq\nu)\\ q^{n-\nu} & (\mu<\nu).\end{cases} \tag{46}$$

We see then that in (42) the matrix corresponding to the first right-hand sum is

$$\frac{q-1}{M+1}U_n=\frac{m-M}{(M+1)^2}U_n,$$

whereas to the second right-hand sum in (42) corresponds the matrix

$$\frac{\lambda Q}{M+1}\, q^{n-1}(qU_n+E_n+V_n),$$

where E_n is the unit matrix. We obtain

$$\Delta_n^{-1}=\Big(\frac{m-M}{(M+1)^2}+\frac{MQq^n}{(M+1)^2}\Big)U_n+\Big(\frac{1}{M+1}+\frac{MQq^{n-1}}{(M+1)^2}\Big)E_n+\frac{MQq^{n-1}}{(M+1)^2}\,V_n.$$

The coefficient of U_n is here equal to $(mQ)/(M+1)^2$, both in the case (41) and (41°), and we have finally

$$\Delta_n^{-1}=\frac{mQ}{(M+1)^2}\,U_n+\Big(\frac{1}{M+1}+\frac{MQq^{n-1}}{(M+1)^2}\Big)E_n+\frac{MQq^{n-1}}{(M+1)^2}\,V_n. \tag{47}$$

We now denote by s_μ the sum of the elements in the μth row of the matrix (47) and by t_ν the corresponding sum in the νth column. If we first assume $m\neq M$, for the matrices U_n and V_n, the μth row sums are, respectively, equal to

$$\frac{q^{n-1}-1}{q-1};\qquad \frac{1-q^{n-n}}{q-1},$$

and the νth column sums are

$$\frac{q^{n-\nu}-1}{q-1};\qquad \frac{1-q^{1-\nu}}{q-1}.$$

We obtain now from (47) by (36)

$$\begin{aligned}(M+1)^2 s_\mu &= mQ\,\frac{q^{n-1}-1}{q-1}+M+1+MQq^{n-1}+MQ\,\frac{q^{n-1}-q^{n-1}}{q-1}\\ &=\frac{Q}{\sigma}\,[mq^{n-1}-m+Mq^n-Mq^{n-1}+Mq^{n-1}-Mq^{n-1}]+M+1\\ &=\frac{M+1}{m-M}\,Q\,[Mq^n-m+(m-M)q^{n-1}]+M+1,\end{aligned}$$

and this is by (41) equal to $(M+1)Qq^{n-1}$. We have finally

$$s_\mu=\frac{Q}{M+1}\,q^{n-1}=\frac{(M+1)^{n-1}}{|\Delta_n|}\,q^{n-1}, \tag{48}$$

and this remains true also for $m=M$, as is immediately seen.

Similarly, we have

$$\begin{aligned}(M+1)^2 t_\nu &= mQ\,\frac{q^{n-\nu}-1}{q-1}+M+1+MQq^{n-1}+MQ\,\frac{q^{n-1}-q^{n-\nu}}{q}\\ &=\frac{Q}{\sigma}\,[mq^{n-\nu}-m+Mq^n-Mq^{n-1}+Mq^{n-1}-Mq^{n-\nu}]+M+1\\ &=\frac{M+1}{m-M}\,Q\,[Mq^n-m+(m-M)q^{n-\nu}]+M+1=(M+1)Qq^{n-\nu},\end{aligned}$$

and we have

$$t_\nu=\frac{Q}{M+1}\,q^{n-\nu}=\frac{(M+1)^{n-1}}{|\Delta_n|}\,q^{n-\nu}, \tag{49}$$

relation which is also immediately verified for the case $m=M$.

4. Bounds for the Determinants, depending on Ω_n and Δ_n

A determinant

$$M=\begin{vmatrix} \alpha_1 & -m_{12} & \dots & -m_{1n} \\ -m_{21} & \alpha_2 & \dots & -m_{2n} \\ \cdot & \cdot & \dots & \cdot \\ \cdot & \cdot & \dots & \cdot \\ \cdot & \cdot & \dots & \cdot \\ -m_{n1} & -m_{n2} & \dots & \alpha_n \end{vmatrix} \tag{50}$$

will be called an *M-determinant* if all diagonal elements α_ν are positive, all elements off the main diagonal $-m_{\mu\nu}$ $(\mu\neq\nu)$ are not positive and the determinant M, as well as all principal (coaxial) minors of M of all degrees, are positive.

In what follows we will have to use a theorem given by the author in 1937 [1], and which will be formulated as the following:

LEMMA I. *If we have for the M-determinant (50) and a determinant* $H=|h_{\mu\nu}|$ $(\mu,\nu=1,\dots,n)$ *of order n, the inequalities*

$$|h_{\nu\nu}|\geqq\alpha_\nu, \qquad |h_{\mu\nu}|\leqq m_{\mu\nu} \qquad (\mu\neq\nu;\ \mu,\nu=1,\dots,n), \tag{51}$$

then $H\neq0$, *and we have*

$$|H|\geqq M. \tag{52}$$

If (H), (M), *respectively, denote the matrices of the determinants H and M, the inverse matrix of* (H) *is majorized by the inverse matrix of* (M)

$$(H)^{-1}\ll(M)^{-1}. \tag{52°}$$

Suppose now that in the determinant Ω_n given by (17) all α_ν are positive and m_ν, M_ν non-negative. Then it follows from (18) that Ω_n is a monotonically decreasing function of all m_ν and from (20) that M is also monotonically decreasing in all M_ν. Suppose now that for a certain set of values of α_ν, m_ν, M_ν the determinant $\Omega_n\neq0$. Then replace the m_ν and M_ν corresponding to certain rows $(\nu_1,\dots,\nu_s)$ by zeros; the determinant Ω_n cannot decrease and remains therefore positive; but then Ω_n becomes equal to the product of $\alpha_{\nu_1}\alpha_{\nu_2}\dots\alpha_{\nu_s}$ with the principal minor complementary to the set of indices $\nu_1,\dots,\nu_s$. Therefore, all principal minors of Ω_n are positive. We see that Ω_n *is an M-determinant, if the conditions*

$$\alpha_\nu>0, \quad m_\nu\geqq0, \quad M_\nu\geqq0 \qquad (\nu=1,\dots,n); \tag{53}$$

are satisfied and $\Omega_n\neq0$. But now we can easily deduce the following theorem.

A. *Consider the set of all determinants* $A=|a_{\mu\nu}|$ *satisfying the conditions*

$$|a_{\mu\nu}|\leqq m_\mu \quad (\nu<\mu), \qquad |a_{\mu\nu}|\leqq M_\mu \quad (\nu>\mu), \qquad |a_{\mu\nu}|\geqq\alpha_\mu \qquad (\mu,\nu=1,\dots,n), \tag{54}$$

where α_μ *are n given positive constants and* m_μ, M_μ *are* $2n-2$ *given nonnegative constants. Then in order that no determinant A of this set vanishes, it is necessary and sufficient that* $\Omega_n>0$. *If this condition is satisfied, we have*

$$|A|\geqq\Omega_n. \tag{55}$$

PROOF: Since in the case $\Omega_n>0$, Ω_n is an M-determinant, the sufficiency of our condition follows immediately from the inequality (52) mentioned above.

If $\Omega_n=0$, we can take obviously $a_{\mu\mu}=\alpha_\mu$ and $a_{\mu\nu}=-m_\mu$ or $a_{\mu\nu}=-M_\mu$ according as $\nu<\mu$ or $\nu>\mu$ and obtain a vanishing determinant A satisfying the condition (54).

Suppose now $\Omega_n<0$, then it follows from the form (17) of Ω_n that Ω_n becomes positive if all m_μ are replaced by zeros. There exists, therefore, such a positive $t<1$ that Ω_n vanishes if all m_μ in (17) are replaced by tm_μ, but then we obtain a vanishing determinant A of our set in taking $a_{\mu\mu}=\alpha_\mu$ and $a_{\mu\nu}=-tm_\mu$ or $a_{\mu\nu}=-M_\mu$, according as $\nu<\mu$ or $\nu>\mu$. The theorem A is proved.

In specializing the matrix of Ω_n to Δ_n and in assuming that in particular $0<m<M$, we obtain immediately from (22) and the theorem A:

B. *Consider for two positive constants m, M, $m\leqq M$, the set of all determinants $A=|a_{\mu\nu}|$ of the nth order for which*

$$|a_{\mu\mu}|\geqq 1 \quad (\mu=1, \ldots, n), \quad |a_{\mu\nu}|\leqq m \quad (\nu<\mu), \quad |a_{\mu\nu}|\leqq M \quad (\nu>\mu), \tag{56}$$

then, in order that no determinant A of this set vanish, it is necessary and sufficient that for $m<M$ the inequality

$$\frac{m}{(1+m)^n}<\frac{M}{(1+M)^n} \qquad (m<M), \tag{57}$$

holds, and if this inequality is satisfied, we have for each determinant A of the set

$$|A|\geqq|\Delta_n|=\frac{(1+m)^n(1+M)^n}{M-m}\left[\frac{M}{(1+M)^n}-\frac{m}{(1+m)^n}\right]. \tag{58}$$

If $m=M$, the condition becomes

$$m<\frac{1}{n-1} \qquad (M=m) \tag{57°}$$

and we have, if (57°) is satisfied,

$$|A|\geqq|\Delta_n|=[1-(n-1)m](1+m)^{n-1} \qquad (m=M). \tag{58°}$$

From theorem B we can deduce the following theorem.

C. *Let $A=(a_{\mu\nu})$ $(\mu,\nu=1, \ldots, n)$ be a matrix satisfying the conditions*

$$|a_{\mu\nu}|\leqq m \quad (\nu<\mu), \qquad |a_{\mu\nu}|\leqq M \quad (\nu>\mu), \tag{59}$$

where m, M are two constants with $0<m<M$. Put

$$\delta(m,M)=\frac{Mm^{1/n}-mM^{1/n}}{M^{1/n}-m^{1/n}}. \tag{60}$$

Then all fundamental roots of the matrix A are contained in the set of the n closed circles described around the elements $a_{\mu\mu}$ with the radius $\delta(m,M)$. The value (60) of $\delta(m,M)$ cannot be improved if $A=\Delta_n$.[7]

Proof: Let λ be a fundamental root of A so that the matrix $\lambda E-A$ is singular. Put $\min_\mu|\lambda-a_{\mu\mu}|=\alpha$; we then have to prove that $\alpha\leqq\delta(m,M)$. If $\alpha=0$, there is nothing to prove. Suppose $\alpha>0$, and consider the matrix

$$\frac{\lambda E-A}{\alpha}=(b_{\mu\nu}).$$

For this matrix we have

$$|b_{\mu\mu}|\geqq 1, \quad |b_{\mu\nu}|\leqq\frac{m}{\alpha} \quad (\nu<\mu), \qquad |b_{\mu\nu}|\leqq\frac{M}{\alpha} \quad (\nu>\mu).$$

[7] For $M=m$, $\delta(m,M)$ becomes $(n-1)m$, but in this case our result is contained in Gerschgorin's theorem, cf. [4]. From the theorem C the result given by Stein and Rosenberg in [3c] as theorem III follows immediately.

Therefore, we have by theorem B

$$\frac{\frac{m}{\alpha}}{\left(1+\frac{m}{\alpha}\right)^n} \geqq \frac{\frac{M}{\alpha}}{\left(1+\frac{M}{\alpha}\right)^n},$$

and therefore,

$$\frac{1+\frac{m}{\alpha}}{m^{1/n}} \leqq \frac{1+\frac{M}{\alpha}}{M^{1/n}},$$

$$\alpha\left(\frac{1}{m^{1/n}}-\frac{1}{M^{1/n}}\right) \leqq \frac{M}{M^{1/n}}-\frac{m}{m^{1/n}},$$

$$\alpha \leqq \frac{M^{1-\frac{1}{n}}-m^{1-\frac{1}{n}}}{m^{-1/n}-M^{-1/n}} = \delta(m, M).$$

5. Bounds of the Matrix Δ_n^{-1}

For an n dimensional vector $\xi=(x_1, \ldots, x_n)$ the Hölder norm corresponding to the exponent $p \geqq 1$ is given by

$$|\xi|_p = \sqrt[p]{|x_1|^p + \ldots + |x_n|^p} \qquad (p \geqq 1). \tag{61}$$

We will only use the three cases corresponding to $p=1, 2, \infty$:

$$|\xi|_p = |x_1| + \ldots + |x_n|, \quad |\xi|_\infty = \max_\nu |x_\nu|, \quad |\xi|_2 = \sqrt{|x_1|^2 + \ldots + |x_n|^2}. \tag{62}$$

We have among these three norms the following inequalities:

$$|\xi|_\infty \leqq |\xi|_1 \leqq n|\xi|_\infty, \tag{63,a}$$

$$|\xi|_\infty \leqq |\xi|_2 \leqq \sqrt{n}|\xi|_\infty, \tag{63,b}$$

$$|\xi|_1 \leqq \sqrt{n}|\xi|_2 \leqq \sqrt{n}|\xi|_1, \tag{63,c}$$

which are immediately verified. The left-hand inequality (63, c) implies the well-known inequality between the arithmetical mean and the arithmetical mean of the squares. If $A=(a_{\mu\nu})$ is an $n \times n$ matrix, we define its norm corresponding to the exponent p $(1 \leqq p \leqq \infty)$ by

$$|A|_p = \max_{\xi \neq 0} \frac{|A\xi|_p}{|\xi|_p} \tag{64}$$

and denote it by $|A|_p$. We will use here too only the cases $p=1, 2, \infty$.

In applying to the definition (64) the formulas (63, b), and (63, c) we obtain immediately

$$\frac{1}{\sqrt{n}}|A|_1 \leqq |A|_2 \leqq \sqrt{n}\,|A|_1, \tag{65, a}$$

$$\frac{1}{\sqrt{n}}|A|_\infty \leqq |A|_2 \leqq \sqrt{n}\,|A|_\infty. \tag{65, b}$$

For $p=1, \infty$ the expressions of $|A|_1$, $|A|_\infty$ are easy to write down; we have, as is well known and very easy to prove,

$$|A|_1 = \max_\nu \sum_\mu |a_{\mu\nu}| \tag{66, a}$$

$$|A|_\infty = \max_\mu \sum_\nu |a_{\mu\nu}|. \tag{66, b}$$

As to $|A|_2$, its expression is irrational; $|A|_2$ is the square root of the maximum fundamental root of the symmetric and nonnegative matrix AA^*. Since the direct computation of $|A|_2$ is difficult in most cases, we prove the following estimate for $|A|_2$:

LEMMA II. *We have for any matrix A*

$$\frac{1}{n}\max(|A|_1,|A|_\infty) \leqq |A|_2 \leqq \sqrt{|A|_1|A|_\infty}, \tag{67}$$

The first part of (67) follows from (65,a) and (65,b). To prove the second part, we introduce the notations

$$s_\mu = \sum_\nu |a_{\mu\nu}|, \quad t_\nu = \sum_\mu |a_{\mu\nu}| \qquad (\mu,\nu = 1,\ldots,n).$$

The sum of the moduli of all elements in the μth row of AA^* can be estimated as follows

$$|\sum_{\nu,\varkappa} a_{\mu\varkappa}a_{\nu\varkappa}| \leqq \sum_\varkappa \sum_\nu |a_{\mu\varkappa}a_{\nu\varkappa}| = \sum_\varkappa |a_{\mu\varkappa}|t_\varkappa \leqq s_\mu|A|_1 \leqq |A|_\infty|A|_1.$$

Equation (67) follows now from the theorem of Frobenius that the modulus of each fundamental root of a square matrix does not exceed the greatest sum of the moduli of the elements of this matrix in different rows.

If we now apply these results to the matrix Δ_n^{-1} discussed in the section 3, we obtain from (48), (49), (66,a) and (66,b)

$$|\Delta_n^{-1}|_1 = |\Delta_n^{-1}|_\infty = \frac{Q}{M+1} = \frac{(M+1)^{n-1}}{|\Delta_n|}, \tag{68}$$

and from (67) and (65,a)

$$\frac{Q}{\sqrt{n}(M+1)} \leqq |\Delta_n^{-1}|_2 \leqq \frac{Q}{M+1} = \frac{(M+1)^{n-1}}{|\Delta_n|}. \tag{69}$$

In combining these inequalities with the results given in section 4, we obtain the following theorem.

D. *Let $A=(a_{\mu\nu})$ be a square matrix of order n satisfying conditions (56), and let (57) be satisfied. Then we have*

$$|A^{-1}|_p \leqq \frac{(M+1)^{n-1}}{|\Delta_n|} \qquad (p=1,2,\infty);$$

and therefore for any vector ξ

$$|A\xi|_p \geqq \frac{|\Delta_n|}{(M+1)^{n-1}}|\xi|_p \qquad (p=1,2,\infty). \tag{70}$$

PROOF: It follows from (52°) of lemma I at once in virtue of (66,a) and (66,b) that

$$|A^{-1}|_p \leqq |\Delta_n^{-1}|_p = \frac{Q}{M+1} \qquad (p=1,\infty);$$

further, the matrix $A^{-1}(A^{-1})^*$ is majorized by $\Delta_n^{-1}(\Delta_n^{-1})^*$. By a well-known theorem of Probenius, therefore, the maximum modulus of a fundamental root of $A^{-1}(A^{-1})^*$ is majorized by that of $\Delta_n^{-1}(\Delta_n^{-1})^*$, and so we also have

$$|A^{-1}|_2 \leqq |\Delta_n^{-1}|_2 \leqq \frac{Q}{M+1}.$$

By definition (64), therefore, in putting $A\xi=\eta$, we have

$$|A^{-1}\eta|_p \leqq \frac{Q}{M+1}|\eta|_p,$$

and this is equivalent to (70).

6. Bounds of the Matrix $\Delta_n^{-1}-\Delta_n^{(0)-1}$

We denote by $\Delta_n^{(0)}$ the matrix obtained from (21) in replacing m by zero:

$$\Delta^{(0)}=\begin{pmatrix} 1 & -M & -M & \dots & -M \\ 0 & 1 & -M & \dots & -M \\ \cdot & \cdot & \cdot & \dots & \cdot \\ \cdot & \cdot & \cdot & \dots & \cdot \\ \cdot & \cdot & \cdot & \dots & \cdot \\ 0 & 0 & 0 & \dots & 1 \end{pmatrix}. \tag{71}$$

We will prove the following theorem:

E. *If $0<m<M$ and (57) is satisfied, then the matrix $\Delta_n^{-1}-\Delta_n^{(0)-1}$ is a nonnegative matrix and we have*

$$|\Delta_n^{-1}-\Delta_n^{(0)-1}|_p=\max_{1\leqq\nu\leqq n}(1+M)^{\nu-1}\frac{(1+m)^{n-\nu}-|\Delta_n|}{|\Delta_n|} \qquad (p=1,\infty). \tag{72}$$

Proof: Since $\Delta_n^{(0)}$ satisfies the inequalities (51), it follows from (52°) that $\Delta_n^{-1}-\Delta_n^{(0)-1}$ is nonnegative. Denote by $s_\mu^{(0)}$ and $t_\nu^{(0)}$ the sums of the elements in the μth row and in the νth column of $\Delta_n^{(0)-1}$, and by $\bar{s}_\mu$ and $\bar{t}_\nu$ the corresponding expressions for the matrix $\Delta_n^{-1}-\Delta_n^{(0)-1}$. We have

$$\bar{s}_\mu=s_\mu-s_\mu^{(0)}, \quad \bar{t}_\nu=t_\nu-t_\nu^{(0)} \qquad (\mu,\nu=1,\dots,n). \tag{73}$$

It follows then from the formulas (48) and (49) that $\bar{s}_\mu$ runs for $\mu=n, n-1, \dots, 1$ through the same set of values as $\bar{t}_\nu$ for $\nu=1, \dots, n$.

Formula (49) can be written in the form

$$t_\nu=\frac{q^{n-\nu}(M+1)^{n-1}}{|\Delta_n|}=\frac{(1+m)^{n-\nu}(1+M)^{\nu-1}}{|\Delta_n|}. \tag{74}$$

Since Δ_n becomes 1 for $m=0$, we have (72) and E is proved.

Discussion of $|\Delta_n^{-1}-\Delta_n^{(0)-1}|_p$. We prove first that $t_\nu-t_\nu^{(0)}$ increases with ν as long as the condition

$$1-\frac{m}{M}\geqq|\Delta_n| \tag{75}$$

is satisfied. Indeed, put

$$k_\nu\equiv\frac{t_{\nu+1}-t_{\nu+1}^{(0)}}{t_\nu-t_\nu^{(0)}}=(M+1)\frac{(1+m)^{n-\nu-1}-|\Delta_n|}{(1+m)^{n-\nu}-|\Delta_n|}. \tag{76}$$

In solving the three inequalities

$$k_\nu\gtreqless 1 \tag{77}$$

with respect to $|\Delta_n|$, we obtain correspondingly

$$|\Delta_n|\lesseqgtr\sigma_\nu\equiv\left(1-\frac{m}{M}\right)(1+m)^{n-\nu-1}. \tag{78}$$

The inequalities $k_\nu\geqq 1$ $(\nu=1, \dots, n)$ are obviously satisfied in virtue of (75) as long as

$\nu \leqq n-1$. We have, therefore, in this case, in using (72)

$$\operatorname*{Max}_{\nu}(t_\nu - t_\nu^{(0)}) = (1+M)^{n-1}\frac{1-|\Delta_n|}{|\Delta_n|} = (1+M)^{n-1}\frac{\delta}{1-\delta},$$

$$|\Delta_n^{-1} - \Delta_n^{(0)-1}|_p = (1+M)^{n-1}\frac{1-|\Delta_n|}{|\Delta_n|} = (1+M)^{n-1}\frac{\delta}{1-\delta} \qquad \left(p=1,\infty;\quad |\Delta_n| \leqq 1-\frac{m}{M}\right). \tag{79}$$

Condition (75) can be written by using the notation (27), as $\delta \geqq m/M$, and in virtue of (29) this is certainly satisfied if we have $MM_n \geqq 1$,

$$(M+1)^n - nM - 2 \geqq 0. \tag{80}$$

Condition (80) becomes for $n=3$: $M \geqq 0.5321$. *For $n \geqq 4$, (80) is in any case satisfied, if we have*

$$M \geqq \frac{1.5}{n} \qquad (n \geqq 4). \tag{81}$$

Indeed, if the relation (80) is satisfied for a positive M, it is satisfied for any greater value because the coefficients of all positive powers of M in the left-hand expression are greater than or equal to 0. To prove the sufficiency of (81), it is sufficient to prove that $(1+1.5/n)^n \geqq 3.5$ $(n \geqq 4)$. But here the left-hand expression is monotonically increasing with n, and this inequality follows, therefore, from $(5.5/4)^4 = 3.75\ \ldots\ > 3.5$.

Suppose now that we have

$$1 - \frac{m}{M} \leqq |\Delta_n| \leqq 1, \quad \delta \leqq \frac{m}{M}. \tag{82}$$

Then we have, since $0 < m < 1/(n-1)$,

$$\frac{(1+m)^{n-\nu}-1}{m} \leqq \frac{\left(1+\frac{1}{n-1}\right)^{n-\nu}-1}{\frac{1}{n-1}} \leqq (n-1)\left(\left(1+\frac{1}{n-1}\right)^{n-1}-1\right) \leqq (e-1)(n-1),$$

$$(1+m)^{n-\nu} = 1 + 1.72\,\theta n m, \quad 0 < \theta < 1$$

$$(1+m)^{n-\nu} - |\Delta_n| = 1.72\,\theta n m + 1 - |\Delta_n|,$$

and therefore by (82) $(1+m)^{n-\nu} - |\Delta_n| \leqq 1.72\theta n m + m/M$.

For $n \geqq 4$ we have in the case (82), since the inequality (81) is not satisfied,

$$\frac{1}{M} \leqq \frac{n}{1.5}$$

and, therefore, finally

$$(1+m)^{n-\nu} - |\Delta_n| \leqq 2.39 n m \qquad (\nu = 1, \ldots, n) \tag{83}$$

On the other hand, since $M < 1.5/n$, $(1+M)^{\nu-1} \leqq (1+1.5/n)^n < e^{1.5} = 4.481689$, and, therefore, from (72) and (73)

$$t_\nu - t_\nu^{(0)} \leqq 10.72 n \frac{m}{|\Delta_n|} \quad \left(\nu = 1, \ldots, n;\quad |\Delta_n| \geqq 1 - \frac{m}{M};\quad n > 3\right),$$

$$|\Delta_n^{-1} - \Delta_n^{(0)-1}|_p \leqq 10.72 n \frac{m}{|\Delta_n|} \quad \left(p = 1, \infty;\quad |\Delta_n| \geqq 1 - \frac{m}{M};\quad n > 3\right). \tag{84}$$

To obtain a lower bound, we take in (74) $\nu = 1$. We obtain, since for $n > 3$, $0 < |\Delta_n| \leqq 1$,

$$t_1 - t_1^{(0)} = \frac{(1+m)^{n-1} - |\Delta_n|}{|\Delta_n|} \geqq \frac{(n-1)m}{|\Delta_n|} \geqq 0.75 n \frac{m}{|\Delta_n|},$$

and, therefore,

$$|\Delta_n^{-1}-\Delta_n^{(0)-1}|_p \geqq 0.75n\,\frac{m}{|\Delta_n|} \qquad (p=1,\infty\,;n\geqq 4). \tag{85}$$

To obtain the exact value of $|\Delta_n^{-1}-\Delta_n^{(0)-1}|_p$ if (75) is not satisfied, we return to the inequalities (78) which are equivalent to (77).

Denote by n_0 the smallest integer between 1 and n, such that we have

$$\sigma_{n_0-1}\geqq|\Delta_n|>\sigma_{n_0} \qquad (1\leqq n_0\leqq n). \tag{86}$$

The parts of this inequality implying σ_0 or σ_n must be disregarded, that is to say, this inequality reduces to $|\Delta_n|>\sigma_1$ for $n_0=1$ and to $\sigma_{n-1}\geqq|\Delta_n|$ for $n_0=n$. Then we see at once that $\max\,(t_\nu-t_\nu^{(0)})=t_{n_0}-t_0^{(0)}$, and therefore

$$|\Delta_n^{-1}-\Delta_n^{(0)-1}|_p=t_{n_0}-t_0^{(0)}=\frac{(1+M)^{n_0-1}(1+m)^{n-n_0}-|\Delta_n|}{|\Delta_n|} \qquad (p=1,\infty). \tag{87}$$

For $m=M$ we have $n_0=1$, and therefore by (23)

$$|\Delta_n^{-1}-\Delta_n^{(0)-1}|_p=\frac{(n-1)m}{1-(n-1)m} \qquad \left(m=M<\frac{1}{n-1}\right). \tag{87°}$$

7. Bounds of $A^{-1}-A^{(0)-1}$

In order to obtain the theorem corresponding to E for a determinant A satisfying conditions (56), (57) of theorem B, we prove first the following important lemma, which generalizes considerably the relation (52°) of lemma I.

LEMMA III. *Consider n positive numbers $\alpha_1,\ \ldots,\ \alpha_n$ and $2n^2-2n$ nonnegative numbers $m_{\mu\nu},\ \epsilon_{\mu\nu}$ $(\mu\neq\nu;\quad \mu,\nu=1,\ \ldots,\ n)$, such that the matrices*

$$M=\begin{pmatrix} \alpha_1 & -m_{12}-\epsilon_{12} & \ldots & -m_{1n}-\epsilon_{1n} \\ -m_{21}-\epsilon_{21} & \alpha_2 & \ldots & -m_{2n}-\epsilon_{2n} \\ \cdot & \cdot & \ldots & \cdot \\ \cdot & \cdot & \ldots & \cdot \\ \cdot & \cdot & \ldots & \cdot \\ -m_{n1}-\epsilon_{n1} & -m_{n2}-\epsilon_{n2} & \ldots & \alpha_n \end{pmatrix}, \tag{88}$$

$$M^{(0)}=\begin{pmatrix} \alpha_1 & -m_{12} & \ldots & -m_{1n} \\ -m_{21} & \alpha_2 & \ldots & -m_{2n} \\ \cdot & \cdot & \ldots & \cdot \\ \cdot & \cdot & \ldots & \cdot \\ \cdot & \cdot & \ldots & \cdot \\ -m_{n1} & -m_{n2} & \ldots & \alpha_n \end{pmatrix} \tag{89}$$

are M-matrices.

Consider n constants A_μ $(\mu=1,\ \ldots,\ n)$, such that

$$|A_\mu|\geqq\alpha_\mu \qquad (\mu=1,\ \ldots,\ n) \tag{90}$$

and $2n^2-2n$ *constants* $a_{\mu\nu}$, $b_{\mu\nu}$ $(\mu\neq\nu;\quad \mu,\nu=1,\ \ldots,\ n)$ *such that*

$$|a_{\mu\nu}|\leqq m_{\mu\nu},\quad |b_{\mu\nu}-a_{\mu\nu}|\leqq \epsilon_{\mu\nu}\quad (\mu\neq\nu;\quad \mu,\nu=1,\ \ldots,\ n), \tag{91}$$

and form the two matrices

$$A=\begin{pmatrix} A_1 & b_{12} & \ldots & b_{1n} \\ b_{21} & A_2 & \ldots & b_{2n} \\ . & . & \ldots & . \\ . & . & \ldots & . \\ . & . & \ldots & . \\ b_{n1} & b_{n2} & \ldots & A_n \end{pmatrix}, \tag{92}$$

$$A^{(0)}=\begin{pmatrix} A_1 & a_{12} & \ldots & a_{1n} \\ a_{21} & A_2 & \ldots & a_{2n} \\ . & . & \ldots & . \\ . & . & \ldots & . \\ . & . & \ldots & . \\ a_{n1} & a_{n2} & \ldots & A_n \end{pmatrix}. \tag{93}$$

Then we have

$$A^{-1}-A^{(0)-1}\ll M^{-1}-M^{(0)-1}. \tag{94}$$

PROOF: We write $M=P-T$, $M^{(0)}=P-T^{(0)}$, where the matrices T, $T^{(0)}$ have zeros in the main diagonal and off the main diagonal, respectively, the nonnegative elements $m_{\mu\nu}+\epsilon_{\mu\nu}$, $m_{\mu\nu}$ and where P is the diagonal matrix

$$\begin{pmatrix} \alpha_1 & & & \\ & \alpha_2 & & 0 \\ & & . & \\ & & & . \\ & 0 & & \\ & & & \alpha_n \end{pmatrix}.$$

We can develop the inverse of $P-T=P(E-P^{-1}T)$ (E is the unit matrix) in the following way:

$$(P-T)^{-1}=\sum_{\kappa=0}^{\infty}(P^{-1}T)^{\kappa}P^{-1}. \tag{96}$$

The convergence of this development and the validity of (96) follow easily from the fact that the determinant of the matrix $P-tT$ does not vanish for $|t|\leqq 1$, which follows immediately from lemma I. The corresponding development holds also for $(P-T^{(0)})^{-1}$, and we obtain therefore

$$M^{-1}-M^{(0)-1}=\sum_{\kappa=1}^{\infty}[(P^{-1}T)^{\kappa}-(P^{-1}T^{(0)})^{\kappa}]P^{-1}. \tag{97}$$

The elements of $P^{-1}T$ are here $(m_{\mu\nu}+\epsilon_{\mu\nu})/\alpha_\mu$ or zeros, and those of $P^{-1}T^{(0)}$ are $m_{\mu\nu}/\alpha_\mu$ or zeros; therefore all elements of the matrices

$$(P^{-1}T)^\kappa-(P^{-1}T^{(0)})^\kappa \qquad (\kappa=1,2,\ \ldots) \tag{98}$$

are polynomials in $m_{\mu\nu}/\alpha_\mu$ and $\epsilon_{\mu\nu}/\alpha_\mu$ with nonnegative coefficients. Denote by Q the diagonal matrix

$$Q=\begin{pmatrix} A_1 & & & \\ & A_2 & & 0 \\ & & \cdot & \\ & & & \cdot \\ & 0 & & \\ & & & A_n \end{pmatrix}.$$

nd write $A=Q-S$, $A^{(0)}=Q-S^{(0)}$, where the elements of S are $b_{\mu\nu}$ or zeros, and those of $S^{(0)}$, $a_{\mu\nu}$ or zeros. Since, therefore, we have

$$Q^{-1}S\ll P^{-1}T, \qquad Q^{-1}S^{(0)}\ll P^{-1}T^{(0)},$$

we have

$$A^{-1}=\sum_{\kappa=0}^{\infty}(Q^{-1}S)^\kappa Q^{-1}, \qquad A^{(0)-1}=\sum_{\kappa=0}^{\infty}(Q^{-1}S^{(0)})^\kappa Q^{-1},$$

$$A^{-1}-A^{(0)-1}=\sum_{\kappa=0}^{\infty}[(Q^{-1}S)^\kappa-(Q^{-1}S^{(0)})^\kappa]Q^{-1}. \tag{99}$$

But now the elements of $(Q^{-1}S)^\kappa-(Q^{-1}S^{(0)})^\kappa$ are obtained from those of (98) in substituting there $a_{\mu\nu}/A_\mu$ instead of $m_{\mu\nu}/\alpha_\mu$ and $(b_{\mu\nu}-a_{\mu\nu})/A_\mu$ instead of $\epsilon_{\mu\nu}/\alpha_\mu$. Further, we have by (90) and (91)

$$\left|\frac{a_{\mu\nu}}{A_\mu}\right|\leqq\frac{m_{\mu\nu}}{\alpha_\mu}, \qquad \left|\frac{b_{\mu\nu}-a_{\mu\nu}}{A_\mu}\right|\leqq\frac{\epsilon_{\mu\nu}}{\alpha_\mu},$$

and therefore, since the coefficients in (98) are as already mentioned not negative,

$$(Q^{-1}S)^\kappa-(Q^{-1}S^{(0)})^\kappa\ll(P^{-1}T)^\kappa-(P^{-1}T^{(0)})^\kappa$$

and

$$\sum_{\kappa=1}^{\infty}[(Q^{-1}S)^\kappa-(Q^{-1}S^{(0)})^\kappa]\ll\sum_{\kappa=1}^{\infty}[(P^{-1}T)^\kappa-(P^{-1}T^{(0)})^\kappa]. \tag{100}$$

But from (100) by virtue of (90) it follows that the development (99) is majorized by (97) and our lemma is proved.

Under the conditions of theorem B in section 4, if the inequalities (56) and (57) are satisfied, we can apply lemma III in replacing the matrix M by Δ_n, $M^{(0)}$ by $\Delta_n^{(0)}$. We obtain

F. *Under the conditions of theorem B, if the inequalities* (56) *and* (57) *are satisfied, we have*

$$|A^{-1}-A^{(0)-1}|_p\leqq|\Delta_n^{-1}-\Delta_n^{(0)-1}|_p=\max_{1\leqq r\leqq n}(1+M)^{r-1}\,\frac{(1+m)^{n-r}-|\Delta_n|}{|\Delta_n|} \qquad (p=1,\infty), \tag{101}$$

where the values and the estimates for the right-hand expression in (101) *are obtained from the formulas* (79) *to* (87°).

Lemma III can be applied to many problems similar to that solved by theorem F. For instance, in the theory of the solutions of linear equations, the following problem has to be dealt with, although its complete discussion is usually avoided:

Consider a "triangular" system of linear equations

$$\sum_{\nu=\mu}^{n} a_{\mu\nu}x_\nu = y_\mu \qquad (\mu=1, \ldots, n), \tag{102}$$

where the coefficients $a_{\mu\nu}$ are only approximate values to the "true" values $b_{\mu\nu}$. Suppose that we have generally

$$|b_{\mu\nu}-a_{\mu\nu}| \leqq \epsilon \qquad (\nu \geqq \mu); \tag{103}$$

how far is the solution of the system

$$\sum_{\nu=\mu}^{n} b_{\mu\nu}x_\nu = y_\mu \tag{104}$$

influenced if the $b_{\mu\nu}$ are replaced by $a_{\mu\nu}$?

If we denote the matrix of (102) by $A^{(0)}$ and that of (104) by A, the question can be answered by giving estimates of $|A^{-1}-A^{(0)-1}|_p$ $(p=1, \infty)$. Suppose that we have generally

$$a_{\mu\mu}=1, \quad |a_{\mu\nu}| \leqq M_\mu \qquad (\mu>\nu; \quad \mu=1, \ldots, n-1) \tag{105}$$

and consider the matrix

$$\Delta(M_1, \ldots, M_{n-1}) = \begin{pmatrix} 1 & -M_1 & \ldots & -M_1 \\ 0 & 1 & \ldots & -M_2 \\ \cdot & \cdot & \ldots & \cdot \\ \cdot & \cdot & \ldots & \cdot \\ \cdot & \cdot & \ldots & \cdot \\ \cdot & \cdot & \ldots & \cdot \\ 0 & 0 & \ldots & 1 \end{pmatrix}, \tag{106}$$

where all elements to the left of the main diagonal are zeros, and all elements to the right of the main diagonal in the μth row are equal to $-M_\mu$.

We obtain from lemma III at once the majorization

$$A^{-1}-A^{(0)-1} \ll \Delta(M_1+\epsilon, \ldots, M_{n-1}+\epsilon)^{-1}-\Delta(M_1, \ldots, M_{n-1})^{-1}.$$

To obtain the inverse of the matrix $\Delta(M_1, \ldots, M_{n-1})$, consider the system of linear equations

$$x_\mu - M_\mu(x_{\mu+1}+\ldots+x_n)=u_\mu \qquad (\mu=1, \ldots, n). \tag{107}$$

To solve it explicitly, we put

$$s_\mu = \sum_{\kappa=\mu}^{n} x_\kappa \qquad (\mu=1, \ldots, n), \tag{108}$$

$$1+M_\mu=N_\mu, \qquad N_\mu N_{\mu+1} \ldots N_n = P_\mu \qquad (\mu=1, \ldots, n-1) \qquad N_n=1, \qquad P_n=1. \tag{109}$$

Then (107) becomes

$$x_\mu = M_\mu s_{\mu+1}+u_\mu \qquad (\mu=1, \ldots, n), \tag{110}$$

$$s_\mu = N_\mu s_{\mu+1}+u_\mu \qquad (\mu=1, \ldots, n), \tag{111}$$

where $s_{n+1}=0$. Dividing (111) by P_μ, we obtain

$$\frac{s_\mu}{P_\mu} = \frac{s_{\mu+1}}{P_{\mu+1}} + \frac{u_\mu}{P_\mu}$$

and therefore

$$s_\mu = P_\mu \sum_{\varkappa=\mu}^{n} \frac{u_\varkappa}{P_\varkappa};$$

introducing this in (110) we have

$$x_\mu = u_\mu + M_\mu P_{\mu+1} \sum_{\varkappa=\mu+1}^{n} \frac{u_\varkappa}{P_\varkappa} \qquad (\mu = 1, \ldots, n;\ P_{n+1} = 0). \tag{112}$$

We obtain therefore for the inverse of our $\Delta(M_1, \ldots, M_{n-1})$, if E denotes the unit matrix,

$$\Delta(M_1, \ldots, M_{n-1})^{-1} = E + DT, \tag{113}$$

where D is the diagonal matrix

$$D = \begin{pmatrix} M_1P_2 & & & & & \\ & M_2P_3 & & & & \\ & & \ddots & & & \\ & & & & 0 & \\ & 0 & & & & \\ & & & & M_{n-1}P_n & \\ & & & & & 0 \end{pmatrix}, \tag{114}$$

and T the triangular matrix

$$T = \begin{pmatrix} 0 & \frac{1}{P_2} & \frac{1}{P_3} & \cdots & \frac{1}{P_n} \\ & 0 & \frac{1}{P_3} & \cdots & \frac{1}{P_n} \\ & & 0 & \cdots & \frac{1}{P_n} \\ & & & \ddots & \\ & 0 & & & \\ & & & & 0 \end{pmatrix}. \tag{115}$$

The expressions

$$\Delta(M_1+\epsilon, \ldots, M_{n-1}+\epsilon)^{-1} - \Delta(M_1, \ldots, M_{n-1})^{-1} \tag{116}$$

obtained from (113), (114), (115) are rather unwieldy; however, we shall obtain for its norm corresponding to $p=1$ (cf. 66,a) a very simple and elegant expression.

Indeed, if we take the sum of the elements in the νth column of $\Delta(M_1, \ldots, M_{n-1})^{-1}$ and denote it by l'_ν, we have

$$l'_\nu = 1 + \frac{1}{P_\nu} \sum_{\mu=1}^{\nu-1} M_\mu P_{\mu+1} = 1 + \sum_{\mu=1}^{\nu-1} M_\mu \prod_{\varkappa=\mu+1}^{\nu-1} (1+M_\varkappa).$$

If we now write out $l'_{\nu+1}$, we obtain

$$l'_{\nu+1} = 1 + \left[\sum_{\mu=1}^{\nu-1} M_\mu \prod_{\varkappa=\mu+1}^{\nu-1} (1+M_\varkappa) \right] (1+M_\nu) + M_\nu;$$

and in comparing this with the expression for t'_ν we see that we have $t'_{\nu+1}\equiv(1+M_\nu)t'_\nu$ and therefore

$$t'_\nu=\prod_{\kappa=1}^{\nu-1}(1+M_\kappa). \tag{117}$$

We obtain now for the sum of the elements in the νth column of (116)

$$t_1=0, \quad t_2=\epsilon,$$

$$t_\nu=\prod_{\kappa=1}^{\nu-1}(1+M_\kappa+\epsilon)-\prod_{\kappa=1}^{\nu-1}(1+M_\kappa) \qquad (\nu=1,\ldots,n).$$

In multiplying this by $1+M_\nu+\epsilon$, we obtain

$$\prod_{\kappa=1}^{\nu}(1+M_\kappa+\epsilon)-\prod_{\kappa=1}^{\nu}(1+M_\kappa)-\epsilon\prod_{\kappa=1}^{\kappa-1}(1+M_\kappa),$$

and comparing this with $t_{\nu+1}$,

$$t_{\nu+1}=(1+M_\nu+\epsilon)t_\nu+\epsilon\prod_{\kappa=1}^{\nu-1}(1+M_\kappa). \tag{118}$$

Therefore, t_ν is monotonically increasing with ν, and we see that the norm of (116) corresponding to $p=1$ has the value

$$\prod_{\nu=1}^{n-1}(1+M_\nu+\epsilon)-\prod_{\nu=1}^{n-1}(1+M_\nu) \tag{119}$$

and obtain therefore

$$|A^{-1}-A^{(0)-1}|_1\leqq\prod_{\nu=1}^{n-1}(1+M_\nu+\epsilon)-\prod_{\nu=1}^{n-1}(1+M_\nu) \tag{120}$$

as the solution of our problem. In applications it may be better to use the recurrence formula (118). If all M_μ have the same value M, the expression (113) coincides with that obtained in section 5 for Δ_n^{-1} for $m=0$. But in this case we see from (48) and (49) that the row sums run through the same values as the sums in the columns. We obtain, therefore, in this case the expression

$$(M+1+\epsilon)^{n-1}-(M+1)^{n-1}=(n-1)\epsilon(M+1+\theta\epsilon), \quad 0<\theta<1,$$

as the norm of (116), both for $p=1$ and $p=\infty$.

8. Linear Systems With a Nearly Triangular Matrix

The results of the preceding sections give the means to discuss the following problem concerning the system (1) in the introduction under the conditions (2) and the "triangular" system

$$\sum_{\nu=\mu}^{n}a_{\mu\nu}x_\nu=y_\mu \qquad (\mu=1,\ldots,n), \tag{121}$$

with the matrix $A^{(0)}$. In discussing this problem we can obviously assume that $a_{\mu\mu}=1$ $(\mu=1,\ldots,n)$. Then the difference between the solution of (1) and that of (121) is given by the vector $(A^{-1}-A^{(0)-1})\eta$, $\eta=(y_1,\ldots,y_n)$, and the norm of this vector corresponding to one of the indices $p=1,\infty$ does not exceed $|A^{-1}-A^{(0)-1}|_p|\eta|_p$ $(p=1,\infty)$, and can indeed for suitable choice of the vector η attain this limit. Therefore, the norms $|A^{-1}-A^{(0)-1}|_p$ measure the error committed in replacing the system (1) by (121).

For an $\epsilon>0, M>0$ being given, how small must $m>0$ be taken in order that we have

$$|A^{-1}-A^{(0)-1}|_p\leqq\epsilon \qquad (p=1,\infty)? \tag{122}$$

If we introduce the quantities $|\Delta_n|$ and δ corresponding by (22), (23), and (27) to m and M, we obtain from (79) and (94) the condition

$$(1+M)^{n-1}\frac{\delta}{1-\delta}\leqq\epsilon$$

$$\delta\leqq\frac{\epsilon}{(1+M)^{n-1}+\epsilon}\qquad\left(|\Delta_n|\leqq 1-\frac{m}{M}\right)\tag{123}$$

as long as the condition (75) is satisfied and therefore certainly as long as $M\geqq 1.5/n$ $(n\geqq 4)$.

On the other hand, we have by (30)

$$m=\frac{\delta}{M_n+\theta\dfrac{\delta}{M}},\tag{124}$$

and from (123) and (124)

$$m\leqq\frac{\epsilon}{M_n(1+M)^{n-1}+\left(M_n+\dfrac{\theta}{M}\right)\epsilon}\qquad\left(|\Delta_n|\leqq 1-\frac{m}{M}\right).\tag{125}$$

We see that it will be sufficient to take

$$m\leqq m_0\equiv\frac{\epsilon}{M_n(1+M)^{n-1}+\left(M_n+\dfrac{1}{M}\right)\epsilon}\qquad\left(|\Delta_n|\leqq 1-\frac{m}{M}\right)\tag{126}$$

to solve our problem, for instance, if we have $M\geqq 1.5/n$ $(n\geqq 4)$ or $M\geqq 0.5321$ $(n=3)$. For small values of ϵ obviously, only the first term in the denominator is essential, and we have

$$m_0\approx K(n,M)\epsilon,\quad K(n,M)=\frac{1}{M_n(1+M)^{n-1}}.\tag{127}$$

Tables 1 and 2 give the values of $K(n,M)$ for a set of integer M from 1 to 10 and some values of $M>1.5/n$. We have obviously

$$K(n,M)<\frac{1}{M^{2n-2}}.\tag{128}$$

TABLE 1. $K(n,M)$

M	$n=3$	$n=4$	$n=5$	$n=6$	$n=7$	$n=8$	$n=9$	$n=10$
1	.0625	.0114	.(2)240	.(3)548	.(3)130	.(4)316	.(5)778	.(5)192
2	.0111	.(2)103	.(3)106	.(4)115	.(5)126	.(6)140	.(7)155	.(8)172
3	.(2)347	.(3)193	.(4)116	.(6)719	.(7)448	.(8)280	.(9)175	.(10)109
4	.(2)143	.(4)526	.(5)206	.(7)821	.(8)328	.(9)131	.(11)524	.(12)210
5	.(3)694	.(4)182	.(6)498	.(7)138	.(9)383	.(10)106	.(12)295	.(14)821
6	.(3)378	.(5)736	.(6)149	.(8)204	.(10)619	.(11)126	.(13)258	.(15)526
7	.(3)223	.(5)336	.(7)522	.(9)815	.(10)127	.(12)199	.(14)211	.(16)486
8	.(3)140	.(5)168	.(7)207	.(9)255	.(11)315	.(13)389	.(15)480	.(17)592
9	.(4)926	.(6)903	.(8)900	.(10)900	.(12)900	.(14)900	.(16)900	.(18)900
10	.(4)636	.(6)515	.(8)424	.(10)351	.(12)290	.(14)239	.(16)198	.(18)164

TABLE 2. $K(n, M)$

M	$n=3$	$n=4$	$n=5$	$n=6$	$n=7$	$n=8$	$n=9$	$n=10$
.1	------	------	------	------	------	------	------	------
.2	------	------	------	------	------	.0328	.0197	.0121
.3	------	------	.0866	.0399	.0196	.0101	.(2)533	.(2)289
.4	------	.117	.0438	.0180	.(2)788	.(2)359	.(2)169	.(3)809
.5	.254	.0718	.0241	.(2)891	.(2)349	.(2)142	.(3)592	.(3)252
.6	.181	.0464	.0141	.(2)470	.(2)165	.(3)602	.(3)224	.(4)848
.7	.134	.0313	.00864	.(2)260	.(3)825	.(3)270	.(4)902	.(4)305
.8	.102	.0218	.00548	.(2)150	.(3)431	.(3)127	.(4)382	.(4)116
.9	.0789	.0156	.00359	.(3)894	.(3)233	.(4)623	.(4)169	.(5)462
1.0	.0625	.0114	.00240	.(3)548	.(3)120	.(4)316	.(5)778	.(5)193
	$n=15$	$n=20$	$n=25$	$n=30$	$n=35$	$n=40$	$n=45$	$n=50$
.1	.0157	.(2)439	.(2)138	.(3)469	.(3)166	.(4)604	.(4)224	.(5)841
.2	.(2)137	.(3)188	.(4)281	.(5)439	.(6)697	.(6)112	.(7)180	.(8)290
.3	.(3)167	.(4)112	.(6)793	.(7)570	.(8)413	.(9)299	.(10)217	.(11)157
.4	.(4)242	.(6)809	.(7)277	.(9)957	.(10)331	.(11)114	.(13)395	.(14)137
.5	.(5)399	.(7)681	.(8)118	.(10)204	.(12)354	.(14)613	.(15)106	.(17)184
.6	.(6)729	.(8)658	.(10)597	.(12)543	.(14)494	.(16)449	.(18)409	.(20)372
.7	.(6)146	.(9)721	.(11)357	.(13)177	.(16)879	.(18)436	.(20)216	.(22)107
.8	.(7)317	.(10)886	.(12)248	.(15)695	.(17)195	.(20)545	.(22)153	.(25)428
.9	.(8)743	.(10)121	.(13)197	.(16)322	.(19)525	.(22)856	.(24)140	.(27)228
1.0	.(8)186	.(11)182	.(14)178	.(17)173	.(20)169	.(23)165	.(26)162	.(29)158

The bound in (126) is obviously the "best" under the condition (75), save that the factor $1/M$ of ϵ in the denominator could be replaced by an (unknown) fraction of it.

If $M<1.5/n$, the use of the general formula (87) is very cumbersome. We can, however, obtain a good working limit for m in the following way. If the inequalities (2) are valid for an $M<1.5/n=M^{(n)}$, then they are also satisfied if M is replaced by $M^{(n)}$, but then the limit for m obtained for $M^{(n)}$ is also sufficient for our M. We obtain therefore in this case the sufficient condition for (122) in the form

$$m \leqq m_0' \equiv \frac{\epsilon}{M_n^{(n)}(1+M^{(n)})^{n-1}+\left(M_n^{(n)}+\frac{1}{M_n}\right)\epsilon}. \tag{129}$$

Table 3 gives the values of $K(n,M^{(n)})$ for $n=1,2,\ldots,50$.

TABLE 3. $M=M^{(n)}=1.5/n$

n	$(1+M)^n-nM-1$	$K(n,M)$	n	$(1+M)^n-nM-1$	$K(n,M)$
3	.871	.255	27	1.805	.00755
4	1.074	.134	28	1.811	.00723
5	1.213	.0866	29	1.817	.00694
6	1.315	.0623	30	1.822	.00667
7	1.393	.0480	31	1.827	.00642
8	1.454	.0387	32	1.831	.00619
9	1.504	.0323	33	1.836	.00597
10	1.546	.0276	34	1.840	.00577
11	1.580	.0240	35	1.844	.00558
12	1.610	.0213	36	1.848	.00540
13	1.635	.0190	37	1.851	.00524
14	1.658	.0172	38	1.854	.00508
15	1.677	.0157	39	1.857	.00493
16	1.695	.0144	40	1.860	.00480
17	1.710	.0133	41	1.863	.00466
18	1.724	.0124	42	1.866	.00454
19	1.736	.0116	43	1.869	.00442
20	1.748	.0109	44	1.871	.00431
21	1.758	.0102	45	1.873	.00420
22	1.768	.00965	46	1.876	.00410
23	1.776	.00914	47	1.878	.00401
24	1.784	.00869	48	1.880	.00391
25	1.792	.00827	49	1.882	.00383
26	1.799	.00789	50	1.884	.00374

The expression for m_0' can be written in introducing the value of $M_n^{(n)}$ as

$$\frac{3}{2n}\cdot\frac{\epsilon}{\left(1+\frac{1.5}{n}\right)^{n-1}\left(\left(1+\frac{1.5}{n}\right)^{n}-2.5\right)+\left(\left(1+\frac{1.5}{n}\right)^{n}-1.5\right)\epsilon}.$$

We observe now that for any positive α and positive x the expression $(1+x/n)^{n-\alpha}$ monotonically increases and tends to e^x if the positive n increases monotonically to ∞. Indeed, if we put $u=1/n$, take the logarithm of this expression, differentiate it with respect to u, and multiply by u^2, we obtain

$$\frac{x(u-\alpha u^2)}{1+ux}-\log(1+ux)$$

but this expression vanishes for $u=0$ and decreases for positive u, since its derivative is

$$\frac{-xu}{(1+ux)^2}(2\alpha+x+\alpha xu).$$

We see, therefore, that

$$\left(1+\frac{1.5}{n}\right)^{n-1}\uparrow e^{1.5},\qquad\left(1+\frac{1.5}{n}\right)^{n}\uparrow e^{1.5}$$

and our bound for m can therefore be replaced by

$$\frac{3}{2n}\cdot\frac{\epsilon}{e^{1.5}(e^{1.5}-2.5)+(e^{1.5}-1.5)\epsilon}>\frac{\epsilon}{(5.93+1.99\epsilon)n};$$

we can replace therefore the condition $m\leqq m_0'$ by the simpler condition

$$m\leqq m_0=\frac{\epsilon}{n}\,\frac{1}{6+2\epsilon}. \tag{130}$$

On the other hand, we obtain at once the solution of our problem in the case $m=M<1/(n-1)$ from (87°).

$$m \leqq m_0 \equiv \frac{1}{n-1}\frac{\epsilon}{1+\epsilon} \qquad \left(m=M<\frac{1}{n-1}\right). \tag{131}$$

This is a "best" condition, whereas the condition (130) can still be improved. We see however, in comparing (130) with (131), that the bound in (130) cannot be improved by a factor greater than 6.

From the condition (130) we can finally derive the inequality (7) of the introduction. Indeed, if positive $m_0<1/2n$ is given, we can solve (130) with respect to ϵ,

$$\epsilon=\frac{6nm_0}{1-2nm_0},$$

and obtain therefore, in applying (130) for $m=m_0$, the inequality

$$|A^{-1}-A^{(0)-1}|_p \leqq \frac{6nm_0}{1-2nm_0}\,\varepsilon,$$

which holds for all positive $m_0<1/2n$ and gives the inequality (7) if we replace here m_0 by m.

9. References

[1] A. Ostrowski, Über die Determinanten mit überwiegender Hauptdiagonale, Comm. Math. Helv. **10,** 69–96 (1937).

[2] A. Ostrowski, Sur les conditions générales pour la régularité des matrices, Rendic. di Mat. e. d. s. applicaz. [V] **10,** 156–168 (1951).

[3] A. Ostrowski, Sur le matrices peu différentes d'une matrice triangulaire, Compt. rend. **233,** 1558–1560 (1951).

[3a] P. Stein and R. L. Rosenberg, On the solution of linear simultaneous equations by iteration, J. London Math. Soc. **23,** 111–117 (1948).

[4] O. Taussky-Todd, A recurring theorem on determinants, Am. Math. Monthly **56,** 672–676 (1949).

Washington, January 27, 1953.

INDEX TO VOLUME 52

A

Page

Absolute calibration of NBS standard thermal neutron density, RP2477 ... 93
Acetylenic hydrocarbons and intermediates, synthesis and physical properties, RP2472 ... 51
Achromatism of optical systems, RP2471 ... 43
Acquista, N., D. E. Mann, E. K. Plyler, Vibrational spectra of tetrafluoroethylene and tetrachloroethylene, RP2474 ... 67
Adiabatic demagnetization of chromic alums, RP2469 ... 33
Alaska, radio interference at 30 to 42 Mc, in, RP2468 ... 21
Aliphatic and alicyclic hydrocarbons, synthesis and physical properties, RP2473 ... 59
Allen, Jr., H. G., E. K. Plyler, Infrared spectrum of hydrogen sulfide in the 6,200-cm^{-1} region, RP2490 ... 205
Alloys, aluminum, fatigue-notch sensitivity, RP2495 ... 235
Alumina, lime, and water, phase equilibrium system of, from 50° to 250° C, RP2476 ... 75
Aluminum alloys, fatigue-notch sensitivity, RP2495 ... 247
Alums, chromic, tables for use in interpretation of paramagnetic behavior below 1° K, RP2469 ... 33
Amalgams, silver-tin-(copper-zinc), dimensional stability, RP2487 ... 185
Atmospheric ozone, continuous measurement by automatic photoelectric method, RP2481 ... 133
Attenuators, variable, mismatch errors in measurement of ultrahigh-frequency and microwave, RP2465 ... 7
Atypical pH response of some nonsilicate glasses, RP2497 ... 251
Audio, frequency, multirange, thermocouple instruments of high accuracy, RP2494 ... 227

B

Bagg, T. C., F. Stair, R. G. Johnson, Continuous measurement of atmospheric ozone by an automatic photoelectric method, RP2481 ... 133
Bass, A. M., W. S. Benedict, E. K. Plyler, Flame emission spectrum of water vapor in the 1.9-micron region, RP2485 ... 161
Beatty, R. W., Mismatch errors in the measurement of ultrahigh-frequency and microwave variable attenuators, RP2465 ... 7
Belknap, M. A., H. J. Keegan, D. J. Cordrey, Spectral transmissive properties of five selected optical glasses, RP2505 ... 305
Benedict, W. S., A. M. Bass, E. K. Plyler, Flame emission spectrum of water vapor in the 1.9-micron region, RP2485 ... 161
Bennett, J. A., J. G. Weinberg, Fatigue notch sensitivity of some aluminum alloys, RP2495 ... 235
Benzene, toluene, ethylbenzene, and 2-butanone, apparent specific volume of polystyrene in, RP2492 ... 217
Bingham and Cannon Master viscometers, precise measurements with, RP2479 ... 105
Bolt materials for underground mechanical joints, electrical measurements in selection of, RP2499 ... 265
Borate, phosphate, and germaniate glasses, pH response, RP2497 ... 251
Bovey, H. L., M. F. Shafer, Applications of dimensional analysis to spray-nozzle performance data, RP2482 ... 141
Broida, H. P., H. J. Morowitz, M. Seigin, Optical spectroscopic determination of hydrogen isotopes in aqueous mixtures, RP2503 ... 293
2-Butanone, benzene, toluene, and ethylbenzene, apparent specific volume of polystyrene in, RP2492 ... 217
Buzzard, R. W., D. P. Fickle, J. J. Park, Silver-uranium system, RP2483 ... 149

C

Callendar's radio-balance, use of for measurement of energy emission from radioactive sources, RP2486 ... 177
Cannon Master and Bingham viscometers, precise measurements with, RP2479 ... 105
Carbon dioxide in the ideal gas state, thermodynamic functions for, RP2502 ... 289
Characterization of normal matrices, RP2467 ... 17
Chloride, nickel, high-purity, preparation, RP2475 ... 73
Chromatic aberration of lenses, RP2471 ... 43
Clabaugh, W. S., J. W. Donovan, R. Gilchrist, Preparation of nickel chloride of high purity, RP2475 ... 73
Cleek, G. W., H. F. Shermer, G. F. Rynders, D. Hubbard, Atypical pH response of some nonsilicate glasses, RP2497 ... 251
Coaxial radio-frequency connectors and their electrical quality, RP2480 ... 121
Cobalt-free nickel chloride, preparation, RP2475 ... 73
Cogliano, J. A., M. Griffel, F. S. Jessup, F. P. Park, Apparent specific volume of polystyrene in benzene, toluene, ethylbenzene, and 2-butanone, RP2492 ... 217
Collett, C. T., Densities of five selected optical glasses, RP2506 ... 309
—, Simplification of calculations in routine density and volumetric determination, RP2489 ... 201
Colorimeter for measuring chromaticities of pyrotechnic smokes, RP2488 ... 195
Combination bands of hydrogen sulfide, RP2490 ... 205
Compressibilities of crystalline and glassy modifications of selenium and glucose, RP2496 ... 247
Connectors, coaxial radio-frequency, electrical quality, RP2480 ... 121
Conrady's chromatic condition, RP2471 ... 43
Cordrey, D. J., H. J. Keegan, M. A. Belknap, Spectral transmissive properties of five selected optical glasses, RP2505 ... 305
Corrosion, underground, of bolt materials, RP2499 ... 265
Cottington, R. L., J. F. Swindells, R. C. Hardy, Precise measurements with Bingham viscometers and Cannon Master viscometers, RP2479 ... 105
Coughanour, L. W., R. S. Roth, V. A. DeProsse, Phase equilibrium relations in the systems lime-titania and zirconia-titania, RP2470 ... 37
Cryoscopic study of solubility of uranium in liquid sodium, RP2503 ... 223
Cyclic and aliphatic hydrocarbons, synthesis and physical properties, RP2473 ... 59
Current sheet approximations in reference to high-frequency magnetic measurements, RP2501 ... 279

D

Page

De Juren, J. A., H. Rosenwasser, Absolute calibration of NBS standard thermal neutron density, RP2477 ... 93
Densities of optical glasses, RP2506 ... 309
Density and volumetric determinations, simplification of calculations, RP2489 ... 201
DeProsse, V. A., L. W. Coughanour, R. S. Roth, Phase equilibrium relations in the systems lime-titania and zirconia-titania, RP2470 ... 37
Deuterium oxide, optical spectroscopic determination, RP2503 ... 293
Dickson, G., J. A. Mitchell, I. C. Schoonover, H. C. Vacker, Some factors affecting the dimensional stability of the silver-tin-(copper-zinc) amalgams, RP2487 ... 185
Dimensional analysis, application to spray-nozzle performance, RP2482 ... 141
Dimensional stability of silver-tin-(copper-zinc) amalgams, RP2487 ... 185
Donovan, J. W., W. S. Clabaugh, R. Gilchrist, Preparation of nickel chloride of high purity, RP2475 ... 73
Douglas, T. B., A cryoscopic study of the solubility of uranium in liquid sodium at 97.8° C, RP2503 ... 223

E

Electrical measurements in the selection of bolt materials for underground mechanical joints, RP2499 ... 265
Electrical quality of coaxial radio-frequency connectors, RP2480 ... 121
Electron-optical shadow method of magnetic field mapping, RP2478 ... 97
Energy emission from radioactive sources, use of Callendar's radio-balance for measurement of, RP2486 ... 177
Ethylbenzene, benzene, toluene, and 2-butanone, apparent specific volume of polystyrene in, RP2492 ... 217
Exponential integral for large complex arguments, evaluation, RP2508 ... 313

F

Fatigue-notch sensitivity of aluminum alloys, RP2495 ... 235
Feder, D. P., Conrady's chromatic condition, RP2471 ... 43
Fickle, D. P., R. W. Buzzard, J. J. Park, Silver-uranium system, RP2483 ... 149
Field mapping, magnetic, electron-optical shadow method, RP2478 ... 97
Flame emission spectrum of water vapor, RP2485 ... 161
Flieger, Jr., H. W., J. F. Masi, J. S. Wicklund, Heat capacity of gaseous perfluoropropane, RP2500 ... 275
Fookson, A., P. Pomerantz, T. W. Mears, S. Rothberg, F. L. Howard, Synthesis and physical properties of several acetylenic hydrocarbons, RP2472 ... 51
—, —, —, —, —, Synthesis and physical properties of several aliphatic and alicyclic hydrocarbons, RP2473 ... 59
Formulas for facilitating osculatory interpolation, RP2491 ... 211
Fuel spray nozzles, performance, RP2482 ... 141
Furukawa, G. T., R. E. McCoskey, M. L. Reilly, Heat capacity, heats of transitions, fusion, and vaporization, and vapor pressure of octafluorocyclobutane, RP2466 ... 11
Futterman, W., E. Osborne, D. S. Saxon, A numerical solution of Schrödinger's equation in the continuum, RP2498 ... 259

G

Gas analysis, apparatus for determination of minor components, RP2464 ... 1
Gautier, Jr., T. N., C. J. Sargent, Predication of the likelihood of interference at frequencies of 30 to 42 megacycles in Alaska, RP2468 ... 21
Germaniate, borate, and phosphate glasses, pH response, RP2497 ... 251
Gilchrist, R., W. S. Clabaugh, J. W. Donovan, Preparation of nickel chloride of high purity, RP2475 ... 73
Glasses, nonsilicate, atypical pH response, RP2497 ... 251
Glasses optical:
Refractive indices RP2504 ... 303
Spectral transmissive properties, RP2505 ... 305
Densities, RP2506 ... 309
Thermal expansions, RP2507 ... 311
Glucose and selenium, compressibilities of crystalline and glassy, RP2496 ... 247
Griffel, M., R. S. Jessup, J. A. Cogliano, R. P. Park, Apparent specific volume of polystyrene in benzene, toluene, ethylbenzene, and 2-butanone, RP2492 ... 217

H

Haas, P. H., B. Kostyshyn, Discussion of current-sheet approximations in reference to high-frequency magnetic measurements, RP2501 ... 279
Hardy, R. C., J. F. Swindells, R. L. Cottington, Precise measurements with Bingham viscometers and Cannon Master viscometers, RP2479 ... 105
Heat capacity of gaseous perfluoropropane, RP2500 ... 275
Heat capacity, vapor pressure, and heats of vaporization, transition, and fusion of octafluorocyclobutane, RP2466 ... 11
Heavy water, optical spectroscopic determination, RP2503 ... 293
Hermach, F. L., E. S. Williams, Multirange, audiofrequency thermocouple instruments of high accuracy, RP2494 ... 227
Hidnert, P., Thermal expansion of five selected optical glasses, RP2507 ... 311
High-frequency magnetic measurements, current-sheet approximations, RP2501 ... 279
Hoffman, A. J., O. Taussky, A characterization of normal matrices, RP2467 ... 17
Howard, F. L., P. Pomerantz, A. Fookson, T. W. Mears, S. Rothberg, Synthesis and physical properties of several acetylenic hydrocarbons, RP2472 ... 51
—, —, —, —, —, Synthesis and physical properties of several aliphatic and alicyclic hydrocarbons, RP2473 ... 59
Hubbard, D., G. F. Rynders, G. W. Cleek, A typical pH response of some nonsilicate glasses, RP2497 ... 251
Hudson, R. P., C. K. McLane, Tables for use in the interpretation of paramagnetic behavior below 1° K, for the chromic alums (J=3/2), RP2469 ... 33
Hydrocarbons, acetylenic and intermediates, synthesis and physical properties, RP2472 ... 51

Page

Hydrocarbons, aliphatic and alicyclic, synthesis and physical properties, RP2473 ... 59
Hydrogen isotopes, in aqueous mixtures, optical spectroscopic analysis, RP2503 ...
Hydrogen-oxygen and acetylene-oxygen flames, emission spectra, RP2485 ... 161
Hydrogen-sulfide spectrum, RP2490 ... 205

I

Inductance, current-sheet approximations in measurements of, RP2501 ... 279
Infrared absorption spectrum of hydrogen sulfide, RP2490 ... 205
Infrared spectra of tetrafluoroethylene and tetrachloroethylene, RP2474 ... 67
Iron and steel bolts, low-alloy, soil corrosion, RP2499 ... 265
Isotopes, hydrogen, in aqueous mixtures, optical spectroscopic determination, RP2503 ... 293

J

Jessup, R. S., M. Griffel, J. A. Cogliano, R. P. Park, Apparent specific volume of polystyrene in benzene, toluene, ethylbenzene, and 2-butanone, RP2492 ... 217
Jickling, R. M., M. C. Selby, E. C. Wolzein, Coaxial radio-frequency connectors and their electrical quality, RP2480 ... 121
Johnson, R. G., R. Stair, T. C. Bagg, Continuous measurement of atmospheric ozone by an automatic photoelectric method, RP2481 ... 133

K

Keegan, H. J., M. A. Belknap, D. J. Cordrey, Spectral transmissive properties of five selected optical glasses, RP2505 ... 305
Kostyshyn, B., P. H. Haas, Discussion of current-sheet approximations in reference to high-frequency magnetic measurements, RP2501 ... 279

L

Lachenbruch, S. H., L. Marton, J. A. Simpson. Electron-optical shadow method of magnetic-field mapping, RP2478 ... 97
Lenses, achromatism of, RP2471 ... 43
Lime, alumina, and water, phase equilibrium system of, from 50° to 250°C., RP2476 ... 75
Lime-titania and zirconia-titania, phase equilibrium relations, RP2470 ... 37
Lukacs, E., O. Szasz, Nonnegative trigonometric polynominals and certain rational characteristic functions, RP2484 ... 153

M

Magnetic field mapping, electron-optical shadow method, RP2478 ... 97
Magnetic measurements, high-frequency, current-sheet approximations, RP2501 ... 279
Mann, D. E., N. Acquista, E. K. Plyler, Vibrational spectra of tetrafluoroethylene and tetrachloroethylene, RP2474 ... 67
Mann, W. B., Use of Callendar's "radio-balance" for the measurement of the energy emission from radioactive sources, RP2486 ... 177
Marton, L., J. A. Simpson, S. H. Lachenbruch, Electron-optical shadow method of magnetic-field mapping, RP2478 ... 97
Masi, J. F., H. W. Flieger, Jr., J. S. Wicklund, Heat capacity of gaseous perfluoropropane, RP2500 ... 275
Matrices, normal, characterization of, RP2467 ... 17
Matrices, triangular, RP2509 ... 319
McCoskey, R. E., G. T. Furukawa, M. L. Reilly, Heat capacity, heats of transitions, fusion, and vaporization, and vapor pressure of octafluorocyclobutane, RP2466 ... 11
McLane, C. K., R. P. Hudson, Tables for use in the interpretation of paramagnetic behavior below 1° K; for the chromic alums (J=3/2), RP2469 ... 33
Mears, T. W., P. Pomerantz, A. Fookson, S. Rothberg, F. L. Howard, Synthesis and physical properties of several acetylenic hydrocarbons, RP2472 ... 51
—, —, —, —, —, Synthesis and physical properties of several aliphatic and alicyclic hydrocarbons, RP2473 ... 59
Metals, aluminum alloys, fatigue failures, RP2495 ... 235
Mitchell, J. A., I. C. Schoonover, G. Dickson, H. C. Vacker, Some factors affecting the dimensional stability of the silver-tin-(copper-zinc) amalgams, RP2487 ... 185
Molecular structure of tetrafluoroethylene and tetrachloroethylene, RP2474 ... 67
Morowitz, H. J., H. P. Broida, M. Selgin, Optical spectroscopic determination of hydrogen isotopes in aqueous mixtures, RP2503 ... 293

N

NBS standard thermal neutron density, absolute calibration of, RP2477 ... 93
Neutron density, thermal, absolute calibration of NBS standard, RP2477 ... 93
Nickel chloride, high-purity, preparation, RP2475 ... 73
Nimeroff, I., S. W. Wilson, A colorimeter for pyrotechnic smokes, RP2488 ... 195
Nonnegative trigonometric polynomials and certain rational characteristic functions, RP2484 ... 153
Nonsilicate glasses, atypical pH response, RP2497 ... 251
Notch sensitivity of aluminum alloys in fatigue, RP2495 ... 235
Nozzles, fuel spray, performance, RP2482 ... 141
Numerical analysis:
Characterization of normal matrices, RP2467 ... 17
Evaluation of the exponential integral for large complex arguments, RP2508 ... 313
Matrices, triangular, RP2509 ... 319
Nonnegative trigonometric polynomials, RP2484 ... 153
Osculatory interpolation, formulas for facilitating, RP2491 ... 211
Schrödinger's equation in the continuum, RP2498 ... 259

O

Octafluorocyclobutane, entropy, heat capacity, heats of transition, fusion, and vaporization, and vapor pressure of, RP2466 ... 11
Optical-electron shadow method of magnetic-field mapping, RP2478 ... 97

Page

Optical glasses:
Refractive indices, RP2504 ... 303
Spectral transmissive properties, RP2505 ... 305
Densities, RP2506 ... 309
Thermal expansion, RP2507 ... 311
Optical spectroscopic determination of hydrogen isotopes in aqueous mixtures, RP2503 ... 293
Optical systems, achromatism of, RP2471 ... 43
Osborne, E., W. Futterman, D. S. Saxon, A numerical solution of Schrödinger's equation in the continuum, RP2498 ... 259
Osculatory interpolation, formulas for facilitating, RP2491 ... 211
Ostrowski, A. M., On nearly triangular matrices, RP2509 ... 319
Ozone, atmospheric, continuous measurement of by automatic photoelectric method, RP2481 ... 133

P

Paramagnetic behavior of chromic alums, RP2469 ... 33
Park, J. J., R. W. Buzzard, D. P. Fickle, Silver-uranium system, RP2483 ... 149
Park, R. P., M. Griffel, R. S. Jessup, J. A. Cogliano, Apparent specific volume of polystyrene in benzene, toluene, ethylbenzene, and 2-butanone, RP2492 ... 217
Peppler, R. B., L. S. Wells, The system of lime, alumina, and water from 50° to 250° C, RP2476 ... 75
Perfluoropropane, gaseous, heat capacity, RP2500 ... 275
pH response, atypical, of some nonsilicate glasses, RP2497 ... 251
Phase diagram of silver-uranium diagram, RP2483 ... 149
Phase equilibrium relations in the system lime-titania and zirconia-titania, RP2470 ... 37
Phase equilibrium system of lime, alumina, and water, RP2476 ... 75
Phosphate, borate, and germaniate glasses, pH response, RP2497 ... 251
Photoelectric colorimeter for measuring chromaticities of pyrotechnic smokes, RP2488 ... 195
Photoelectric method, automatic, for continuous measurement of atmospheric ozone, RP2481 ... 133
Picnometers, simplification of calculations in use of, RP2489 ... 201
Plyler, E. K., H. C. Allen, Jr., Infrared spectrum of hydrogen sulfide in the 6,290-cm^{-1} region, RP2490 ... 205
—, *W. S. Benedict, A. M. Bass,* Flame emission spectrum of water vapor in the 1.9-micron region, RP2485 ... 161
—, *D. E. Mann, N. Acquista,* Vibrational spectra of tetrafluoroethylene and tetrachloroethylene, RP2474 ... 67
Polystyrene, apparent specific volume, RP2492 ... 217
Pomerantz, P., A. Fookson, T. W. Mears, S. Rothberg, F. L. Howard, Synthesis and physical properties of several acetylenic hydrocarbons, RP2472 ... 51
—, —, —, —, —, Synthesis and physical properties of several aliphatic and alicyclic hydrocarbons, RP2473 ... 59
Pyrotechnic smokes, colorimeter for measuring chromaticities, RP2488 ... 195

R

Radioactive sources, use of Callendar's radio-balance for measurement of energy emission from, RP2486 ... 177
Radio-balance, Callendar's, use of for measurement of energy emission from radioactive sources, RP2486 ... 177
Radio-frequency connectors, coaxial, electrical quality, RP2480 ... 121
Radio interference in Alaska at frequencies 30 to 42 Mc, prediction, RP2468 ... 21
Radio, mismatch errors in measurement of ultrahigh-frequency and microwave variable attenuators, RP2465 ... 7
Refractive indices of optical glasses, RP2504 ... 303
Reilly, M. L., G. T. Furukawa, R. E. McCoskey, Heat capacity, heats of transitions, fusion, and vaporization, and vapor pressure of octafluorocyclobutane, RP2466 ... 11
Rodney, W. S., R. E. Stephens, Refractive indices of five selected optical glasses, RP2504 ... 303
Rosenwasser, H., J. A. De Juren, Absolute calibration of NBS standard thermal neutron density, RP2477 ... 93
Roth, R. S., L. W. Coughanour, V. A. DeProsse, Phase equilibrium relations in the systems lime-titania and zirconia-titania, RP2470 ... 37
Rothberg, S., P. Pomerantz, A. Fookson, T. W. Mears, F. L. Howard, Synthesis and physical properties of several acetylenic hydrocarbons, RP2472 ... 51
—, —, —, —, —, Synthesis and physical properties of several aliphatic and alicyclic hydrocarbons, RP2473 ... 59
Rynders, G. F., G. W. Cleek, D. Hubbard, Atypical pH response of some nonsilicate glasses, RP2497 ... 251

S

Salzer, H. E., New formulas for facilitating osculatory interpolation, RP2491 ... 211
Sargent, C. J., T. N. Gautier, Jr., Prediction of the likelihood of interference at frequencies of 30 to 42 megacycles in Alaska, RP2468 ... 21
Saxon, D. S., W. Futterman, E. Osborne, A numerical solution of Schrödinger's equation in the continuum, RP2498 ... 259
Schoonover, I. C., J. A. Mitchell, G. Dickson, H. C. Vacker, Some factors affecting the dimensional stability of the silver-tin-(copper-zinc) amalgams, RP 2487 ... 185
Schrödinger's equation in the continuum, numerical solution, RP2498 ... 259
Schwerdtfeger, W. J., Electrical measurements in the selection of bolt materials for service underground, RP2499 ... 265
Selby, M. C., E. C. Wolzein, R. M. Jickling, Coaxial radio-frequency connectors and their electrical quality, RP2480 ... 121
Selenium and glucose, compressibilities of crystalline and glassy modifications of, RP2496 ... 247
Selgin, M., H. P. Broida, H. J. Morowitz, Optical spectroscopic determination of hydrogen isotopes in aqueous mixtures, RP2503 ... 293
Shafer, M. R., H. L. Bowey, Applications of dimensional analysis to spray-nozzle performance data, RP2482 ... 141
Shepherd, M, Apparatus for the determination of minor components of a gas mixture, RP2464 ... 1
Shermer, H. F., G. F. Rynders, G. W. Cleek, D. Hubbard, Atypical pH response of some nonsilicate glasses, RP2497 ... 251
Silver-tin-(copper-zinc) amalgams, dimensional stability, RP2487 ... 185

Page

Silver-uranium system, phase diagram, RP2483 149
Simpson, J. A., L. Marton, S. H. Lachenbruch, Electron-optical shadow method of magnetic-field mapping, RP2478 97
Smokes, pyrotechnic, colorimeter for measuring chromaticities, RP2488 195
Sodium, liquid, cryoscopic study of solubility of uranium in, RP2493 223
Soil corrosion of bolt materials, RP2499 265
Solubility of uranium in liquid sodium, cryoscopic study, RP2493 223
Specific-gravity determinations, simplification of calculations, RP2489 201
Specific volume, apparent, of polystyrene in benzene, toluene, ethylbenzene, and 2-butanone, RP2492 217
Spectra, vibrational, of tetrafluoroethylene and tetrachloroethylene, RP2474 67
Spectral transmissive properties of optical glasses, RP2505 305
Spectroscopic determination of hydrogen isotopes in aqueous mixtures, RP2503 293
Spectrum, flame emission, of water vapor, RP2485 161
Spectrum, infrared, of hydrogen sulfide, RP2490 205
Spray nozzles, fuel, performance, RP2482 141
Stair, R., T. C. Bagg, E. G. Johnson, Continuous measurement of atomspheric ozone by an automatic photoelectric method, RP2481 133
Standard thermal neutron density, NBS, absolute calibration, RP2477 93
Stephens, R. E., W. S. Rodney, Refractive indices of five selected optical glasses, RP2504 303
Swindells, J. F., R. C. Hardy, R. L. Cottington, Precise measurements with Bingham viscometers and Cannon Master viscometers, RP2479 105
System, phase equilibrium, of lime, alumina, and water from 50° to 250° C., RP2476 75
Szasz, O., E. Lukacs, Nonnegative trigonometric polynomials and certain rational characteristic functions, RP2484 153

T

Tables for use in interpretation of paramagnetic behavior below 1° K, for the chromic alums ($J=3/2$), RP2469 33
Taussky, O., A. J. Hoffman, A characterization of normal matrices, RP2467 17
Tetrafluoroethylene and tetrachloroethylene, vibrational spectra, RP2474 67
Thermal expansion of optical glasses, RP2507 311
Thermal neutron density, NBS standard, absolute calibration, RP2477 93
Thermocouple instruments, high-accuracy, multirange, audiofrequency, RP2494 227
Thermodynamic functions for carbon dioxide in the ideal gas state, RP2502 289
Titania, zirconia, and lime, phase equilibrium relations, RP2470 37
Todd, J., Evaluation of the exponential integral for large complex arguments, RP2508 313
Toluene, benzene, ethylbenzene, and 2-butanone, apparent specific volume of polystyrene in, RP2492 217

U

Page

Ultrahigh-frequency and microwave variable attenuators, mismatch errors in measurement of, RP2465 7
Underground corrosion of bolt materials, RP2499 265
Uranium, cyroscopic study of solubility in liquid sodium, RP2493 223
Uranium-silver system, phase diagram, RP2483 149

V

Vacher, H. C., J. A. Mitchell, I. C. Schoonover, G. Dickson, Some factors affecting the dimensional stability of the silver-tin-(copper-zinc) amalgams, RP2487 185
Vapor pressure of octafluorocyclobutane, RP2466 11
Vibrational spectra of tetrafluoroethylene and tetrachloroethylene, RP2474 67
Viscometers, Bingham and Cannon Master, precise measurements with, RP2479 105
Volumetric analysis of trace constituents in gas mixtures, RP2464 1
Volumetric and density determinations, simplification of calculations, RP2489 201

W

Water analysis, optical spectroscopic method, RP2503 293
Water, lime, and alumina, phase equilibrium system of, from 50° to 250° C, RP2476 75
Water vapor, flame emission spectrum, RP2485 161
Weighing, hydrostatic, simplification of calculations, RP2489 201
Weinberg, J. G., J. A. Bennett, Fatigue notch sensitivity of some aluminum alloys, RP2495 235
Weir, C. E., Compressibilities of crystalline and glassy modifications of selenium and glucose, RP2496 247
Wells, L. S., R. B. Peppler, The system of lime, alumina, and water from 50° to 250° C., RP2476 75
Wicklund, J. S., J. F. Masi, H. W. Flieger, Jr., Heat capacity of gaseous perfluoropropane, RP2500 275
Williams, E. S., F. L. Hermach, Multirange, audiofrequency thermocouple instruments of high accuracy, RP2494 227
Wilson, S. W., I. Nimeroff, A colorimeter for pyrotechnic smokes, RP2488 195
Wolzein, E. C., M. C. Selby, R. M. Jickling, Coaxial radio-frequency connectors and their electrical quality, RP2480 121
Woolley, H. W., Thermodynamic functions for carbon dioxide in the ideal gas state, RP2502 289

Z

Zirconia-titania and lime-titania, phase equilibrium relations, RP2470 37

U. S. GOVERNMENT PRINTING OFFICE: 1954

UNITED STATES
GOVERNMENT PRINTING OFFICE
DIVISION OF PUBLIC DOCUMENTS
WASHINGTON 25, D. C.

OFFICIAL BUSINESS

PENALTY FOR PRIVATE USE TO AVOID
PAYMENT OF POSTAGE, $300
(GPO)

Journal of Research of the National Bureau of Standards Vol. 52, No. 6 June 1954

Contents

		Page
Discussion of current-sheet approximations in reference to high-frequency magnetic measurements. Bohdan Kostyshyn and Peter H. Haas.	RP2501	279
Thermodynamic functions for carbon dioxide in the ideal gas state. Harold W. Woolley.	RP2502	239
Optical spectroscopic determination of hydrogen isotopes in aqueous mixtures. Herbert P. Broida, Harold J. Morowitz, and Margaret Selgin.	RP2503	293
Refractive indices of five selected optical glasses. Robert E. Stephens and William S. Rodney.	RP2504	303
Spectral transmissive properties of five selected optical glasses. Harry J. Keegan, Marion A. Belknap, and Dorothy J. Cordrey.	RP2505	305
Densities of five selected optical glasses. Charles T. Collett.	RP2506	309
Thermal expansion of five selected optical glasses. Peter Hidnert.	RP2507	311
Evaluation of the exponential integral for large complex arguments. John Todd.	RP2508	313
On nearly triangular matrices. A. M. Ostrowski.	RP2509	319
Index to volume 52 (January to June 1954, Research Papers RP2464 to RP2509).		347

Single copies of the above Research Papers are not available for sale, but the Superintendent of Documents, U. S. Government Printing Office, Washington 25, D. C., will reprint 100 or more copies, and request for the purchase price should be mailed promptly to that Office.

For sale by the Superintendent of Documents, U. S. Government Printing Office, Washington 25, D. C. Price 70 cents (single copy). Subscription Price: $5.50 a year; $1.25 additional for foreign mailing. Single copies vary in price.

UNITED STATES GOVERNMENT PRINTING OFFICE, WASHINGTON : 1954